

NATIONAL CENTER FOR EARTHQUAKE
ENGINEERING RESEARCH

State University of New York at Buffalo

THE BEHAVIOR AND DESIGN OF NONCONTACT LAP SPLICES SUBJECTED TO REPEATED INELASTIC TENSILE LOADING

by

Vincent E. Sagan, Peter Gergely and Richard N. White

Department of Structural Engineering
School of Civil and Environmental Engineering
Cornell University
Ithaca, New York 14853

Technical Report NCEER-88-0033

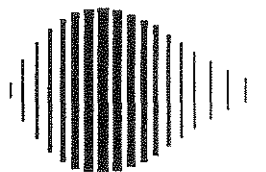
December 8, 1988

This research was conducted at Cornell University and was partially supported by the National Science Foundation under Grant No. ECE 86-07591.

NOTICE

This report was prepared by Cornell University as a result of research sponsored by the National Center for Earthquake Engineering Research (NCEER). Neither NCEER, associates of NCEER, its sponsors, Cornell University or any person acting on their behalf:

- a. makes any warranty, express or implied, with respect to the use of any information, apparatus, method, or process disclosed in this report or that such use may not infringe upon privately owned rights; or
- b. assumes any liabilities of whatsoever kind with respect to the use of, or the damage resulting from the use of, any information, apparatus, method or process disclosed in this report.



**THE BEHAVIOR AND DESIGN OF NONCONTACT LAP SPLICES
SUBJECTED TO REPEATED INELASTIC TENSILE LOADING**

by

Vincent E. Sagan¹, Peter Gergely² and Richard N. White³

December 8, 1988

Technical Report NCEER-88-0033

NCEER Contract Number 87-1005

NSF Master Contract Number ECE 86-07591

- 1 Structural Engineer, Simpson Gumpertz and Heger, Inc.
- 2 Professor, Department of Structural Engineering, Cornell University
- 3 James A. Friend Family Professor of Engineering, Cornell University

NATIONAL CENTER FOR EARTHQUAKE ENGINEERING RESEARCH
State University of New York at Buffalo
Red Jacket Quadrangle, Buffalo, NY 14261

PREFACE

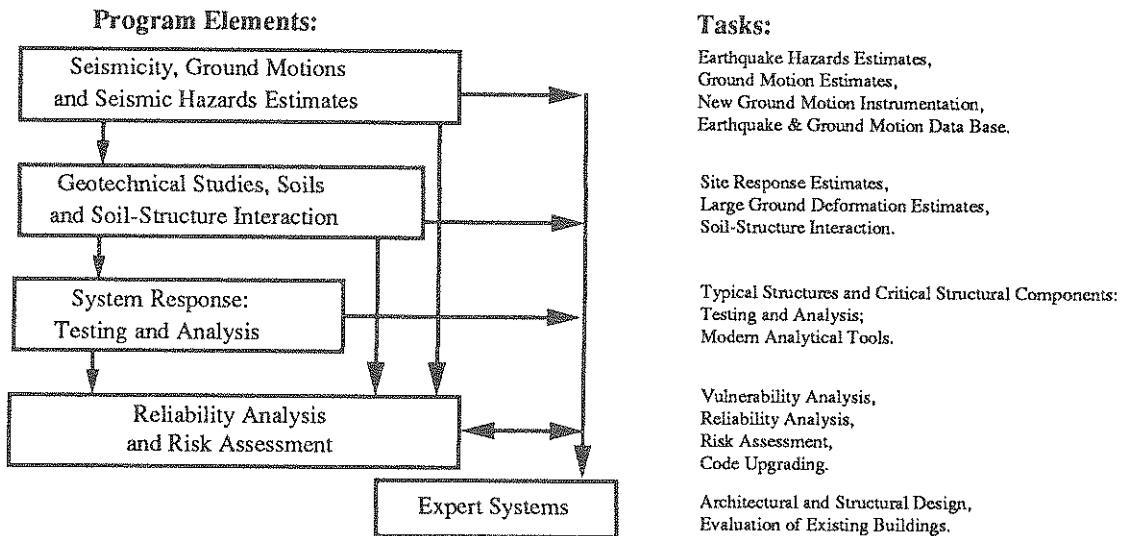
The National Center for Earthquake Engineering Research (NCEER) is devoted to the expansion and dissemination of knowledge about earthquakes, the improvement of earthquake-resistant design, and the implementation of seismic hazard mitigation procedures to minimize loss of lives and property. The emphasis is on structures and lifelines that are found in zones of moderate to high seismicity throughout the United States.

NCEER's research is being carried out in an integrated and coordinated manner following a structured program. The current research program comprises four main areas:

- Existing and New Structures
- Secondary and Protective Systems
- Lifeline Systems
- Disaster Research and Planning

This technical report pertains to Program 1, Existing and New Structures, and more specifically to system response investigations.

The long term goal of research in Existing and New Structures is to develop seismic hazard mitigation procedures through rational probabilistic risk assessment for damage or collapse of structures, mainly existing buildings, in regions of moderate to high seismicity. The work relies on improved definitions of seismicity and site response, experimental and analytical evaluations of systems response, and more accurate assessment of risk factors. This technology will be incorporated in expert systems tools and improved code formats for existing and new structures. Methods of retrofit will also be developed. When this work is completed, it should be possible to characterize and quantify societal impact of seismic risk in various geographical regions and large municipalities. Toward this goal, the program has been divided into five components, as shown in the figure below:



System response investigations constitute one of the important areas of research in Existing and New Structures. Current research activities include the following:

1. Testing and analysis of lightly reinforced concrete structures, and other structural components common in the eastern United States such as semi-rigid connections and flexible diaphragms.
2. Development of modern, dynamic analysis tools.
3. Investigation of innovative computing techniques that include the use of interactive computer graphics, advanced engineering workstations and supercomputing.

The ultimate goal of projects in this area is to provide an estimate of the seismic hazard of existing buildings which were not designed for earthquakes and to provide information on typical weak structural systems, such as lightly reinforced concrete elements and steel frames with semi-rigid connections. An additional goal of these projects is the development of modern analytical tools for the nonlinear dynamic analysis of complex structures.

As part of the systems response area, several projects are concerned with the response of lightly reinforced concrete structures. This report summarizes work on the safety of concrete elements containing lapped splices built such a way that the spliced bars do not touch. Design guidelines are formulated for earthquake-type loading.

ABSTRACT

The results of an investigation on the behavior and design of noncontact lap splices under monotonic and repeated inelastic is presented. This is the final phase of an extensive investigation on the behavior of lap splices subjected to inelastic cyclic loading. The goal of the study is to understand the behavior of noncontact tensile lap splices and to formulate improved design guidelines and equations that conform to existing unified design equations. Forty-seven full-scale, flat plate tension specimens were tested to determine the effects of specimen geometry, bar size, concrete strength, splice length, transverse steel area and spacing, repeatability, and primarily, the spacing of the splice bars.

The test data and other literature suggest that the load transfer between two bars of the splice is by a truss-like mechanism. The failure mode is an in-plane crack produced by a combination of bond-induced bursting forces and Poisson strain produced by the in-plane compressive stresses. The behavior is influenced by the added confinement that comes from spacing of the splice bars, and the reduction in concrete tensile strength with the compression field of the force transfer that is needed to resist the bursting. Equations for the design of noncontact lap splices for both monotonic and seismic loading are derived that take into account these effects and are modifications of existing state-of-the-art lap splice design equations.

ACKNOWLEDGEMENTS

The work here reported is sponsored by the National Science Foundation, Earthquake Hazard Mitigation Program under grant number CEE-8505676 and partially by NCEER grant number 87-1005B. The research project also received assistance from Richmond Screw Anchor Co., Inc. The work was performed in the George Winter Lab for Experimental Structural Research, Cornell University.

The people behind the scenes, which included Kenneth C. Hover, Tim Bond, Dave Farmer, and Paul Jones on the Structural Engineering faculty and staff, laboratory assistants Robert Hovey, Alex Milton, Hayes Concannon, and Anders Carlson, and the people at Saunders Concrete, are gratefully acknowledged for the guidance and assistance they provided in the experimental program.

TABLE OF CONTENTS

	Page
1 INTRODUCTION	
1.1 The Problem	1-1
1.2 Objectives and Scope	1-3
2 LITERATURE REVIEW	
2.1 Introduction	2-1
2.2 Tensile Lap Splice Summary	2-1
2.2.1 Design of Tensile Lap Splices and Anchorages	2-2
2.2.2 General Behavior	2-4
2.2.3 Load History	2-8
2.2.4 Factors Affecting Splice Behavior	2-11
2.3 Noncontact Tensile Lap Splices	2-18
2.3.1 Code Provisions on Noncontact Lap Splices	2-18
2.3.2 Noncontact Splice Research	2-19
3 DESCRIPTION OF EXPERIMENTAL PROGRAM	
3.1 Introduction	3-1
3.2 Specimen Description	3-1
3.3 Loading System	3-16
3.4 Instrumentation	3-18
3.5 Data Acquisition	3-18
3.6 Materials	3-21
3.7 Test Procedure	3-31
4 DISCUSSION OF EXPERIMENTAL RESULTS	
4.1 Introduction	4-1
4.2 Monotonically Loaded Specimens	4-1
4.3 Repeatedly Loaded Specimens	4-8
4.3.1 Number of Load Cycles	4-8
4.3.2 Development of Cracking	4-15
4.3.3 Development of Strains	4-17
4.3.4 Ultimate Load	4-30
4.3.5 Post-ultimate Investigation of Internal Cracking	4-33
4.4 Summary	4-36

5 DESIGN RECOMMENDATIONS

5.1	Introduction	5-1
5.2	Truss Model	5-2
5.2.1	Evidence	5-2
5.2.2	Design Equation Derivations	5-10
5.3	Critical Evaluation	5-21

6 SUMMARY AND CONCLUSIONS

6.1	Summary	6-1
6.2	Conclusions	6-2
6.3	Suggestions for Further Research	6-6

REFERENCES	7-1
------------------	-----

LIST OF TABLES

	Page
SECTION 3	
3.1 Tension test specimen dimensions.....	3-8
3.2 Tension test specimen reinforcement details....	3-10
3.3 Tension test specimen instrumentation.....	3-20
3.4 Tension test specimen material properties.....	3-24
3.5 Reinforcing steel properties.....	3-26
3.6 Concrete mix designs.....	3-29
 SECTION 4	
4.1 Tension test specimen behavior summary.....	4-2
4.2 Effects of transverse reinforcement distribution.....	4-13
 SECTION 5	
5.1 Bond stress reevaluation.....	5-6
5.2 Tension specimen evaluation of based on noncontact lap splice design and performance - satisfactory.....	5-26
5.3 Tension specimen evaluation of based on noncontact lap splice design and performance - marginal.....	5-27
5.4 Tension specimen evaluation of based on noncontact lap splice design and performance - unsatisfactory.....	5-28

LIST OF FIGURES

	Page
SECTION 2	
2.1	Failure patterns in deformed bars and splices (Orangun, et al. 1975).....2-5
2.2	Schematic representation of bursting force distribution, splice versus anchorage (Panahshahi, et al. 1987).....2-7
2.3	Comparison of Tepfers' and Reynolds' models for tension splice behavior (Panahshahi, et al. 1987).....2-9
2.4	Failure patterns for wide sections with multiple splices (Thompson, et al. 1975, Lem, et al. 1983).....2-16
2.5	Force transfer in tensile lap splices (Robinson, et al. 1974).....2-20
2.6	Lap splice internal cracking (Goto and Otsuka 1979).....2-20
2.7	Secondary cracking pattern in tension splices (Ferguson and Krishnaswamy 1971).....2-20
SECTION 3	
3.1	Simplified sketch of a typical tension test specimen3-3
3.2	Reinforcement in a typical tension test specimen.....3-4
3.3	Lap splice study specimen from Kluge, et al. (1986).....3-5
3.4	Specimen description terminology.....3-7
3.5	Deep beam tensile cracking.....3-13
3.6	Transverse steel details.....3-15
3.7	Experimental tension test frame and specimen.....3-17
3.8	Test frame used by Kluge, et al. (1986).....3-19
3.9	Data acquisition and loading system.....3-22

3.10	Load cell details.....	3-23
3.11	Mechanical splicing system used for load application.....	3-28

SECTION 4

4.1	Specimen identification.....	4-4
4.2	Experimental parameter distribution.....	4-5
4.3	Experimental parameter distribution, concrete compressive strength versus splice bar spacing.....	4-6
4.4	Ultimate load performance of the monotonically loaded specimens.....	4-7
4.5	Load cycle performance versus splice bar spacing, considering bar size and concrete strength.....	4-10
4.6	Concrete cracking progression of specimen TH8-4-5Sv.....	4-16
4.7	Surface concrete cracking patterns at failure for different splice bar spacings.....	4-18
4.8	Load versus splice bar strains.....	4-20
4.9	Splice bar strain redistribution.....	4-21
4.10	Splice bar strain distribution and the effect of splice bar spacing.....	4-24
4.11	Transverse reinforcement strains and splice bar spacing, $40d_b$ splices.....	4-25
4.12	Transverse reinforcement strains and splice bar spacing, $30d_b$ splices.....	4-26
4.13	Transverse steel reinforcement strains and splice length, $4d_b$ splice bar spacing.....	4-27
4.14	Transverse steel reinforcement strains and splice length, $8d_b$ splice bar spacing.....	4-28
4.15	Transverse reinforcement strains and transverse reinforcement spacing.....	4-29
4.16	Ultimate load performance of the repeatedly loaded specimens.....	4-32
4.17	In-plane cracking of specimen TL6-2-5Sv.....	4-34

4.18	Isolated in-plane cracking failure mode.....	4-35
4.19	Pulse-velocity readings and in-plane cracking for specimen TH6-8-10Ws at failure.....	4-37

SECTION 5

5.1	Effective lap length.....	5-4
5.2	End splice crack.....	5-9
5.3	Strength in concrete in biaxial stress (Nilson and Winter 1986).....	5-13
5.4	Stress diagram for interior splices not confined by supplementary stirrup-ties (Sivakumar, et al. 1982).....	5-16
5.5	Added confinement due to splice bar spacing.....	5-17
5.6	Lap length design equation comparison.....	5-23

NOTATION

- A = angle defining the compressive stress field between the spaced bars of a noncontact lap splice, degrees.
- A_{tr} = area of transverse reinforcement.
- c = thickness of concrete cover measured from the extreme tension fiber to the edge of the bar, inches.
- d = effective depth of section, measured from extreme compression fiber to centroid of tension reinforcement.
- d_b = diameter of main reinforcement.
- f'_c = specified compressive strength of concrete, psi.
- f_t = tensile strength of the concrete, psi.
- f_y = yield strength of main reinforcement.
- f_{yt} = yield strength of transverse reinforcement.
- l_d = development length, in.
- l_{dh} = development length for hooks.
- l_{eff} = effective splice lap length, inches.
- l_s = total splice lap length, inches.
- P_u = ultimate tensile force developed by main reinforcement on final load cycle.
- P_{sy} = tensile force developed by main reinforcement at the specified yield strength.
- P_y = tensile force developed by main reinforcement at yield.
- P_{yt} = tensile force developed by transverse reinforcement at yield.
- P_{60} = nominal tensile force developed by main reinforcement.

- s = maximum spacing of transverse reinforcement within l_s , center-to-center, inches.
- s_p = clear spacing between the two bars of a lap splice, inches.

SECTION 1

INTRODUCTION

1.1 The Problem

A noncontact lap splice is a structural detail in reinforced concrete that provides continuity to the steel reinforcement by overlapping the ends of the steel bars, without the bars touching. A comprehensive study of noncontact tensile lap splices was undertaken because the behavior of noncontact lap splices is not thoroughly understood, there is a lack of design guidelines, and they are a common occurrence in construction. One source of noncontact lap splices is construction workmanship mistakes in steel reinforcement placement and tying, but other sources exist. Considering the deformations on steel reinforcement, contact lap splice bars are not really in "contact". Concrete will find itself between two bars of a lap splice during proper consolidation of fresh concrete, even if they are tied. Finally, the American Concrete Institute allows spaced splices (ACI Committee 318, 1983).

The American Concrete Institute provides minimal guidance on the behavior and design of noncontact lap splices. ACI Committee 116 (1985) on cement and concrete terminology defines a lap splice as "a connection of reinforcing steel made by lapping the ends of the bars." It further defines lapping as "the overlapping of reinforcing steel bars, welded fabric, or expanded metal so that there may be continuity of stress in the reinforcing when the concrete member is subjected to flexural or tensile

loading." There is no mention of spaced or contact bars. The subject of spacing is addressed in the Building Code Requirements for Reinforced Concrete (ACI Committee 318, 1983) and the accompanying commentary. The requirement is ACI 318-83 Section 12.14.2.3 and states that "bars spliced by noncontact lap splices in flexural members shall not be spaced transversely farther than one-fifth the required lap splice length, nor 6 inches." The commentary supports the provision stating that it is based on tests and that it is undesirable to have an unreinforced concrete section (ACI Committee 318, 1983). At one time the American Concrete Institute Building Code required spaced lap splices (ACI Committee E-1, 1928). By 1963, the code allowed spaced or contact lap splices (ACI Committee 318, 1963). The current provision limiting the spacing of noncontact lap splices was incorporated in the 1971 building code. Therefore, the current provisions are based on research performed before 1971.

The majority of the experimental work on noncontact lap splices was performed before 1960. Walker (1951), Chinn, et al. (1955), and Chamberlin (1952, 1958) all concluded that there was little or no behavioral difference between spaced and contact splices. Their conclusion was based on tests having concrete compressive strengths less than 5000 psi, monotonic loading, limited or no transverse reinforcement, and maximum splice bar spacings of 3 bar diameters, $3d_b$, or 2 inches. When viewed in light of current concrete design and construction practices, the scope of the experimental work appears limited, especially with higher strength concretes and seismic-type load histories.

Only recently were any seismic studies performed on contact lap splices. A series of experimental and analytical projects were performed at Cornell University with the primary goal of designing a seismically resistant lap splices for beams, columns, and wide sections. The resulting design equations advocated closely spaced, uniformly distributed transverse reinforcement (Sivakumar, et al. 1983). Other seismic splice work has been performed by Aristizobal-Ochoa (1983), Sparling and Rezansoff (1986), and Rezansoff, et al. (1988), but none of these studies addressed noncontact lap splices.

The lack of research on noncontact lap splices is the reason for vagueness of design guidelines; the latter leave many questions unanswered. For example, what behavioral changes occur when the bars of a splice are spaced apart, especially under seismic loading? And are new design equations or modifications required? These questions are addressed in this research project, which is a continuation of the lap splice research performed at Cornell University.

1.2 Objectives and Scope

The noncontact lap splice research had several goals. The first was to gain a better understanding of noncontact lap splice behavior. Noncontact lap splice behavior was studied using 47 full-scale, flat plate specimens each having two splices subjected to tensile loading. Splice bar spacing, concrete compressive strength, splice bar size, the amount and distribution of transverse reinforcement, and lap length were varied.

Several specimen designs were duplicated to check the repeatability of the results. All specimens were slowly loaded in tension. If a specimen survived the first loading to yield it was slowly unloaded and then reloaded to yield. This procedure was repeated until failure.

The second goal was to develop a model to explain the spaced splice behavior and then to formulate rational design guidelines and equations. Test data and observations obtained from this study were the basis of the model and equations. An effort was made to incorporate other state-of-the-art research findings on splice behavior, monotonic and seismic, and the compression field theory in order to make a unified theory on lap splice behavior, both contact and spaced, under monotonic and seismic loading.

SECTION 2

LITERATURE REVIEW

2.1 Introduction

The study of noncontact lap splices requires not only a familiarity of the research performed on spaced splices but also a thorough understanding of tensile lap splice behavior and design in general. Because of the abundance of research studies on lap splices that have been performed recently, such as the Cornell seismic splice research, extensive and thorough literature reviews exist on bond, anchorage, and lap splices. Instead of repeating that review, a summary of the current state of knowledge on tensile contact lap splices is presented here, with particular emphasis on the test parameters investigated in this noncontact splice study. Fagundo, et al. (1979), Sivakumar, et al. (1982), and Panahshahi, et al. (1987) are suggested for additional coverage. The summary will be followed by a detailed review of the literature on spaced tensile lap splices.

2.2 Summary of Current Knowledge on Lap Splices

A complete discussion of lap splices cannot be done without including anchorages or development lengths. Some design codes combine the two because of the similarities in behavior and design. The design aspects will be discussed, as well as the behavior the design is intended to control.

2.2.1 Design of Tensile Lap Splices and Anchorages

A brief overview of the current practices and philosophies regarding the design of tensile lap splices and anchorages for both nonseismic and seismic loading conditions is presented. There exists quite a variety of accepted approaches.

The Building Code Requirements for Reinforced Concrete, ACI 318-83 (1983), considers steel reinforcement size and yield strength, and the concrete strength in determining the basic development length. The only recognition of the influences of concrete cover, bar spacing, and transverse steel are in the form of multiplier factors that can be applied when the bars being developed are spaced at least 6 inches on center and have at least a 3 inch clear side cover, and when the developed bar is enclosed with spiral reinforcement not less than 1/4 inch in diameter and at not more than a 4 inch pitch. For splices, the basic development length is multiplied by a factor ranging from 1.0 to 1.7 depending on the amount of steel spliced at a section. Appendix A, Special Provisions for Seismic Design, requires transverse reinforcement over the lap length and limits the location of lap splices because "such splices are not considered reliable" under inelastic cyclic loading according to the Commentary (ACI 318, 1983).

The New Zealand Code of Practice for the Design of Concrete Structures (1982) is based on the recommendations of ACI Committee 408 (1979). Development lengths can be shortened if one considers the confinement of the concrete cover, the bar

spacing, and the transverse reinforcement. The minimum lap length for deformed bars in tension splices is equal to that of the development length. The New Zealand seismic requirements restrict the location of lap splices and requires additional transverse reinforcement.

The latest draft of the CEB-FIB reinforced concrete code (1986) provides two methods, the standard (more traditional method), and the refined method, for determining lap and development lengths. In the refined method the influence of the concrete cover, bar or splice spacing, and the effective transverse reinforcement can be taken into account. The standard method requires minimum cover and transverse reinforcement.

The Cornell seismic splice equations result from the work performed by Fagundo, et al. (1979), Tocci, et al. (1981), Lukose, et al. (1982), Sivakumar, et al. (1983), and Panahshahi, et al. (1987). The proposed equations advocate relatively short lap lengths and closely spaced, uniformly distributed transverse reinforcement in the splice region. The design equations are valid for both tensile and compression splices under loading conditions subjecting the structural member to a minimum of 12 inelastic load cycles with the steel reinforcement reaching three times the yield strain. The proposed provisions are being experimentally evaluated by several other researchers at different institutions (Sparling and Rezansoff 1986, Rezansoff, et al. 1988).

2.2.2 General Behavior

Much evidence has accumulated on the similarities between lap splices and anchorages, or development lengths. To explain the similarities and lap splice behavior in general, several theories have been proposed.

2.2.2.1 Anchorages Versus Splices

Orangun, et al. (1975, 1977) performed a parameter study on development length and splice test data. They developed a strength equation, which has excellent correlation with experimental results for both development lengths and splices. If in addition to the traditional considerations (concrete compressive strength, steel reinforcement size and yield strength), the main reinforcement cover and spacing, and transverse reinforcement are considered, lap splice lengths and anchorage lengths can be designed with the same equation. This study was the basis for the current ACI 408 proposal (1979).

Orangun, et al. (1975, 1977) observed that the cracking failure modes for anchorages and splices, which are summarized in Figure 2.1, are the same. Additional behavioral similarities were observed by other researchers. Reynolds and Beeby (1982) reported that for a lap splice, "Orientation thus has no effect on the bond strength and therefore it is reasonable to assume that the bursting force in all direction around a lap is uniform," as in a single anchored bar.

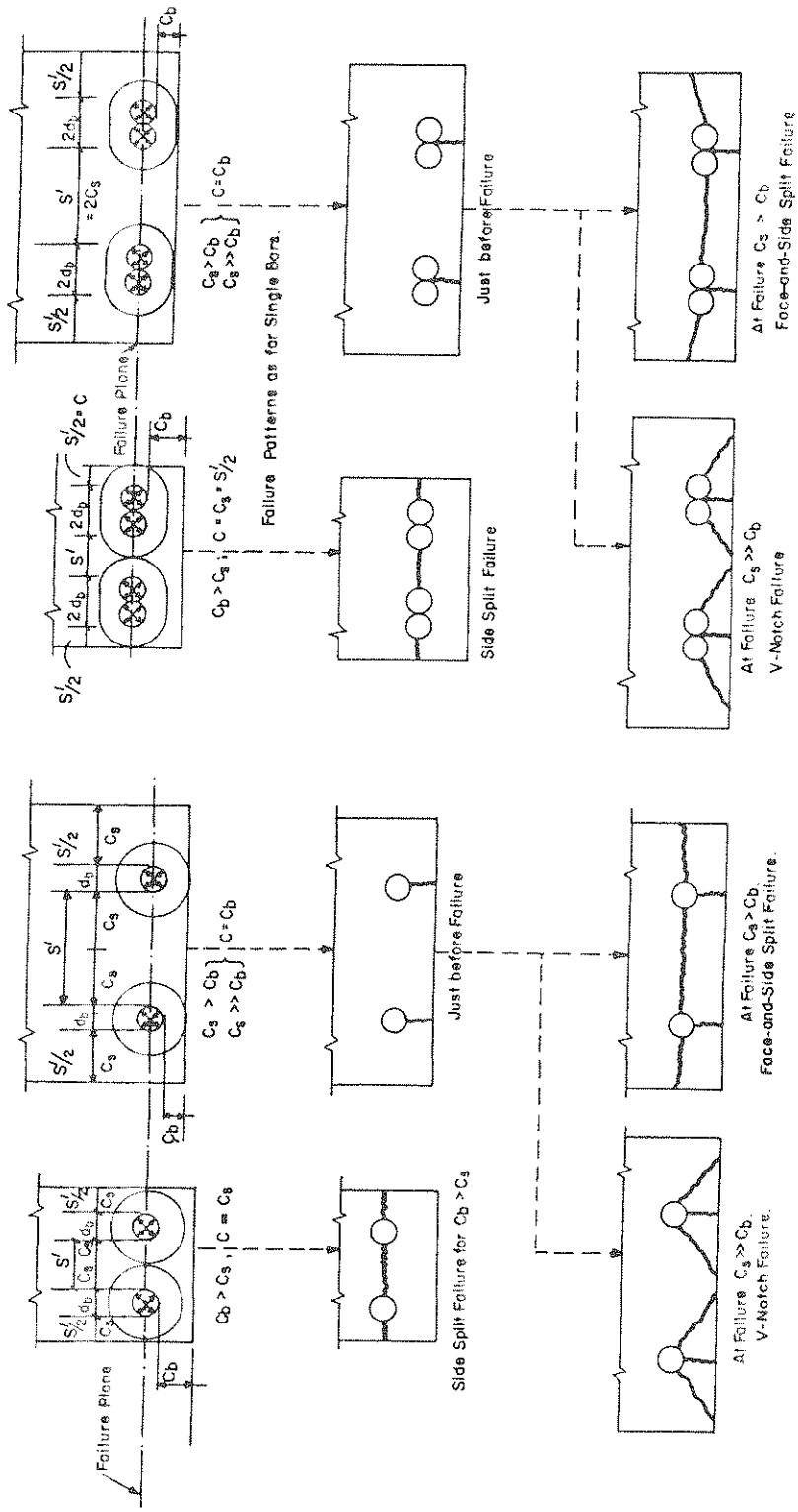


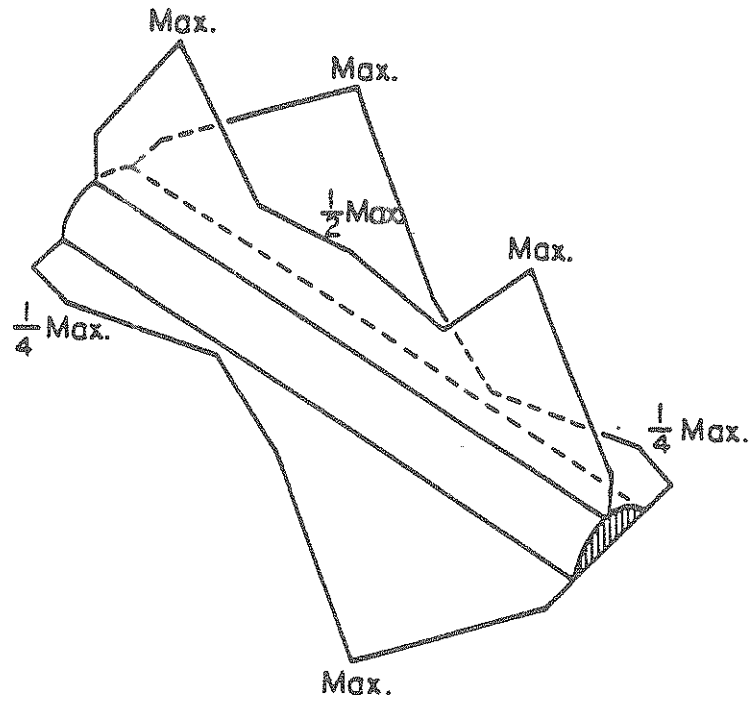
Figure 2.1 Failure patterns in deformed bars and splices (Orangun, et al. 1975).

A three-dimensional nonlinear finite element analysis was performed on a splice and anchorage of similar dimensions loaded monotonically to yield by overall performance of the lap splice and anchored bar were similar. The performance parameters that were similar included the load-end deflection curves, maximum circumferential stress in the concrete cover, and the bursting force intensities. The bursting force distributions are compared in Figure 2.2.

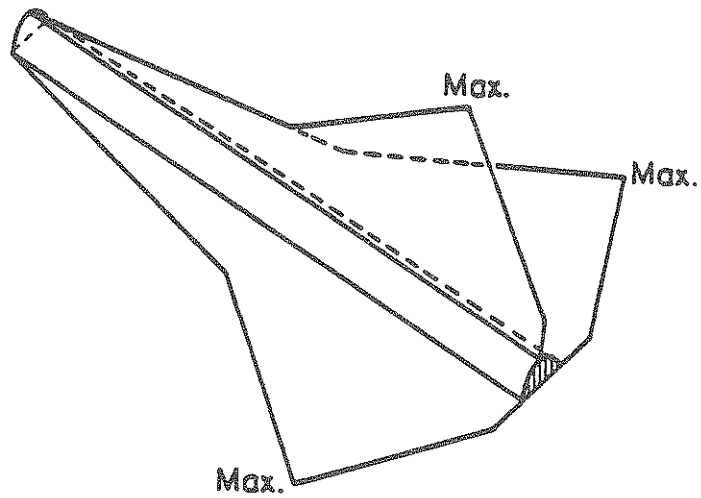
Research reporting differences between splice and anchorage behavior are rare and inconclusive. For example, the results from finite element fracture analyses performed by Tocci, et al. (1981) indicated that spliced bars require greater confinement than an anchorage of equal length. Under high level cyclic loading, Lukose, et al. (1982) reported that there are indications that spliced bars and anchored bars behave differently.

2.2.2.2 Load Transfer Theories

Even though there is similarity in the behavior of lap splices and anchorages, their load transfer mechanisms are different. Splices transfer the tensile forces from one bar of a lap splice to another through the surrounding concrete, while an anchorage transfers the tensile load to the surrounding concrete. In order to explain the load transfer in the splice and to account for the similarities in behavior to an anchorage, Tepfers (1973) suggested two theories for the force transfer in a lap splice; both predicted bursting force behavior different from



a) Lap splice



b) Anchored bar (axisymmetrical)

Figure 2.2 Schematic representation of bursting force distribution, splice versus anchorage (Panahshahi, et al. 1987).

that of an anchored bar. By changing the assumption regarding the angle at which the compressive forces are transferred through the concrete, Reynolds and Beeby (1982) developed a model that produces a bursting force distribution resembling that of an anchored bar. They suggested that the concrete between the bars of a lap splice provides the shortest and stiffest path for force transfer. Besides the predicted behavioral similarities, work done by Panahshahi, et al. (1987) and Goto and Otsuka (1979) support the theory of Reynolds and Beeby. The theories of Tepfers, and Reynolds and Beeby, are summarized in Figure 2.3.

Robinson, et al. (1974) proposed a truss model to explain and predict the behavior of lap splices. The lapped bars act as the truss chords and the transverse reinforcement act as the tension ties, while the concrete between the lapped bars transfers the load in diagonal compression.

2.2.3 Load History

The basic design provisions and guidelines are for noncyclic and nonseismic loading conditions. Most research on reinforced concrete was performed under monotonic loading. Only recently (within the last 20 years) has it been recognized that a structural member's behavior is strongly dependent on load history and this phenomenon requires much research. Loading history includes load intensity, duration, frequency, and application.

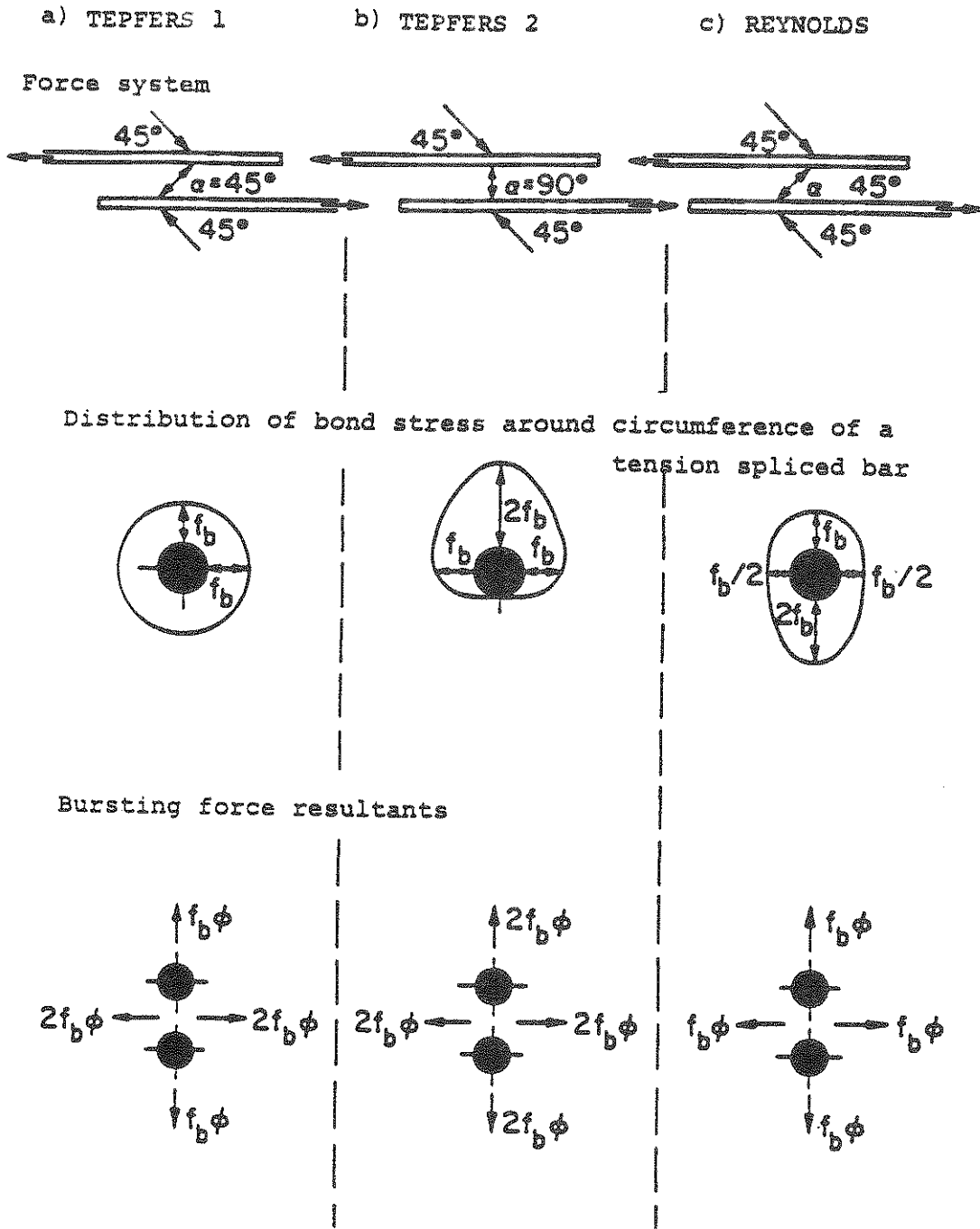


Figure 2.3 Comparison of Tepfers' and Reynolds' models for tension splice behavior (Panahshahi, et al. 1987).

Load application can be categorized as repeated, which is common in fatigue situations, and reversed cyclic, which is common in earthquakes. Yet much of the seismic work was done under repeated loading. Repeated loading causes the face of a structural member or a splice to be alternatively unstressed and stressed in compression or tension. Reversed cyclic loading causes the face of a structural member or a splice to be in the alternating states of tension and compression.

At low load intensities, the design problem becomes one of fatigue and indications are that monotonic design is sufficient (Lukose, et al. 1982). For example, Fagundo, et al. (1979) states that "the ACI 408 proposal is adequate for monotonic loads up to yield and for repeated loads below 80 percent of the monotonic failure load."

Seismic research is considered having load intensities at or above a level that causes the main steel reinforcement to yield. At these load levels, reversed cyclic loading is more damaging than repeated loading (Tocci, et al. 1981, Lukose, et al. 1982, Sparling and Rezansoff 1986). But the failure modes for repeated and reversed cyclic loading are the same (Lukose, et al. 1982). Lukose, et al. (1982) reported that a splice failure under cyclic loads was determined by the resistance of the combined two-bar splice system and generally not by the weaker bar as in monotonic loading. Under reversed cyclic loading there is a progressive deterioration of the force transfer mechanism, yield penetration

along the splice length, and longitudinal splitting (Tocci, et al. 1981). The cumulative damage results in changes of energy absorption capacities and stiffness from cycle to cycle (Lukose, et al. 1981). But Lukose also observed that during a load cycle the damage in the compressive loading was not as severe as in the tensile loading.

2.2.4 Factors Affecting Splice Behavior

A large number of parameters affect lap splice behavior. The more significant factors and those specifically studied in the noncontact lap splice investigation are discussed.

2.2.4.1 Splice Length

The lack of understanding of lap splice behavior is reflected by reinforced concrete code provisions which specify factors to increase the lap lengths. For example, ACI 318-83 requires increases of the basic development length by a factor of 1.0, 1.3, and 1.7 depending on the amount of reinforcement spliced at a section to obtain the lap length. Jirsa, et al. (1979) showed that these factors are not necessary if the splice bar cover, spacing, and transverse reinforcement is accounted for in the design.

Many researchers have investigated the effect of lap length and splice behavior under monotonic loading. Tepfers (1973) reported that the strength added to a lap splice decreases with increasing lap length. The ineffectiveness of added length is

due to the bond stress distribution. Ferguson and Breen (1965) observed that the bond stresses are the highest at the splice ends leaving an idle middle third which does not contribute to the ultimate strength of the splice.

Goto and Otsuka (1979) found that the cracking in the concrete between two bars of a lap splice, which is an indication of the load transfer, varied with lap length. For shorter splices, the crack angles were 30 to 45 degrees with the bar axis along the entire lap length. As the lap length increased, larger crack angles were observed in the middle portion of the splice length. In some cases, the cracks were at 90 degrees to the bar in the middle portion while at the ends of the bar the cracks remained at 30 to 45 degrees.

Performance of lap splices subjected to repeated and cyclic inelastic loading indicates that lap splices with lengths considerably shorter than required by many codes for monotonic loading are sufficient. Fagundo, et al. (1979) suggested that a minimum lap length of 30 bar diameters be used for inelastic cyclic loading. Advantages of the shorter splice length under seismic loading include better bond stress redistribution and having overreinforced sections kept to a minimum as reported by Tocci, et al. (1981). Lap lengths as short as 20 bar diameters are allowed by the seismic design equations proposed by Sivakumar, et al. (1982), provided that the concrete compressive strength is greater than 8650 psi.

2.2.4.2 Concrete Strength

The strength of the concrete surrounding the bars of the lap splice has long been recognized as a significant parameter affecting splice behavior and design. Because of the splitting of the concrete around deformed bars, the tensile strength of the concrete is critical and is used in the design equations.

Relating tensile strength to the compressive strength is done by raising the compressive concrete strength to a power ranging from 0.33 to 0.71 with 0.5 being most common (Carino and Lew 1982, Zsutty 1985).

With higher concrete strengths, shorter lap lengths can be used (Lukose, et al. 1982, Sivakumar, et al. 1982). But Tepfers (1973) showed experientially that a limit exists in the beneficial effects of increased concrete strengths. Higher strength concretes have better integrity and an increase in stiffness, and can resist higher bond stresses, but they also have lower energy absorption capacities. (Cowell, et al. 1982, Lukose, et al. 1981, 1982, Sivakumar, et al., 1982).

2.2.4.3 Size of Steel Reinforcement

Along with concrete strength, the size of the steel reinforcement has also been a major factor in lap splice and anchorage design. Theoretically, the amount of force that can be developed in steel reinforcement is dependent on its cross-sectional area, and the intensity of the bond stress, which is dependent on the surface area, and thus, the perimeter of the

bar. Chinn, et al. (1955) found from experiments that the bar diameter must be considered explicitly as a parameter in lap splice behavior even if splice length, beam width, and bar cover were all expressed in bar diameters. Lukose, et al. (1982) observed that bars with larger diameters caused greater damage to the concrete cover in splices during reversing curvatures associated with seismic loading cycles. The ultimate load per unit length for deformed bars with improved confinement depends increasingly on bar diameter as was reported by Lutz and Gergely (1967).

2.2.4.4 Splice Confinement

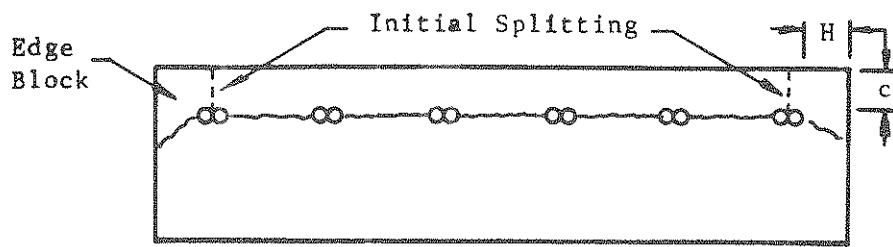
Orangun, et al. (1975) and other research, the code proposal by ACI Committee 408 (1979), and the New Zealand code (1982) have documented the influence of confinement for splices and anchorages. Confinement can be provided by increasing the strength of the concrete surrounding the bars of the splice, increasing the concrete cover and the spacing of the steel reinforcement, and adding transverse reinforcement (Chinn, et al. 1955, Roberts and Ho 1973). Of these sources, only the concrete compressive strength has traditionally been considered in anchorage and lap splice design (ACI 318, 1983) and has been previously discussed in detail.

The confinement of deformed bars provided by concrete involves both the bar cover and spacing (Ferguson 1977). The failure patterns for splices and anchorages depend on the smaller

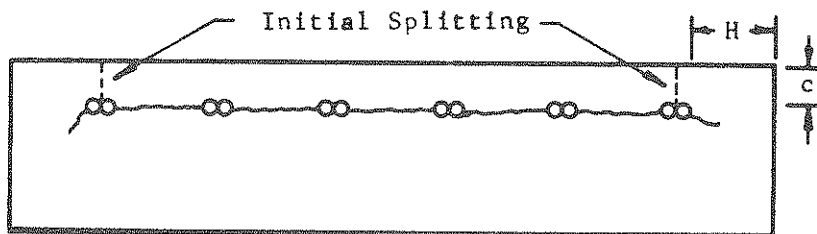
of the clear cover, side cover, and the half-spacing between the bars as shown in Figure 2.1 (Orangun, et al. 1975, 1977, Kemp and Wilhelm 1979). Many proposed development length and splice provisions, including those of ACI Committee 408 (1979), combine bar cover and spacing into one variable. A symptom of insufficient spacing is that the ultimate moment carrying capacities of beams are not being reached. Untrauer and Warren (1977) reported that the smaller the clear spacing, the smaller the developed stress at ultimate loading.

Wider beams with multiple bars or splices (greater than two) require special considerations. The dominant failure modes are summarized in Figure 2.4. Zsutty (1985) recommended a factor for a proposed development length equation specifically addressing the multiple-bar effect. Panahshahi, et al. (1987) reported that under inelastic cyclic loading, flat elements sustained a lower number of load cycles before failure than beam or column-type specimens. For seismic loading it was determined that additional transverse reinforcement is required for multiple spliced sections unless the splices were spaced greater than 4 bar diameters (Lukose, et al. 1982, Sivakumar, et al. 1983, Panahshahi, et al. 1987).

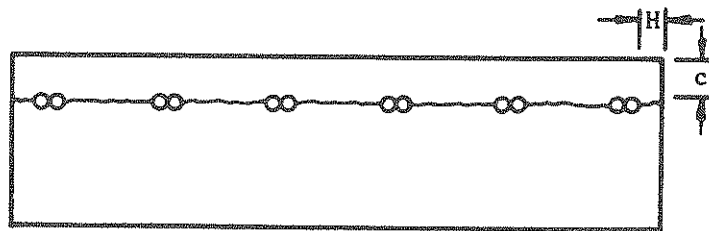
In high cyclic loading, where the loss of cover around the splice is inevitable, the concrete cover thickness did not appear to be a major parameter influencing the strength of the splice (Tocci, et al. 1981). The concrete cover was neglected in the



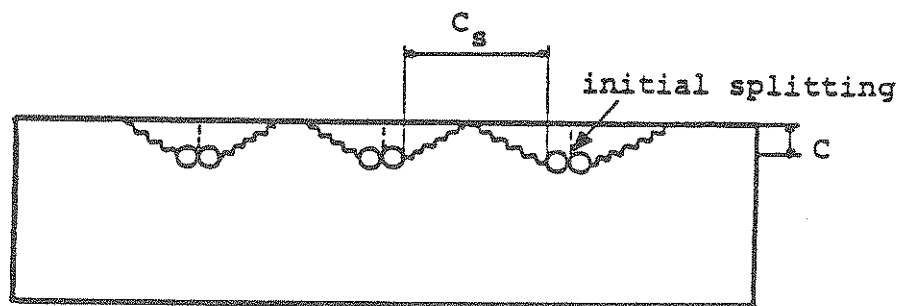
(a) Face and side split failure ($c \leq H < 2c$)



(b) Confined face split failure ($H > 2c$)



(c) Face split failure ($H < c$)



(d) V-type failure ($C_s \gg c$)

Figure 2.4 Failure patterns for wide sections with multiple splices (Thompson, et al. 1975, Lem, et al. 1983).

development of the proposed seismic splice design equations of Sivakumar, et al. (1982). However, the concrete cover is an essential part of the load transfer mechanism in the splice region. Minimum cover of 1.5 bar diameters for seismic loading is recommended (Lukose, et al. 1982).

The initial occurrence of splitting does not necessarily result in failure (Lukose, et al. 1982). Many of the problems associated with improper spacing or small cover can be compensated for with properly placed transverse reinforcement. The closer the spacing of stirrups along the splice length, the less important is the cover in influencing splice strength because of the added confinement and the stirrups acting as crack initiators (Tocci, et al. 1981). Tests show that smaller diameter and more closely spaced reinforcement are more effective than larger diameter more widely spaced stirrups because of their limited zone of influence (Lukose, et al. 1982).

The location of the transverse reinforcement along the splice for the added confinement is also critical. The bond stresses are maximum at the splice ends under monotonic loading, but at failure the steel reaches its yield stress and the peak bond stresses move toward the center of the splice (Roberts and Ho 1973). With monotonic loading that produces stresses above yield, and also with inelastic cyclic loading, yielding of the splice bars in the interior of the splice occurs causing higher bond stresses and increased bursting forces (Roberts and Ho 1973,

Fagundo, et al. 1979, Tocci, et al. 1981, Sivakumar, et al. 1982). The stirrups should be spaced evenly along a splice and outside the splice region a distance d when designing for seismic loading (Sivakumar, et al. 1983). Transverse reinforcement is essential for ductility, energy absorption, and force redistribution for seismic loading (Tocci, et al. 1981, Lukose, et al., 1982, Aristizobal-Ochoa 1983, Sparling and Rezansoff 1986).

2.3 Noncontact Tensile Lap Splices

2.3.1 Code Provisions on Noncontact Lap Splices

The current reinforced concrete codes consider noncontact lap splices in flexural members to be the same as contact splices provided that their spacing is limited to a certain distance. The Building Code Requirements for Reinforced Concrete, ACI 318-83, places the upper limit at the lesser of "one-fifth the required length of lap" and 6 inches. The 1982 New Zealand reinforced concrete code has an identical provision while the proposed European building code, CEB-FIB (1986), recommends the separation to be as small as possible and should not exceed 4 bar diameters. There are no special requirements for noncontact lap splices subjected to seismic loading and proposed seismic splice guidelines, such as Sivakumar, et al. (1982), also do not address the issue.

2.3.2 Noncontact Splice Research

2.3.2.1 Experimental

The common conclusion from the noncontact splice research performed thus far is that there is little or no difference between spaced and contact splices under monotonic loading. The researchers, including Walker (1951), Chamberlain (1952, 1958), Chinn, et al. (1955), and Tepfers (1973), used both pullout and full-scale beam specimens. Their conclusions are reflected in the current code provisions on tensile lap splices where the upper limit on spacing is the extent of the experimentation.

More recently, comparisons of average bond stresses were made with noncontact and contact splices. Cairns and Jones (1982) calculated higher ultimate bond stresses for contact splices than for noncontact splices. But Reynolds and Beeby (1982) also compared bond stresses and found good correlation with contact lap splices when they took into account the "effective" lap length of noncontact lap splices.

In order to explain the behavior of lap splices in general, and specifically noncontact lap splices, Robinson, et al. (1974) proposed the truss model for lap splice behavior, which incorporated the effective lap length as shown in Figure 2.5. Goto and Otsuka (1979) physically showed (see as in Figure 2.6) diagonal cracking of the concrete between two spaced splice bars. The lap length and spacing of the bars affected the angle of cracking. The concrete between the diagonal cracks resembles compressive struts of a truss. Ferguson and Krishnaswamy (1971)

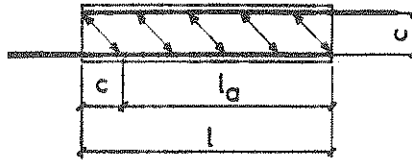


Figure 2.5 Force transfer in tensile lap splices (Robinson, et al. 1974).

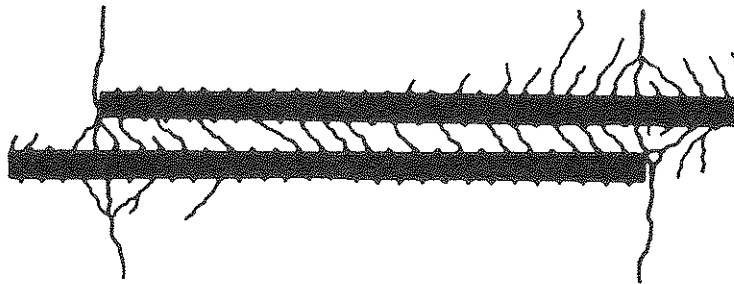


Figure 2.6 Lap splice internal cracking (Goto and Otsuka 1979).

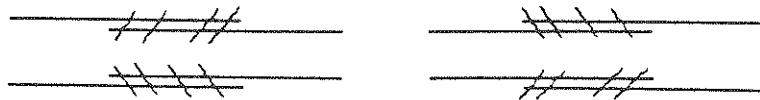


Figure 2.7 Secondary cracking patterns in tension splices (Ferguson and Krishnaswamy 1971).

observed similar diagonal cracking with lap splices, reproduced in Figure 2.7, but the cracking occurred on the surface of beams that contained #14 and #18 splice bars in contact.

2.3.2.2 Analytical Studies

Several analytical investigations were performed to gain a greater understanding of the behavior of lap splices. Betzle (1978) performed a photoelastic analysis of the force transfer in anchorages and spaced lap splices. The study showed that the force transfer between the steel reinforcement and the concrete of splice bars spaced 4 bar diameters apart resembled that of isolated end anchorages. It was also observed that with widely spaced bars the force transfer is "terminated after reaching a few ribs" and "the bond stress peaks are remarkably higher at the beginning and end of the splice" when compared to a narrower spacing. The narrower spaced bars had a force transfer over a greater length. Due to the inelastic behavior of reinforced concrete, the photoelastic analysis is limited in explaining splice behavior.

Panahshahi, et al. (1987) performed an inelastic finite element analytical study of a lap splice with the bars spaced at a fixed distance of 0.25 inches (one quarter of the bar diameter) and found similar results. "At the unloaded end of the splice bar, high bond stresses occurred in the region between spliced bars while the bond stresses around the remaining portion of the splice bar are negligible."

SECTION 3

DESCRIPTION OF EXPERIMENTAL PROGRAM

3.1 Introduction

The experimental program was designed to gain a thorough understanding of noncontact lap splice behavior. From the program, data and observations were obtained and used with other researchers' findings to develop a behavioral model and design requirements. Full-scale wall or slab specimens were selected as the most effective way to study a greater number and wider range of test variables. The test variables included the splice bar spacing, concrete compressive strength, splice bar size, lap length, transverse reinforcement, and repeatability. This chapter describes the properties of the specimens, and the devices and techniques used in the testing.

3.2 Specimen Description

The test specimen was the means to investigate noncontact lap splice behavior and had to meet three objectives:

- 1) It must be a full-scale structural member that would be smaller than a beam or a wall, but behaved as a section of a the larger member containing lap splices when loaded under direct tension.
- 2) The lap splices needed to behave as interior splices with limited influence on one another.

3) The specimen must allow for changes in splice bar spacing, splice length, splice bar size, concrete strength, and transverse reinforcement.

A flat plate specimen loaded in direct tension, as shown in Figure 3.1, was selected to permit the use of a full-scale member. The requirement of full-scale testing eliminated the use of beams because of their size. The smaller specimen permitted more tests to be performed, and therefore, a wider range of parameters were examined. A large number of specimens needed to be tested to obtain an in-depth understanding of the behavior of noncontact tensile lap splices under repeated inelastic loading. The size of the flat plate specimen permitted a number of them to be cast at one time and to significantly reduce the construction time.

Modeled as two interior splices in half a wall thickness, this geometry could be used to idealize the tension zone of a flexural member. The test slab had transverse steel close to one face anchored with ACI Code provision 180 degree hooks into a large side cover, and a thicker unreinforced face. Figure 3.2 is an example of the reinforcement in a typical specimen. The specimen is very similar to the ones tested by Kluge, et al. (1986) as shown in Figure 3.3.

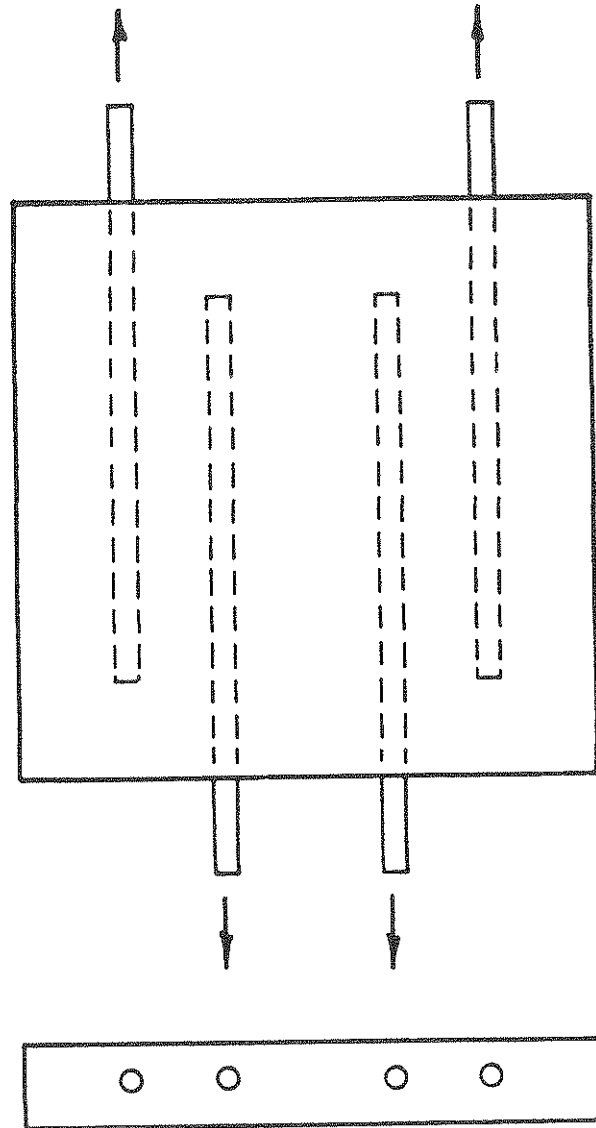


Figure 3.1 Simplified sketch of a typical tension test specimen.

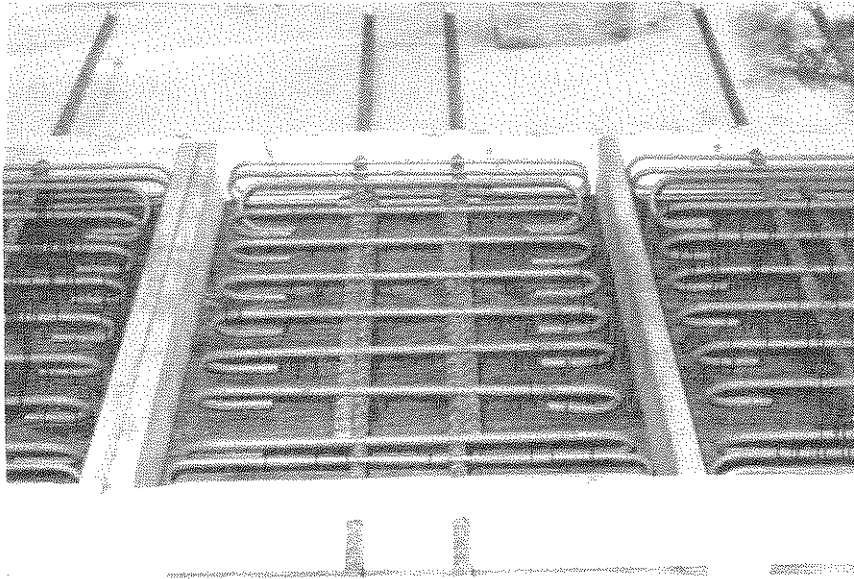


Figure 3.2 Reinforcement in a typical tension test specimen.

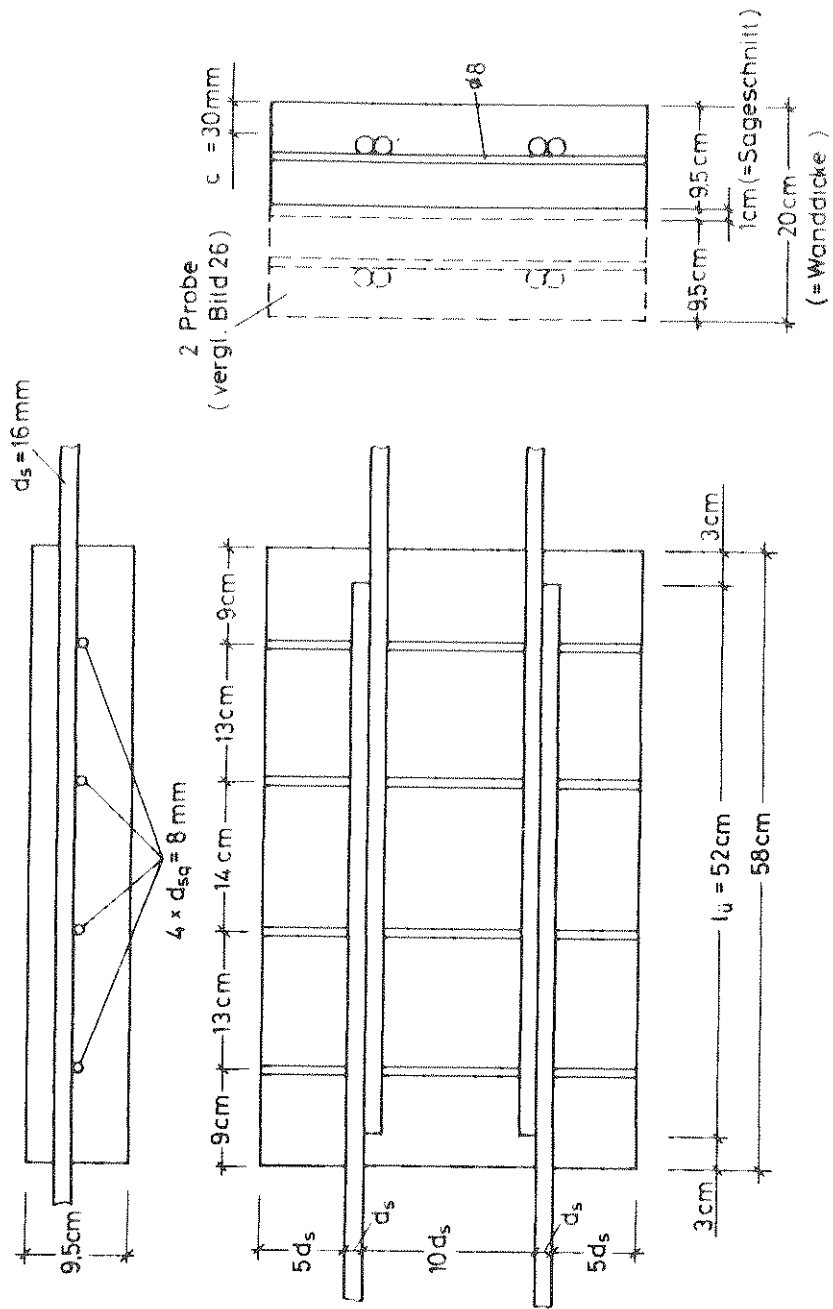
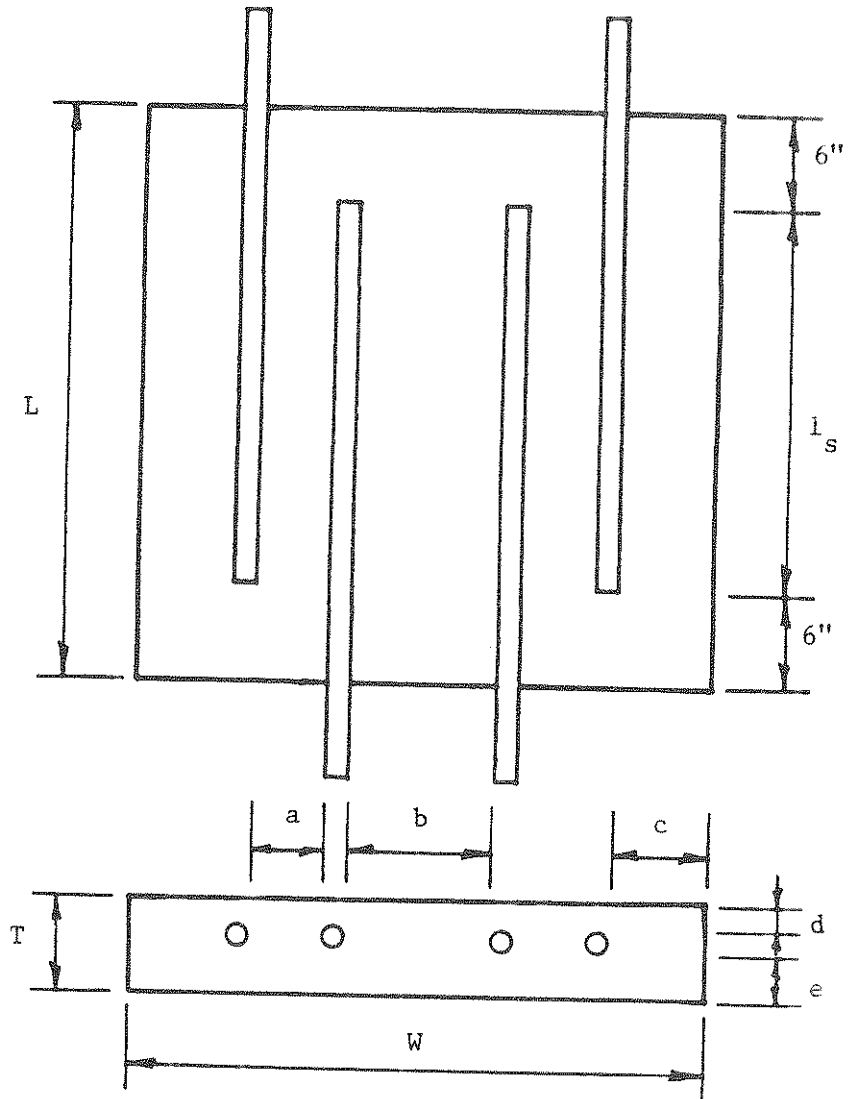


Figure 3.3 Lap splice study specimen from Kluge, et al. (1986).

The terminology used to describe the specimen is defined in Figure 3.4. The spacing and cover dimensions of the specimen were in terms of bar diameter, d_b . The top cover was $1.5d_b$, the bottom cover was $3.0d_b$, and the side cover was approximately $11d_b$, except for the test specimens that used #8 splice bars at a clear spacing of 8 inches. In that case the side cover was 8 inches clear, which proved to be sufficient. The bar and splice spacings were such that the splices were spaced further apart than the individual splice bars. When the splice bar clear spacing was 0, 2, or 4 bar diameters, the splice group clear spacing was 5 bar diameters. The splice group clear spacing was increased to 8 and 10 bar diameters as the splice bar clear spacing was increased to 6 and 8 bar diameters, respectively.

The specimen length equalled the splice length plus 12 inches. The splice length was in terms of bar diameters and was 30 or 40 bar diameters long. The specimen length included a 6 inch length at both ends of the splice, which was reinforced with two closed full-width steel hoops of #3 bars.

Of the 47 specimens, 15 did not match the above description. Seven of those were the preliminary tension specimens. The other 8 had a side cover that was half of the splice group spacing and used welded plates instead of the 180 degree hooks to anchor the transverse steel. Table 3.1 summarizes the cover, spacing, and other dimensions of the specimens, while the reinforcing details are found in Table 3.2.



- | | |
|--------------------------|---------------------------|
| a = splice bar spacing | L = specimen length |
| b = splice group spacing | T = specimen thickness |
| c = side cover | W = specimen width |
| d = top cover | |
| e = bottom cover | l_s = splice lap length |

Figure 3.4 Specimen description terminology.

Table 3.1 Tension test specimen dimensions.

No.	Specimen I.D.	Overall Dimensions		Splice Bar Clear Spacing (in.)
		Length (in.)	Width Thickness (in.)	
1.	PtN8-0-3MNO	42.0	10.0	5.0
2.	PtN8-2-3RNO	42.0	14.0	5.0
3.	PtN8-0-GSt	42.0	13.5	5.0
4.	PtN8-0-5.5St	42.0	13.5	5.0
5.	PtN8-2-GSt	42.0	17.5	5.0
6.	PtN8-4-GSt	42.0	21.5	5.0
7.	PtN8-4-5.5St	42.0	21.5	5.0
8.	TL6-0-5SV	34.5	23.75	4.125
9.	TL6-2-5SV	34.5	26.75	4.125
10.	TL6-4-5SV	34.5	29.75	4.125
11.	TL6-4-5SV-1	34.5	29.75	4.125
12.	TL8-0-5SV	42.0	14.5	5.5
13.	TL8-2-5SV	42.0	18.5	5.5
14.	TL8-4-5SV	42.0	22.5	5.5
15.	TL8-6-8SV	42.0	32.5	5.5
16.	TL8-4-5OF	42.0	22.5	5.5
17.	TL8-0-5S1	42.0	14.0	5.5
18.	TL8-4-5S1	42.0	22.0	5.5
19.	TL8-6-8S1	42.0	32.0	5.5
20.	TN6-0-5SV	34.5	23.75	4.125
21.	TN6-2-5SV	34.5	26.75	4.125
22.	TN6-4-5SV	34.5	29.75	4.125
23.	TN6-6-8SV	34.5	35.0	4.125
24.	TN8-0-5SV	42.0	31.0	5.5

Table 3.1 (Continued) Tension test specimen dimensions.

No.	Specimen I.D.	Overall Dimensions		Splice Bar Clear	Splice Bar Clear	Splice Group Clear Spacing (in.)		
		Length (in.)	Width Thickness (in.)					
25.	TN8-2-5SV	42.0	35.0	5.5	1.5	3.0	11.0	5.0
26.	TN8-4-5SV	42.0	39.0	5.5	1.5	3.0	11.0	5.0
27.	TN8-6-8SV	42.0	46.0	5.5	1.5	3.0	11.0	8.0
28.	TN8-8-10SV	42.0	46.0	5.5	1.5	3.0	8.0	10.0
29.	TN8-8-10SV-1	42.0	46.0	5.5	1.5	3.0	8.0	10.0
30.	TN8-8-10SV-2	42.0	46.0	5.5	1.5	3.0	8.0	10.0
31.	TN8-8-10WS	42.0	46.0	5.5	1.5	3.0	8.0	10.0
32.	TN8-8-10WS-1	42.0	46.0	5.5	1.5	3.0	8.0	10.0
33.	TN8-8-10WS-2	42.0	46.0	5.5	1.5	3.0	8.0	10.0
34.	TH6-0-5SV	34.5	23.75	4.125	1.125	2.25	8.5	3.75
35.	TH6-2-5SV	34.5	26.75	4.125	1.125	2.25	8.5	3.75
36.	TH6-4-5SV	34.5	29.75	4.125	1.125	2.25	8.5	3.75
37.	TH6-6-8SV	34.5	35.0	4.125	1.125	2.25	8.5	6.0
38.	TH6-8-10SV	34.5	39.5	4.125	1.125	2.25	8.5	7.5
39.	TH6-2-5WS	34.5	26.75	4.125	1.125	2.25	8.5	3.75
40.	TH6-4-5WS	34.5	29.75	4.125	1.125	2.25	8.5	3.75
41.	TH6-8-10WS	34.5	39.5	4.125	1.125	2.25	8.5	7.5
42.	T ⁺ H6-4-5WS	42.0	29.75	4.125	1.125	2.25	8.5	3.75
43.	T ⁺ H6-8-10WS	42.0	39.5	4.125	1.125	2.25	8.5	7.5
44.	TH8-0-5SV	42.0	31.0	5.5	1.5	3.0	11.0	5.0
45.	TH8-2-5SV	42.0	35.0	5.5	1.5	3.0	11.0	5.0
46.	TH8-4-5SV	42.0	39.0	5.5	1.5	3.0	11.0	5.0
47.	TH8-6-8SV	42.0	46.0	5.5	1.5	3.0	11.0	8.0

Table 3.2 Tension test specimen reinforcement details.

No.	Specimen I.D.	Lap Length (in.)	Spliced Bar Dia. Spacing (in.)	Transverse Steel		
				Along Splice Dia. Spacing (in.)	Along Splice Area (in. ² /ft.)	Along Splice Area (in. ² /ft.)
1.	PtN8-0-3MNO	30.0	1.0	0.0	NA	NA
2.	PtN8-2-3RNO	30.0	1.0	2.0	NA	NA
3.	PtN8-0-GSt	30.0	1.0	0.0	NA	NA
4.	PtN8-0-5.5St	30.0	1.0	0.0	NA	NA
5.	PtN8-2-GSt	30.0	1.0	2.0	NA	NA
6.	PtN8-4-GSt	30.0	1.0	4.0	NA	NA
7.	PtN8-4-5.5St	30.0	1.0	4.0	NA	NA
8.	TL6-0-5SV	22.5	0.75	0.0	0.375	4.25
9.	TL6-2-5SV	22.5	0.75	1.5	0.375	4.25
10.	TL6-4-5SV	22.5	0.75	3.0	0.375	4.25
11.	TL6-4-5SV-1	22.5	0.75	3.0	0.375	4.25
12.	TL8-0-5SV	30.0	1.0	0.0	0.5	4.5
13.	TL8-2-5SV	30.0	1.0	2.0	0.5	4.5
14.	TL8-4-5SV	30.0	1.0	4.0	0.5	4.5
15.	TL8-6-8SV	30.0	1.0	6.0	0.5	4.5
16.	TL8-4-50F	30.0	1.0	4.0	0.375	24.0
17.	TL8-0-5S1	30.0	1.0	0.0	NA	NA
18.	TL8-4-5S1	30.0	1.0	4.0	NA	NA
19.	TL8-6-8S1	30.0	1.0	6.0	NA	NA
20.	TN6-0-5SV	22.5	0.75	0.0	0.375	4.25
21.	TN6-2-5SV	22.5	0.75	1.5	0.375	4.25
22.	TN6-4-5SV	22.5	0.75	3.0	0.375	4.25
23.	TN6-6-8SV	22.5	0.75	4.5	0.375	4.25
24.	TN8-0-5SV	30.0	1.0	0.0	0.5	4.5

Table 3.2 (Continued) Tension test specimen reinforcement details.

No.	Specimen I.D.	Lap Length (in.)	Spliced Bar		Transverse Steel		
			Splicing Dia. (in.)	Spacing (in.)	Along Splice Dia. (in.)	Spacing Area (in. ² /ft.)	
25.	TN8-2-5SV	30.0	1.0	2.0	0.5	4.5	0.53
26.	TN8-4-5SV	30.0	1.0	4.0	0.5	4.5	0.53
27.	TN8-6-8SV	30.0	1.0	6.0	0.5	4.5	0.53
28.	TN8-8-10SV	30.0	1.0	8.0	0.5	4.5	0.53
29.	TN8-8-10SV-1	30.0	1.0	8.0	0.5	4.5	0.53
30.	TN8-8-10SV-2	30.0	1.0	8.0	0.5	4.5	0.53
31.	TN8-8-10WS	30.0	1.0	8.0	0.625	7.0	0.53
32.	TN8-8-10WS-1	30.0	1.0	8.0	0.625	7.0	0.53
33.	TN8-8-10WS-2	30.0	1.0	8.0	0.625	7.0	0.53
34.	TH6-0-5SV	22.5	0.75	0.0	0.375	4.25	0.31
35.	TH6-2-5SV	22.5	0.75	1.5	0.375	4.25	0.31
36.	TH6-4-5SV	22.5	0.75	3.0	0.375	4.25	0.31
37.	TH6-6-8SV	22.5	0.75	4.5	0.375	4.25	0.31
38.	TH6-8-10SV	22.5	0.75	6.0	0.375	4.25	0.31
39.	TH6-2-5WS	22.5	0.75	1.5	0.375	5.75	0.23
40.	TH6-4-5WS	22.5	0.75	3.0	0.375	5.75	0.23
41.	TH6-8-10WS	22.5	0.75	6.0	0.375	5.75	0.23
42.	T ⁺ H6-4-5WS	30.0	0.75	3.0	0.375	5.75	0.23
43.	T ⁺ H6-8-10WS	30.0	0.75	6.0	0.375	5.75	0.23
44.	TH8-0-5SV	30.0	1.0	0.0	0.5	4.5	0.53
45.	TH8-2-5SV	30.0	1.0	2.0	0.5	4.5	0.53
46.	TH8-4-5SV	30.0	1.0	4.0	0.5	4.5	0.53
47.	TH8-6-8SV	30.0	1.0	6.0	0.5	4.5	0.53

3.2.1 Specimen Development

The goals for the specimen were met by various changes in the shape of the specimen and the location of the transverse reinforcement. The primary means of developing the test member was through the seven preliminary tension specimens, that can be identified by the Pt prefix in its identification name. These specimens specifically studied the isolation of splice behavior and the control of deep beam tensile cracking. This experimental series also evaluated the general test setup, including the data acquisition and loading system.

Initially the splice bars were located in the midplane of the specimen thickness, but to meet the behavior requirements they were moved closer to one face, which was more like a wall or beam specimen. In an attempt to limit the influence of one splice group on another, the splices were physically separated with a 1.5 inch gap in the concrete in several specimens. Due to difficulties in the formwork and transverse reinforcement placement this technique was discontinued in favor of clear bar spacings between the splice groups of at least 5 bar diameters, and greater than the splice bar spacing. Transverse reinforcement was required, in addition to the splice confinement, to control the deep beam tensile cracking in the specimen, as shown in Figure 3.5. Full-width, closed hoops were used in the end blocks of the specimen and straight bars with 180 degree bends were placed along the lap length. The transverse reinforcement along the lap length was anchored in a large cover so that they

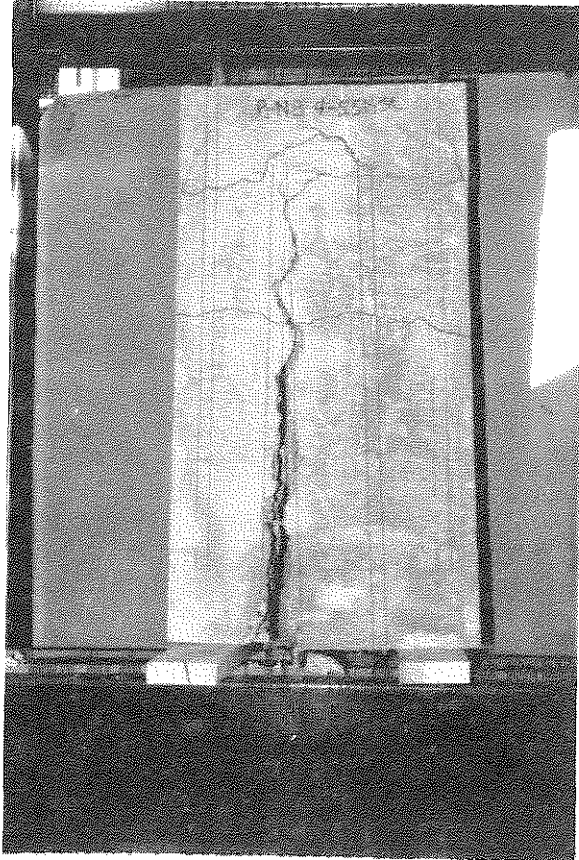


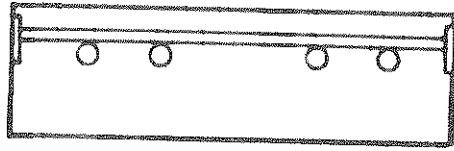
Figure 3.5 Deep beam tensile cracking.

would be fully developed at the edge splice bar. The hooks replaced welded bar end plates for anchorage. The side cover in either case was at least equal to half the splice group spacing. The transverse steel details are depicted in Figure 3.6.

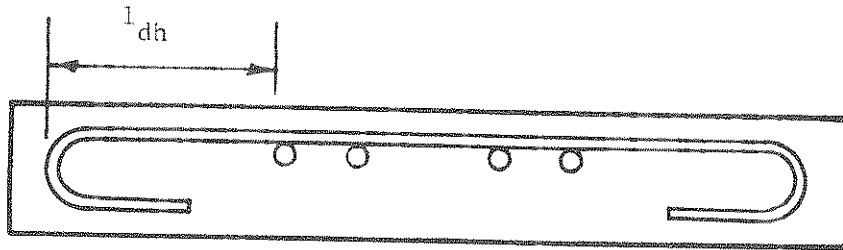
3.2.2 Specimen Evaluation

The behavior of the specimen in its final configuration confirmed its applicability to studying the effect of splice bar spacing in tensile lap splices. During testing and especially at failure, concrete cracking was observed inside and on the surface of the specimen similar to that documented by Chamberlin (1958), Orangun, et al. (1975), Thompson, et al. (1975), Lem, et al. (1983), and others. The concrete covers and splice spacings proved to be sufficient to model an interior splice because the in-plane failure cracking failed to propagate through the entire specimen, from edge to edge. The length added to the ends of the specimen allowed the splice to behave as it was part of a larger structure and provided an area to continue the splice transverse reinforcement.

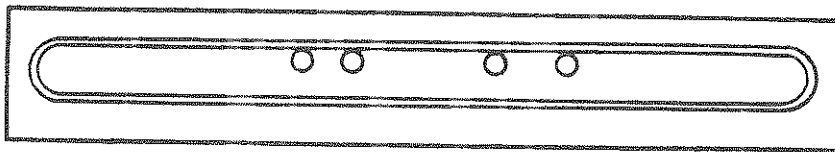
Repeatability of the results also proved the suitability of the specimen. Duplicate specimens sustained a similar number of load cycles before failure, and had similar reinforcement strains, as well as surface and in-plane cracking when compared with the original. Symmetric cracking patterns and propagation in the specimens, and similar splice bar strains, indicated that the two splices within a specimen were acting alike.



a) End plate anchorage



b) ACI Code 180° hook anchorage



c) End block reinforcement

Figure 3.6 Transverse steel details.

Unfortunately, the loading capacities of the flat plate specimens, in terms of ultimate load and number of inelastic load cycles, were less than expected. Several specimens that should have reached yield as predicted by accepted design methods, did not. When compared to contact lap splices in beam and column-type specimens subjected to inelastic flexural cyclic loading, the flat plate specimens generally attained a lower number of repeated direct tensile load cycles before failure.

3.3 Loading System

The test frame was designed to load a flat plate specimen in tension. The frame could accommodate a specimen as large as 5.5 inches thick, 46 inches long, and 46 inches wide. The specimen was vertically oriented to eliminate any dead weight flexural effects and to permit observations of all sides, as shown in Figure 3.7. The frame was a simple reaction frame which anchored one end of the specimen and loaded the other end. The bars were anchored in the test frame and the loading device by nuts on the threaded ends of the bars that were part of the mechanical splicing system.

The loading system consisted of a hand powered pump, Enerpac Model P-80 CL6, and two hydraulic jacks, Enerpac Model RCH 302. The jacks were connected to a common hydraulic line so that each pump exerted an equal force. The magnitude of the load applied bar was measured by a load cell located between the hydraulic



Figure 3.7 Experimental tension test frame and specimen.

jack and the test frame. As shown in Figure 3.8, the test frame and loading system was similar to the set up used by Kluge, et al. (1986).

3.4 Instrumentation

Strain gages were attached directly to the reinforcing steel. The gages were 120 ohm resistance, metal foil, polyimide encapsulated, with integral copper-coated terminals produced by Micro-Measurement Division, Measurement Group Inc. Where possible gages were placed between the bar deformations to reduce the disruption of the concrete-steel interface. The surface preparation included sand-blasting to remove the mill scale, fine filing, and paper sanding. The gages were attached using the Micro-Measurement M-Bond 200 adhesive system. After wiring, the gage was protected by a general purpose coating, M-Coat A, and beeswax. Before testing, each gage was wired in a quarter-bridge circuit. Strain gages were not used in all the specimens, and Table 3.3 indicates which specimens were instrumented.

3.5 Data Acquisition

The data acquisition system, which measured and recorded loads and strains, consisted of the two load cells, strain gages, the HP 3455A digital voltmeter, the HP 3495A scanner, and the HP 9845B desktop computer. A BASIC computer program controlled the collection of voltages from several channels through the scanner/voltmeter combination and converted them to loads and strains,

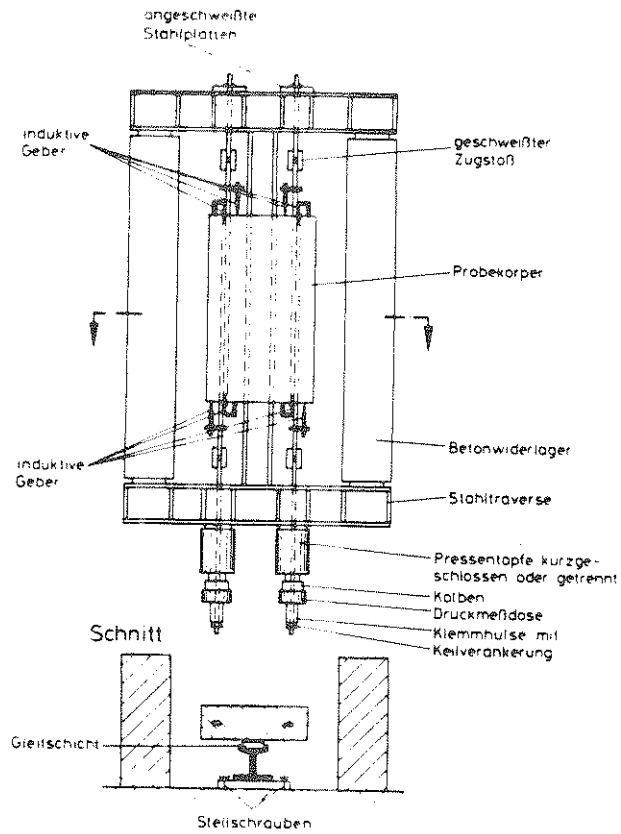


Figure 3.8 Test frame used by Kluge, et al. (1986).

Table 3.3 Tension test specimen instrumentation.

No.	Specimen I.D.	Strain Gages	
		Splice Bar	Transv. Stl.
2.	PtN8-2-3RNo	YES	NO
8.	TL6-0-5Sv	YES	NO
9.	TL6-2-5Sv	YES	NO
10.	TL6-4-5Sv	YES	NO
11.	TL6-4-5Sv-1	YES	NO
28.	TN8-8-10Sv	YES	YES
29.	TN8-8-10Sv-1	YES	YES
30.	TN8-8-10Sv-2	YES	YES
31.	TN8-8-10Ws	YES	YES
32.	TN8-8-10Ws-1	YES	YES
33.	TN8-8-10Ws-2	YES	YES
35.	TH6-2-5Sv	YES	NO
37.	TH6-6-8Sv	YES	NO
38.	TH6-8-10Sv	YES	YES
39.	TH6-2-5Ws	YES	YES
40.	TH6-4-5Ws	YES	YES
41.	TH6-8-10Ws	YES	YES
42.	T ⁺ H6-4-5Ws	YES	YES
43.	T ⁺ H6-8-10Ws	YES	YES
44.	TH8-0-5Sv	YES	NO
46.	TH8-4-5Sv	YES	NO

Note: Specimens not included in the table were not instrumented with strain gages.

which were stored, printed, and plotted. A schematic of the system is given in Figure 3.9.

The loads applied by the hydraulic jacks were measured from two load cells, one on each bar, placed between the hydraulic jack and the test frame as shown in Figure 3.10. The load cell was a machined piece of 1018 seamless steel tubing with a yield strength of 70 ksi. The two end bearing plates were made of A36 steel. Each cell had eight 350 ohm resistance strain gages wired in a full-bridge circuit with 2 gages on each arm of the bridge. The working load capacity of the load cell was 60,000 pounds.

3.6 Materials

The materials selected for the experimental program were typical of those used in today's construction practices. Industry standards and procedures were followed so the results can be applied directly. The material properties of the individual specimens are listed in Table 3.4.

3.6.1 Steel Reinforcement

The transverse reinforcement consisted of #3, #4, and #5 bars, and the longitudinal reinforcement, or splice bars, were #6 and #8 bars. All the steel reinforcement used was Grade 60 and satisfied ASTM A615. The nominal yield strength was 60 ksi, but the actual yield strength varied, as shown in Table 3.5.

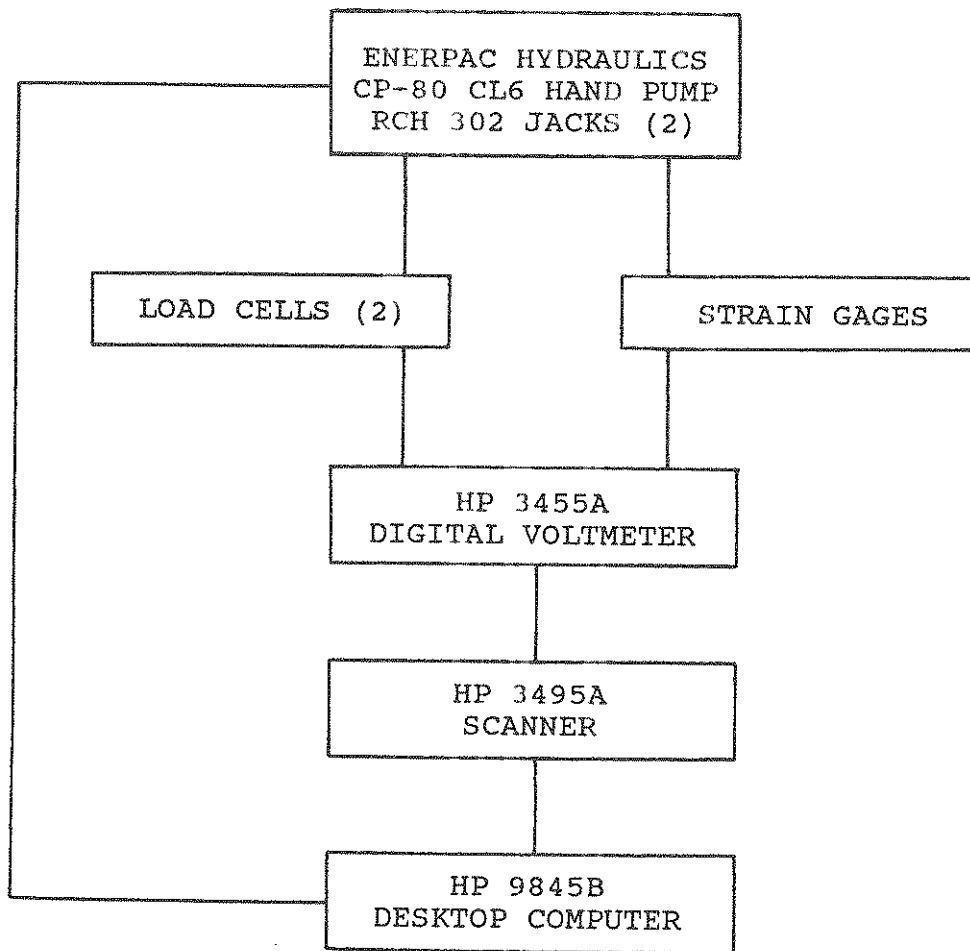


Figure 3.9 Data acquisition and loading system.

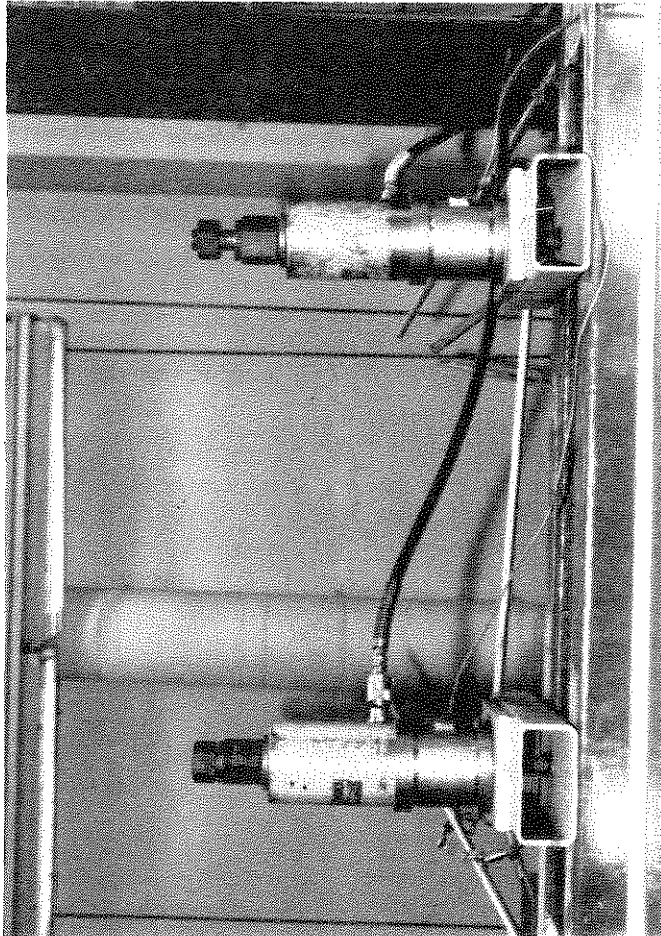
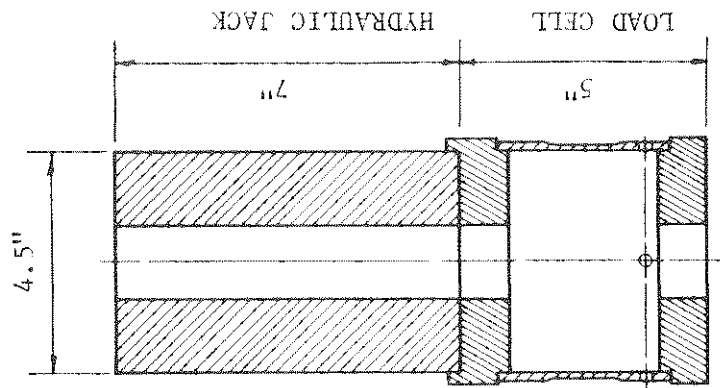


Figure 3.10 Load cell details.

Table 3.4 Tension test specimen material properties.

No.	Specimen I.D.	Concrete Cylinder f'c (psi)	Concrete Core f'c (psi)	Concrete Age at Testing (days)	Spliced Bar fy (ksi)	Splice Transverse Steel fy (ksi)
1.	PtN8-0-3MNO	5470	-	59	69.11	NA
2.	PtN8-2-3RNO	5940	-	61	69.11	NA
3.	PtN8-0-GSt	4110	-	14	69.11	NA
4.	PtN8-0-5.5St	4440	-	15, 27	69.11	NA
5.	PtN8-2-GSt	4110	-	16	69.11	NA
6.	PtN8-4-GSt	4150	-	19	69.11	NA
7.	PtN8-4-5.5St	4440	-	28	69.11	NA
8.	TL6-0-5SV	3060	-	15	66.93	61.8
9.	TL6-2-5SV	3130	-	18	66.93	61.8
10.	TL6-4-5SV	3140	-	20	66.93	61.8
11.	TL6-4-5SV-1	3180	-	22	66.93	61.8
12.	TL8-0-5SV	3170	-	19	69.11	61.8
13.	TL8-2-5SV	3120	-	20	69.11	61.8
14.	TL8-4-5SV	3200	-	22	69.11	61.8
15.	TL8-6-8SV	3460	-	23	69.11	61.8
16.	TL8-4-5OF	3210	-	27	69.11	61.8
17.	TL8-0-5S1	3210	-	17	69.11	NA
18.	TL8-4-5S1	3200	-	28	69.11	NA
19.	TL8-6-8S1	3310	-	29	69.11	NA
20.	TN6-0-5SV	4650	-	22	66.93	61.8
21.	TN6-2-5SV	4650	-	23	66.93	61.8
22.	TN6-4-5SV	4650	-	24	66.93	61.8
23.	TN6-6-8SV	4650	-	25	66.93	61.8
24.	TN8-0-5SV	4310	-	14	69.11	61.8

Table 3.4 (Continued) Tension test specimen material properties.

No.	Specimen I.D.	Concrete Cylinder f' C (psi)	Concrete Core f' C (psi)	Concrete Age at Testing (days)	Spliced Bar f _y (ksi)	Splice Transverse Steel f _{yt} (ksi)
25.	TN8-2-5SV	4360	-	16	69.11	61.8
26.	TN8-4-5SV	4650	-	20	69.11	61.8
27.	TN8-6-8SV	4650	-	21	69.11	61.8
28.	TN8-8-10SV	4870	-	14	69.11	63.0
29.	TN8-8-10SV-1	4870	-	18	69.11	63.0
30.	TN8-8-10SV-2	4870	-	25	69.11	63.0
31.	TN8-8-10WS	4870	-	20	69.11	60.0
32.	TN8-8-10WS-1	4870	-	21	69.11	60.0
33.	TN8-8-10WS-2	4870	-	23	69.11	60.0
34.	TH6-0-5SV	5440	-	25	66.93	61.8
35.	TH6-2-5SV	5450	-	27	66.93	61.8
36.	TH6-4-5SV	5450	-	31	66.93	61.8
37.	TH6-6-8SV	5460	6670	32	66.93	61.8
38.	TH6-8-10SV	5280	-	16	66.93	63.0
39.	TH6-2-5WS	5580	-	23	66.93	63.0
40.	TH6-4-5WS	5940	7040	48	66.93	63.0
41.	TH6-8-10WS	5140	-	14	66.93	63.0
42.	T ⁺ H6-4-5WS	5460	-	21	66.93	63.0
43.	T ⁺ H6-8-10WS	6110	-	60	66.93	63.0
44.	TH8-0-5SV	5470	-	38	69.11	61.8
45.	TH8-2-5SV	5480	-	41	69.11	61.8
46.	TH8-4-5SV	5500	-	47	69.11	61.8
47.	TH8-6-8SV	5510	-	51	69.11	61.8

Table 3.5 Reinforcing steel properties.

Bar Size	Specified Yield * (psi)	Tested Yield (psi)
#8	69,110	69,000
		68,500
		67,100
#6	66,930	63,600
		64,500
		65,000
#5	67,750	60,000
#4	67,500+	61,800
		63,000
#3	73,000+	61,800
		61,400
		63,000

* From steel suppliers records.

On the loaded end of the splice bars a mechanical splicing system described by Lancelot (1986) was incorporated for applying load to the specimen, as shown in Figure 3.11. The threaded splice connection had a larger diameter than the splice bars, so the splice bars in the specimen would yield first.

3.6.2 Concrete

The concrete compressive strength was a major test variable in the investigation and much care was taken with material selection, mix design, casting, curing, and testing. Several concrete mixes were designed, but the same materials were used throughout. The mixes were designed based on ACI Committee 211 procedures for proportioning normal weight concrete (ACI Committee 211, 1985). Crushed limestone aggregate, sand, Type III Portland Cement, water, and at times an admixture were the concrete ingredients. The concrete mix details are summarized in Table 3.6.

Except for two preliminary specimens which made from concrete mixed in the laboratory, mixing was done with a concrete transit mixer. Four to eight specimens incorporating one or two test series were cast at one time to decrease the variability in a particular set of specimens. The mixer arrived with a pre-determined amount of coarse and fine aggregate. Cement was added, followed by enough water to meet the designed 3 to 4 inch slump, which was confirmed before casting.

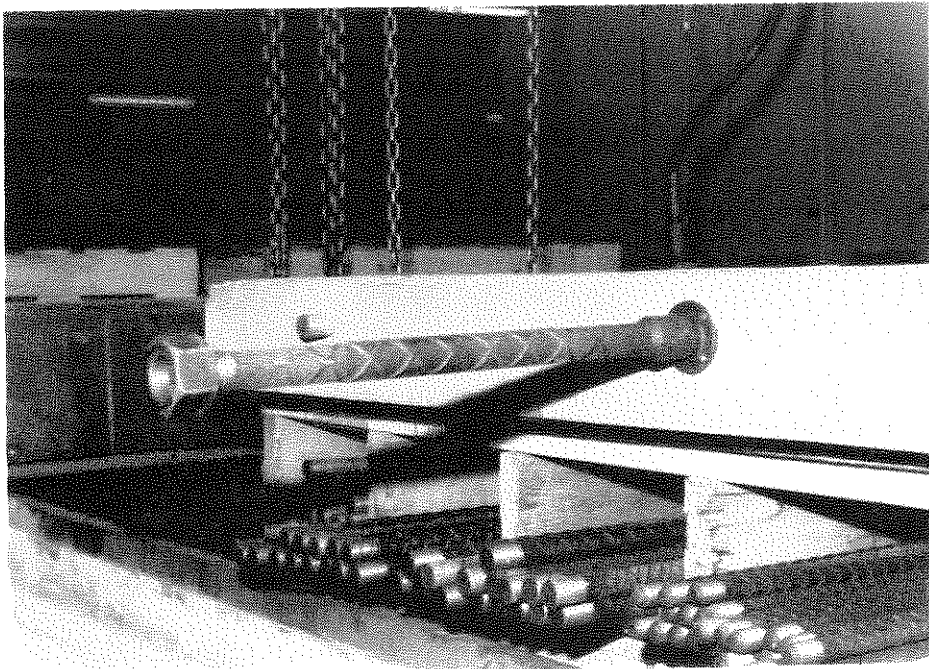


Figure 3.11 Mechanical splicing system used for load application.

Table 3.6 Concrete mix designs.

14 Day Target Strength. Water added until desired slump obtained for mixes 1 and 2.

MIX DESIGN 1: $f'_c = 4000$ psi

Item	Description	Weight (lbs./cu.yd.)
NYDOT #2	Crushed limestone, Max. size 1"	1680
NYDOT #1	Crushed limestone, Max. size 1/2"	300
Sand		1340
Cement	ASTM Type III	658

MIX DESIGN 2: $f'_c = 4000$ psi

Item	Description	Weight (lbs./cu.yd.)
NYDOT #1	Crushed limestone, Max. size 1/2"	1410
Sand		1390
Cement	ASTM Type III	695

Table 3.6 (Continued) Concrete mix designs.

MIX DESIGN 3: $f'_c = 7000$ psi

Item	Description	Weight (lbs./cu.yd.)
NYDOT #2	Crushed limestone, Max. size 1"	1180
NYDOT #1	Crushed limestone, Max. size 1/2"	510
Sand		1220
Cement	ASTM Type III	830
Water		290
Eucon 37	Plasticizer	4230 ml

Specimens were cast horizontally in wood forms, consolidated using internal vibrators, screeded, and finished with a steel trowel. The slabs were wet cured, using burlap and plastic for 7 days in the forms. After wet curing, the formwork was stripped and the specimens were air cured until testing. Testing started no sooner than 14 days after casting. With the Type III cement the strength gain had slowed so that after 14 days the concrete strength was essentially constant.

The concrete compressive strength was determined on the day of testing from 6x12 cylinders following ASTM and ACI procedures. The in-place compressive strength was later confirmed in two specimens with two inch diameter core samples, which proved to be approximately 1000 psi higher than the cylinder strength. The higher strengths were probably due to the small size of the core samples and the thorough consolidation of the concrete in the specimens when it was cast.

Some of the concrete did not meet the specified minimum design strengths due to poor quality cement. For example, specimens with concrete strengths less than 3500 psi were designed for a minimum concrete compressive strength of 4000 psi. The specimens with the lower than expected concrete strengths did not perform as well as anticipated.

3.7 Testing Procedure

After the specimen was placed in the test frame and the equipment set up and checked, the loading of the specimen began.

The loading history was constant for all specimens. The specimens were loaded in tension to the specified yield strength of the splice bar steel. Loading was limited to yield because the load was directly applied to the splice bars extending outside of the concrete slab. If the specimen survived its first cycle up to yield it was unloaded and the process was repeated. During loading and unloading, loads and strains were recorded at predetermined load levels. During testing cracking was marked on the specimen and recorded by sketching, photographs, and audio tape; this continued until failure or termination of testing. Testing was stopped after 35 load cycles with several specimens because of their excellent durability.

To determine the extent of cracking throughout the specimen and when it occurred, nondestructive pulse-velocity measurements were taken before, during, and after testing. The pulse-velocity device measured the time required for a sound wave to pass through the thickness of the specimens. The difference in readings between a cracked section and an uncracked section was a factor of 2 to 20. The mode of failure was easily determined from this process.

Failure was defined as the sudden loss of load carrying capacity to approximately 20 percent or less of the yield load. After failure, the extent of interior cracking was determined with pulse-velocity measurements. For isolated checks for cracking, core holes were drilled and full thickness slices were made in the specimen.

SECTION 4

DISCUSSION OF EXPERIMENTAL RESULTS

4.1 Introduction

The effects of splice bar spacing on particular, but key performance indicators and behavior characteristics will be discussed in detail in this chapter, as well as the effects of the other test parameters. Some of the key performance indicators of the specimens are summarized in Table 4.1 and include the number of load cycles sustained, the failure load, and the failure cracking mode. The specimen identification, explained in Figure 4.1, summarizes the physical and material properties for a particular specimen. Figures 4.2 and 4.3 show that a full range of the test parameters were incorporated in the specimens.

4.2 Monotonically Loaded Specimens

Researchers and code provisions are in agreement that the ultimate load for monotonically loaded splices is independent of the spacing up to a certain point. The results of this study also support this conclusion. The maximum splice bar spacing of the single load cycle tests series was at the current limits of spacing of 6 inches and one-fifth of the required lap length. Depicted in Figure 4.4 are three test series in which the specimens did not reach the actual yield strength of the splice steel. Each line represents a test series where the only difference in the specimens was the splice bar spacing. The

Table 4.1 Tension test specimen behavior summary.

No.	Specimen I.D. *	Load Cycle at Failure	Failure Load/Bar (K)	P_u/P_{60}	P_u/P_{60}	Failure Cracking
1.	PtN8-0-3MNO	1	46	0.84	0.97	Total Cover Loss
2.	PtN8-2-3RNO	10, 8 @ 21k	32.5	0.60	0.69	Deep Beam Flexure
3.	PtN8-0-GSt	1	35.3	0.65	0.74	Total Cover Loss
4.	PtN8-0-5.5St	2, 1 @ 25k	40	0.73	0.84	Total Cover Loss
5.	PtN8-2-GSt	1	32.6	0.60	0.69	Deep Beam Flexure
6.	PtN8-4-GSt	1	25.9	0.47	0.55	Deep Beam Flexure
7.	PtN8-4-5.5St	1	28	0.51	0.59	Deep Beam Flexure
8.	TL6-0-5SV	2, 1 @ 26k	27.9	0.95	1.06	Total In-plane
9.	TL6-2-5SV	1	28.5	0.97	1.08	Total In-plane
10.	TL6-4-5SV	1	28.8	0.98	1.09	Total In-plane
11.	TL6-4-5SV-1	2	29.3	0.99	1.11	Isolated In-plane
12.	TL8-0-5SV	1	43.0	0.79	0.91	Total In-plane
13.	TL8-2-5SV	1	42.2	0.77	0.91	-
14.	TL8-4-5SV	1	47.0	0.86	0.99	-
15.	TL8-6-8SV	1	44.1	0.81	0.93	-
16.	TL8-4-5Of	1	32.0	0.59	0.68	Deep Beam Flexure
17.	TL8-0-5S1	1	32.3	0.59	0.68	Deep Beam Flexure
18.	TL8-4-5S1	1	30.1	0.55	0.64	Deep Beam Flexure
19.	TL8-6-8S1	1	30.1	0.55	0.64	Deep Beam Flexure
20.	TN6-0-5SV	8	28.2	0.96	1.07	-
21.	TN6-2-5SV	16	30.6	1.04	1.16	-
22.	TN6-4-5SV	12	29.9	1.02	1.13	-
23.	TN6-6-8SV	12	29.3	0.99	1.11	-
24.	TN8-0-5SV	5	51.2	0.94	1.08	-

* See Figure 4.1 for I.D. code.

- Failure mode not classifiable.

Table 4.1 (Continued) Tension test specimen behavior summary.

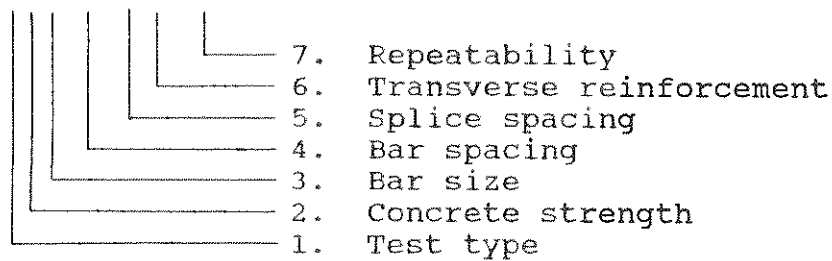
No.	Specimen I.D. *	Load Cycle at Failure	Failure Load/Bar (K)	P _u /P _{sy}	P _u /P ₆₀	Failure Cracking
25.	TN8-2-5SV	8	53.1	0.97	1.12	-
26.	TN8-4-5SV	12	55.6	1.02	1.17	-
27.	TN8-6-8SV	9	51.2	0.94	1.08	-
28.	TN8-8-10SV	6	53.9	0.99	1.14	Isolated In-plane
29.	TN8-8-10SV-1	4	47.7	0.87	1.01	Total In-plane
30.	TN8-8-10SV-2	4	53.0	0.97	1.12	Total In-plane
31.	TN8-8-10WS	1	53.5	0.98	1.13	Total In-plane
32.	TN8-8-10WS-1	1	51.3	0.94	1.08	Isolated In-plane
33.	TN8-8-10WS-2	1	52.5	0.96	1.11	Isolated In-plane
34.	TH6-0-5SV	5	31.2	1.06	1.18	-
35.	TH6-2-5SV	11	31.2	1.06	1.18	-
36.	TH6-4-5SV	4	31.5	1.07	1.19	Total In-plane
37.	TH6-6-8SV	29	31.8	1.08	1.20	Isolated In-plane
38.	TH6-8-10SV	35+	NA	NA	NA	NA
39.	TH6-2-5WS	23	30.1	1.02	1.14	Total In-plane
40.	TH6-4-5WS	35+	NA	NA	NA	NA
41.	TH6-8-10WS	10	30.1	1.02	1.14	Isolated In-plane
42.	T ⁺ H6-4-5WS	35+	NA	NA	NA	NA
43.	T ⁺ H6-8-10WS	35+	NA	NA	NA	NA
44.	TH8-0-5SV	6	55.4	1.02	1.17	Total In-plane
45.	TH8-2-5SV	14	54.1	0.99	1.14	Total In-plane
46.	TH8-4-5SV	25	49.5	0.91	1.04	Total In-plane
47.	TH8-6-8SV	42	55.1	1.01	1.16	Isolated In-plane

* See Figure 4.1 for I.D. code.

+ Testing was stopped at 35 cycles with no sign of failure.

- Failure mode not classifiable.

XX0-0-0Xx-0



1. Test type:
 - T - Tension with splice length = $30d_b$
 - T⁺ - Tension with splice length = $40d_b$
 - Pt - Preliminary tension
2. Concrete strength:
 - L - Low (3000 - 3500 psi)
 - N - Normal (4000 - 5000 psi)
 - H - High (5000 psi and higher)
3. Bar size:
 - 6 - #6
 - 8 - #8
4. Splice bar spacing:
 - Clear distance in bar diameters
5. Splice group spacing:
 - Clear distance in bar diameters
 - G for gap
6. Transverse steel:
 - No - No steel
 - St - End hoop stirrups only, enclosing longitudinal bars
 - S1 - End hoop stirrups only, full width
 - Or - Orangun requirements
 - Sv - Sivakumar requirements
 - Ws - Wider spacing (wider than Sivakumar)
7. Repeatability:
 - Only if a particular specimen is duplicated in physical and material properties.

Figure 4.1 Specimen identification.

SPECIMEN TYPE:

Preliminary tension = 7
Tension = 40

*SPLICE BAR SPACING:

Contact = 7
2d_b = 7
4d_b = 11
6d_b = 6
8d_b = 9

*CONCRETE COMPRESSIVE STRENGTH (psi):

3000 - 3500, Low = 12
4000 - 5000, Normal = 14
5000 and higher, High = 14

*SPLICE BAR SIZE:

#6 = 18
#8 = 22

*SPLICE LAP LENGTH:

30d_b = 38
40d_b = 2

*TRANSVERSE REINFORCEMENT:

Sivakumar requirements = 30
Does not meet Sivakumar = 7
No steel along splice = 3

*LOADING:

One cycle = 13
Repeated = 27

*REPEATABILITY:

Originals = 35
Duplicates = 5

* - Does not include preliminary tension specimens

Figure 4.2 Experimental parameter distribution.

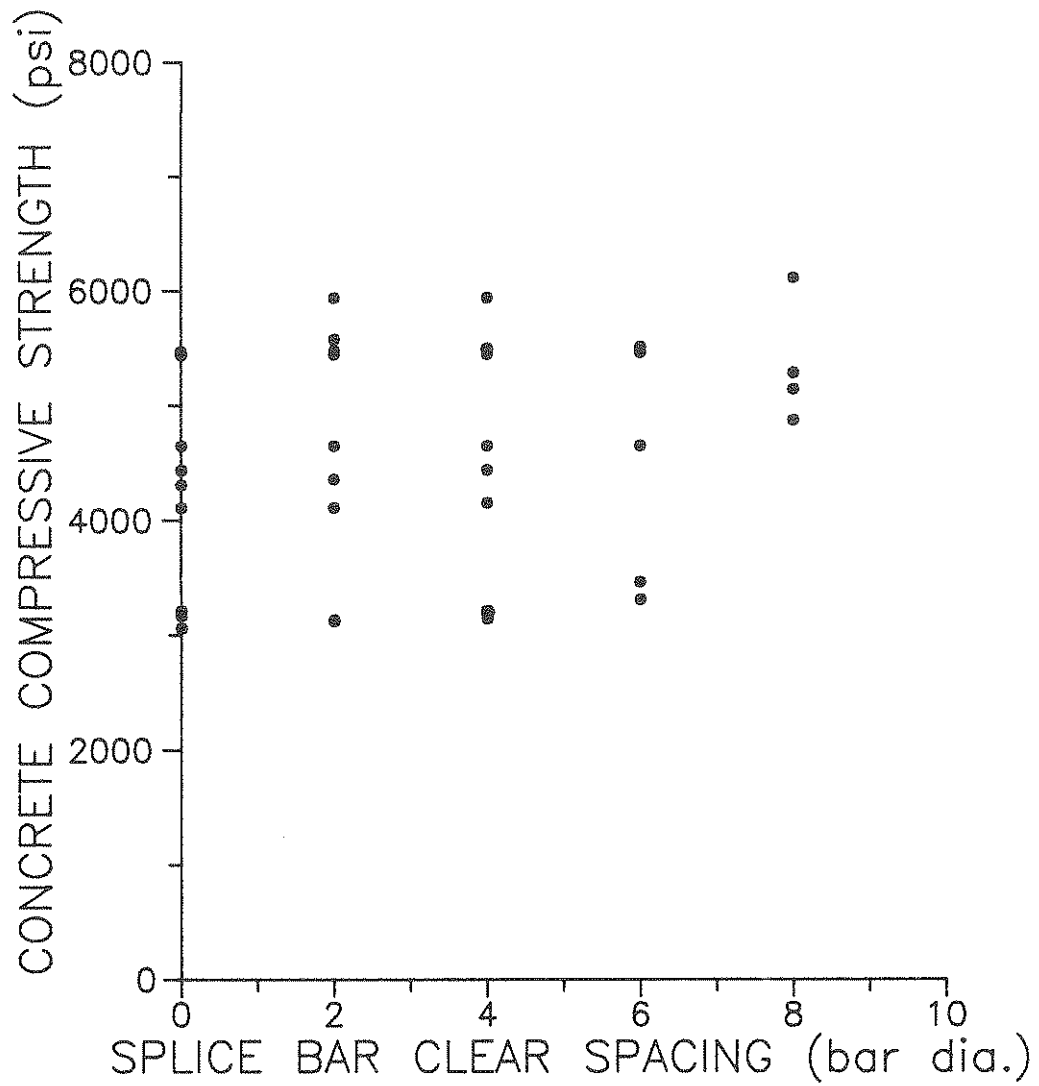


Figure 4.3 Experimental parameter distribution, concrete compressive strength versus splice bar spacing.

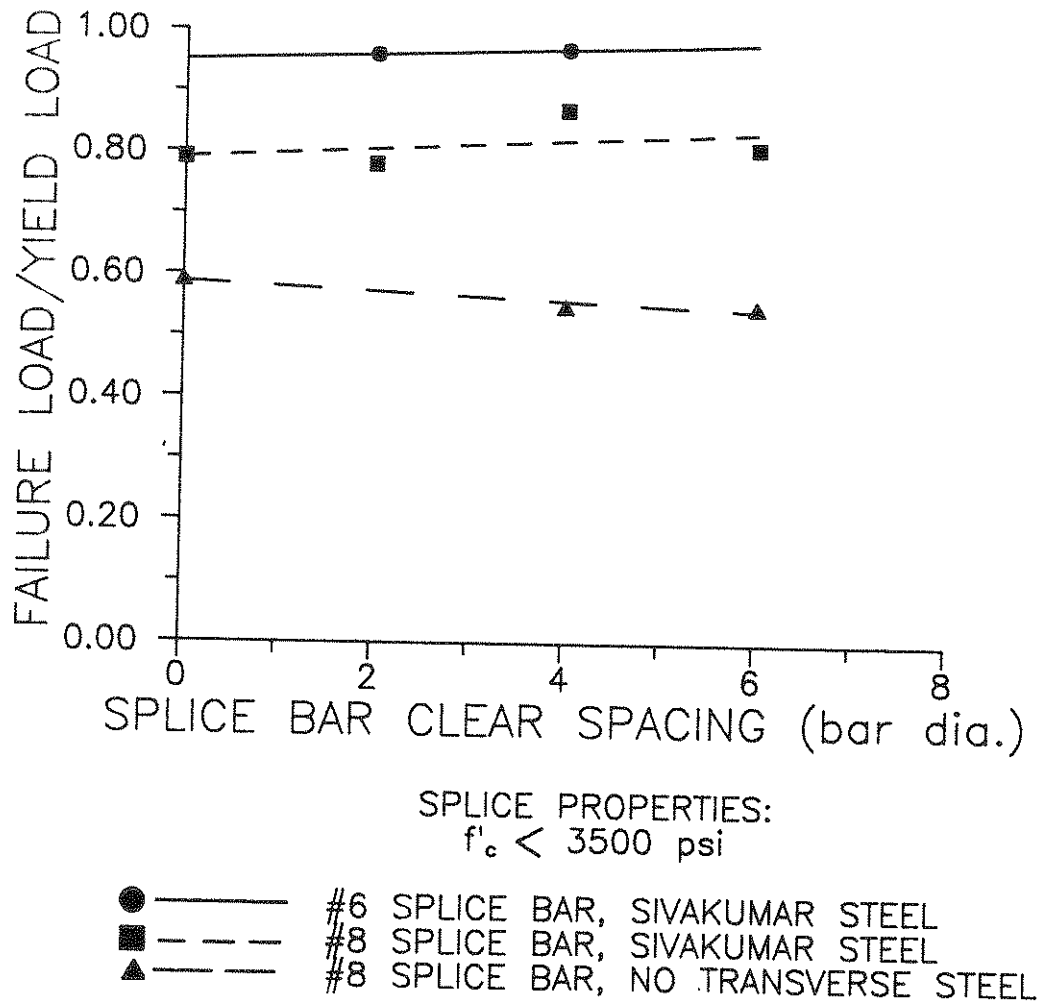


Figure 4.4 Ultimate load performance of the monotonically loaded specimens.

ultimate load reached by these specimens was independent of the spacing of the splice bars.

The monotonically loaded specimens were not designed to fail during the first load cycle. One reason for many of the specimens not surviving more than one or two load cycles was that the splice was designed for a minimum concrete compressive strength of 4000 psi but the resulting concrete strength was less than 3500 psi because of poor quality cement. All the specimens listed in Figure 4.4 shared this condition.

The reason for the at least 20 percent difference in the ultimate strengths between the test series depicted in Figure 4.4 was the amount of transverse reinforcement. The specimens that only reached approximately six-tenths of the specified yield load, which have an S1 suffix, had no transverse reinforcement along the splice length. Without the transverse reinforcement the specimen failed by deep beam tensile cracking. The other specimens had transverse reinforcement that satisfied the seismic design provisions for lap splices proposed by Sivakumar, et al. (1983) and failed by in-plane cracking. The addition of the transverse reinforcement increased the ultimate strength of the splices.

4.3 Repeatedly Loaded Specimens

4.3.1 Number of Inelastic Load Cycles Sustained

Because each specimen was loaded the same way, load history was not a variable and the number of cycles can be used as a

performance indicator. In general, the number of inelastic load cycles was dependent on the amount of confinement to the tensile lap splice provided by the surrounding concrete and transverse reinforcement. Specifically, it was dependent on the spacing of the splice bars, the strength of the surrounding concrete, and the distribution of the transverse reinforcement.

4.3.1.1 Splice Bar Spacing

Changing the spacing between the two splice bars of the splice had a significant effect on the number of inelastic load cycles a specimen sustained. As shown in Figure 4.5, the cyclic performance improved to a certain spacing of the splice bars, which was dependent on the concrete compressive strength. The reason for the improved performance with spacing was probably due to the increased confinement provided by the additional concrete surrounding the bars of the splice. The additional concrete can resist that much more bursting forces from the deformed bars of the splice. A schematic representation of the bursting forces from a splice and an anchored bar are shown in Figure 2.2.

4.3.1.2 Concrete Strength

The compressive strength of the concrete surrounding the noncontact lap splice is critical in the transfer of load from one bar to the other. Also critical is the resistance of the bursting forces caused by a stressed deformed bar resulting in the concrete surrounding the splice to be stressed in tension. Although concrete strength is traditionally measured in terms of

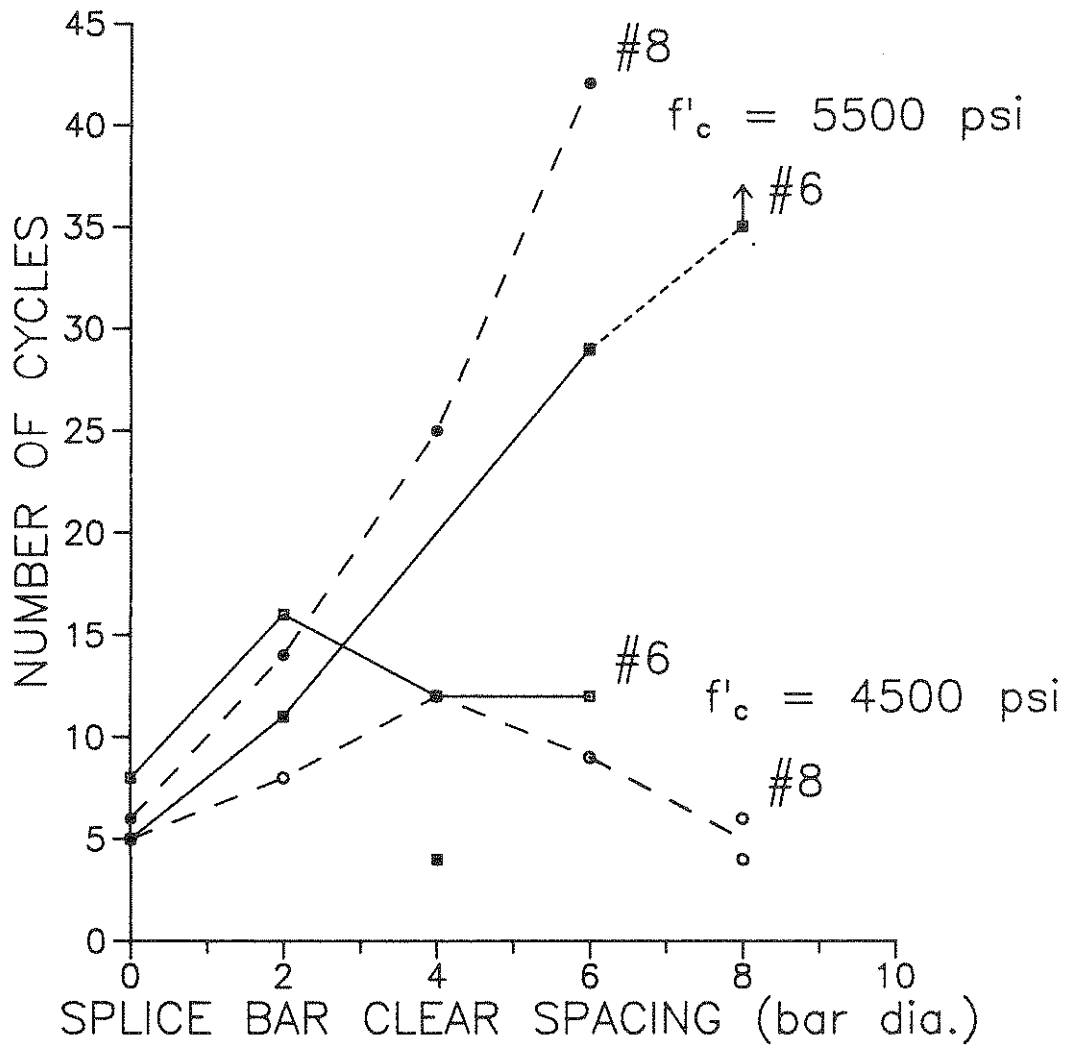


Figure 4.5 Load cycle performance versus splice bar spacing, considering bar size and concrete strength.

compression, the tensile strength is also a critical parameter in the behavior of anchorages and splices. The tensile strength of the concrete was not measured, but a correlation between the two was assumed.

The effect of concrete strength becomes more important on the cyclic performance as the spacing increases, as shown by the test data in Figure 4.5. For example, the number of cycles for a splice of #8 bars spaced at a clear distance of 6 inches increased from 9 yield load cycles to 42 when the concrete compressive strength increased 4650 to 5510 psi. With a greater concrete strength, greater bursting forces can be resisted, resulting in less damage each load cycle. The splice can then resist more cycles. The concrete between the splice bars can also resist a greater compressive loading in the load transfer.

Several of the specimens with the higher concrete strengths sustained less load cycles than expected. The specimens included those with splice bar spacings up to 4 bar diameter spacings that were reinforced meeting the Sivakumar, et al. (1983) requirements. Specimen TH6-2-5Sv failed during the eleventh load cycle and specimen TH6-4-5Sv failed only on the fourth load cycle. Specimen TH6-2-5Ws failed on the twenty-third cycle and specimen TH6-4-5Ws did not fail after 35 load cycles. The Ws specimens had a concrete strength higher than the Sv specimens by several hundred psi, but had less transverse reinforcement. The four contact splice specimens sustained between 5, 5, 6, and 8

cycles even though two of the specimens had a greater concrete strength by about 1000 psi.

The poorer performance is probably due to the concrete quality. Once again, low quality cement was used in some of the higher strength specimens. The target compressive strength was 7000 psi, but a strength of approximately 5500 psi was obtained. The low quality cement may have had an even greater impact on the tensile strength.

4.3.1.3 Transverse Reinforcement

The area and distribution of the transverse reinforcement played a significant role in the number of cycles sustained by a splice, as summarized by Table 4.2. In general, splices reinforced with wider spaced, but still uniformly distributed, transverse steel sustained less load cycles. This occurred even when the same area of reinforcement was provided along the splice length. The spacing, or distribution, of transverse reinforcement is at least as, or more important, than the area of reinforcement provided for cyclic loading performance, and could probably be applied to splices of all spacings. This is in agreement with the conclusion reached in Cornell seismic splice research (Lukose, et al. 1982).

Table 4.2 Effects of transverse reinforcement distribution.

Only specimens from the same concrete cast will be compared to diminish the effects of the concrete. Test series are grouped together.

Specimen I.D.	Load Cycle at Failure	Transverse Steel Along Splice		
		Dia. (in.)	Spacing (in.)	Area (in. ² /ft.)
TN8-8-10Sv	6	0.5	4.5	0.53
TN8-8-10Sv-1	4	0.5	4.5	0.53
TN8-8-10Sv-2	4	0.5	4.5	0.53
TN8-8-10Ws	1	0.625	7.0	0.53
TN8-8-10Ws-1	1	0.625	7.0	0.53
TN8-8-10Ws-2	1	0.625	7.0	0.53
TH6-8-10Sv	35+	0.375	4.25	0.31
TH6-8-10Ws	10	0.375	5.75	0.23

4.3.1.4 Splice Length

The effect of splice length on the behavior of noncontact lap splices was not studied extensively. Only two specimens out of the 47 total had a lap length that differed from 30 bar diameters. These specimens had a longer (40 bar diameter) lap length, which was taken into account when the transverse reinforcement was designed. The longer lap splice specimens were compared with specimens reinforced with the same transverse steel size and spacing, and a 30 bar diameter lap length.

The longer splice made a considerable difference at the wide splice bar spacing of 8 bar diameters. Increasing the lap length increased the number of cycles sustained by the splice by at least 25 inelastic load cycles. Specimen TH6-8-10Ws failed on the tenth cycle, while T+H6-8-10Ws had survived 35 cycles when the testing was stopped. The other specimens, TH6-4-5Ws and T+H6-4-5Ws, did not provide much information because they each sustained 35 inelastic load cycles before the testing was terminated. Nonetheless, increased lap lengths would increase the number of cyclic loads regardless the splice bar spacing if the transverse reinforcement size and spacing remained the same.

4.3.1.5 Bar Size

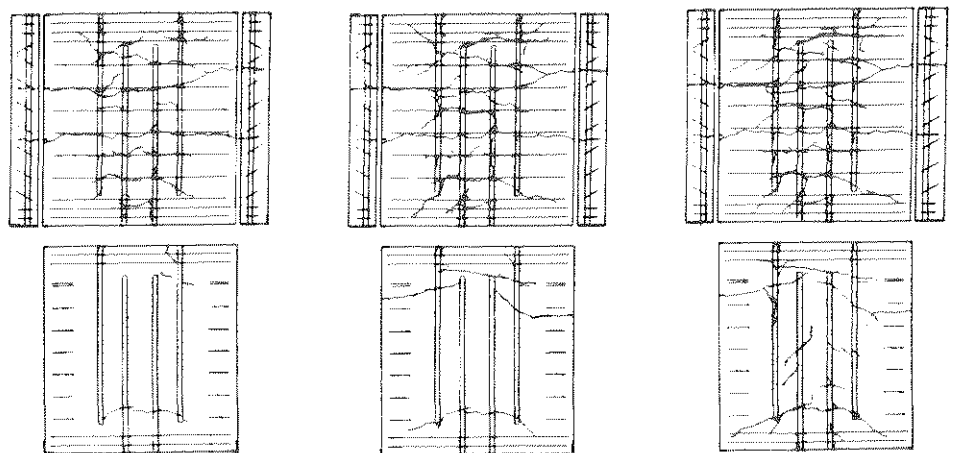
The effect of bar size, another test parameter, on the cyclic performance is difficult to determine for several reasons. The splices, including the transverse reinforcement, were designed using the Sivakumar seismic splice design equations which

take into account the spliced reinforcement size in the determination of the lap length and the spacing of the transverse reinforcement. The specimens plotted in Figure 4.5 each had a lap length of 30 bar diameters, but the transverse steel size and spacing differed depending whether #6 or #8 bars were used. The spliced #6 bars were reinforced with #3 bars spaced at 4.25 inches, while the spliced #8 bars were reinforced with #4 bars spaced at 4.5 inches.

The number of load cycles sustained by a specimen was not clearly dependent on the bar size. In the series with a concrete compressive strength of 4500 psi, the #6 bar specimens sustained at least as many load cycles as the #8 bar specimens regardless the splice bar spacing. But at a concrete strength of approximately 5500 psi, the #8 bar specimens consistently sustained more cycles than the #6 bar specimens at all spacings. The similar cyclic behavior of specimens with different bar sizes demonstrates the general applicability of the Sivakumar equations.

4.3.2 Development of Cracking

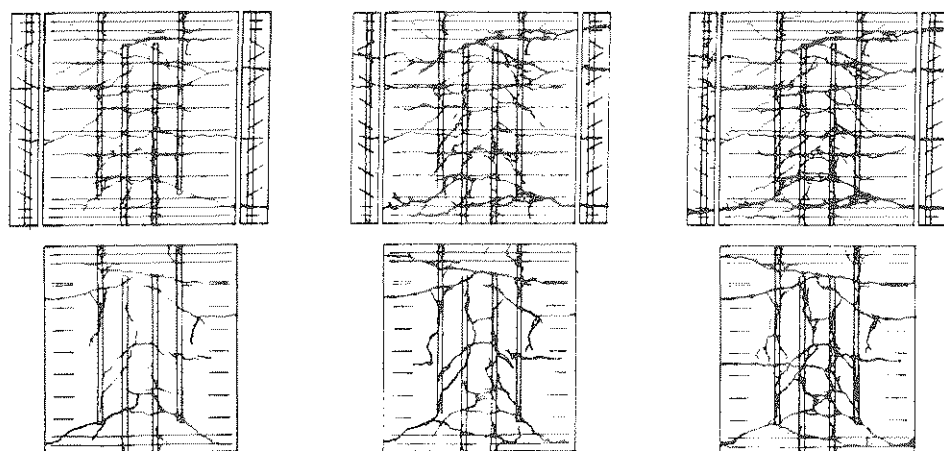
The effect of splice bar spacing was easily noticed in the surface cracking the specimen concrete. The surface cracking was affected by the location of the splice bars and the transverse reinforcement. Figure 4.6 depicts the cracking progression to failure for specimen TH8-4-5Sv, which was representative of all specimens. The first cracks to form during the loading were the along the transverse reinforcement, which was acting as a crack initiator. The transverse cracks were followed by the formation



32 k = 0.59 P_{sy}

40 k = 0.74 P_{sy}

48 k = 0.88 P_{sy}



YIELD - CYCLE 1

YIELD - CYCLE 9

FAILURE - CYCLE 25

Figure 4.6 Concrete cracking progression of specimen TH8-4-5Sv.

of longitudinal cracks along the splice bars. Diagonal cracking, generally located between the splice bars, then formed, including the splice end crack which was diagonal between the splice bars and generally formed through the entire section.

Much of the surface cracking developed during the first load cycle and just prior to failure. After the first cycle, the amount of additional cracking that occurred during a load cycle decreased with each cycle until the onset of failure. At the end of some load cycles no additional cracking was detected. At failure there was a significant increase in surface cracking, as well as a loss in cover, generally at the splice ends. Greater surface cracking and deformation was observed for specimens with wider spaced transverse reinforcement at failure. The surface cracking growth as the number of load cycles increased is documented in Figure 4.6.

The diagonal surface cracking of the concrete between the splice bars became more prominent as the splice bar spacing increased. Even the large crack that formed at the end of the splice was diagonal. Figure 4.7 shows the surface cracking pattern at failure for increasing splice bar spacing. This is not the first evidence of diagonal cracking in tension splices, as discussed in Chapter 2.

4.3.3 Development of Strains

As mentioned earlier 21 of the 47 specimens were instrumented to record reinforcement strains. Many of the instrumented

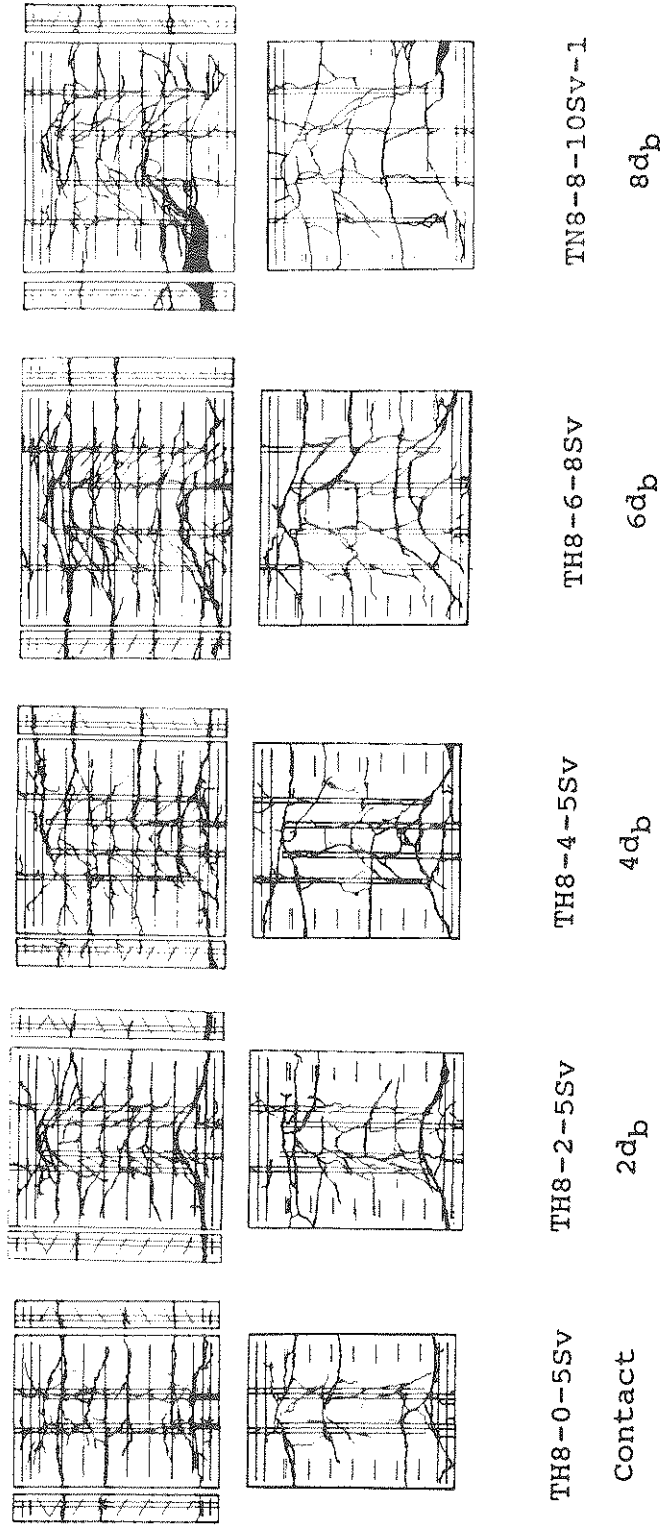


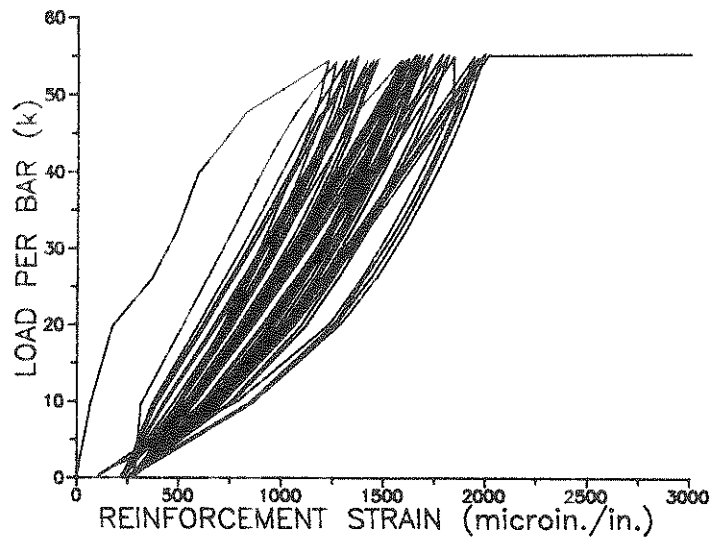
Figure 4.7 Surface concrete cracking patterns at failure for different splice bar spacings.

specimens had a limited number of gages that were used to confirm the yielding of the reinforcement. The data from the remaining gaged specimens was used to understand the splice bar and transverse reinforcement behavior of noncontact lap splice.

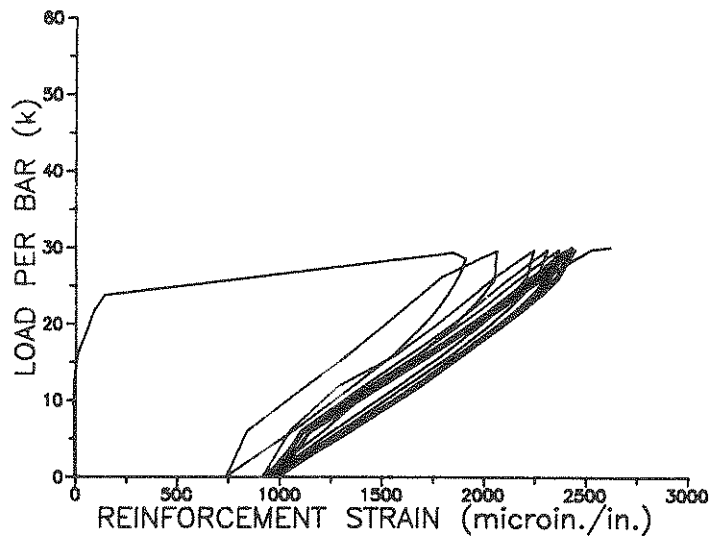
Regardless of the splice bar spacing, the specimens had some common strain behavior. During the first cycle of loading the gages recorded a significant loss of stiffness and an increase in residual strain. The load-strain curves were nearly linear in the following load cycles, except for an occasional, significant change in stiffness that was caused by major cracking and load redistribution, with a slight increase in residual strain and maximum strain with each cycle. Some typical load-strain curves are shown in Figure 4.8.

4.3.3.1 Splice Bar Strains

The splice bar strain distributions were studied with a number of specimens with various splice bar spacings. The comparison was performed with readings from the first and last cycles. It was obvious in the data, some of which is presented in Figure 4.9, that a redistribution occurred with each load cycle which included an increasing yield penetration along the splice length. The yielding, according to Fagundo, et al. (1979), helps distribute the bursting force. The fact that the specimen survived inelastic load cycles demonstrated the ability to redistribute stresses and strains associated with inelastic repeated loading.

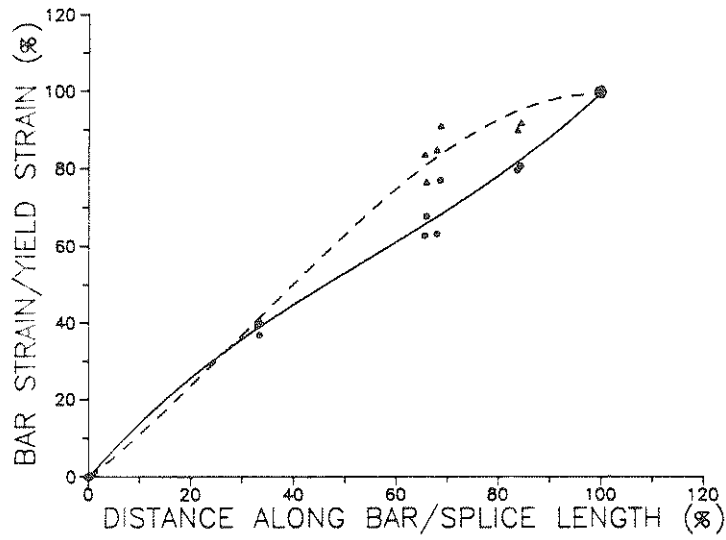


d) SPECIMEN TH8-4-5Sv, SPLICE BAR STRAINS



b) SPECIMEN TH6-8-10Ws, TRANSVERSE STEEL STRAINS

Figure 4.8 Load versus splice bar strains.



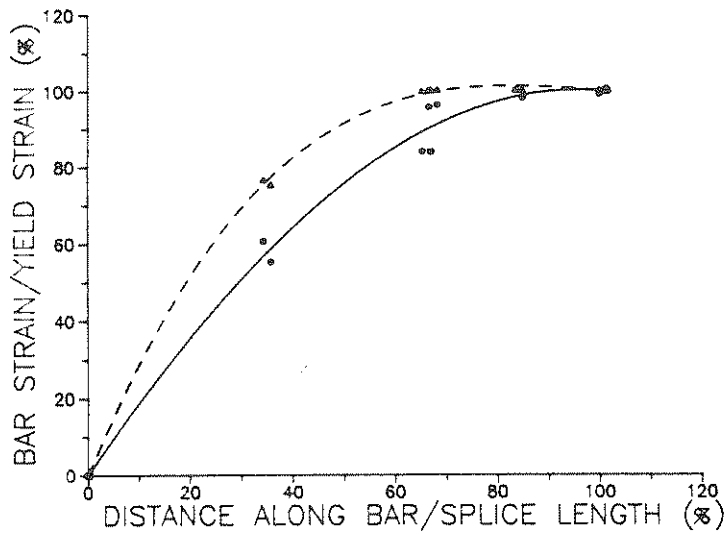
a) SPECIMEN TH8-0-5Sv



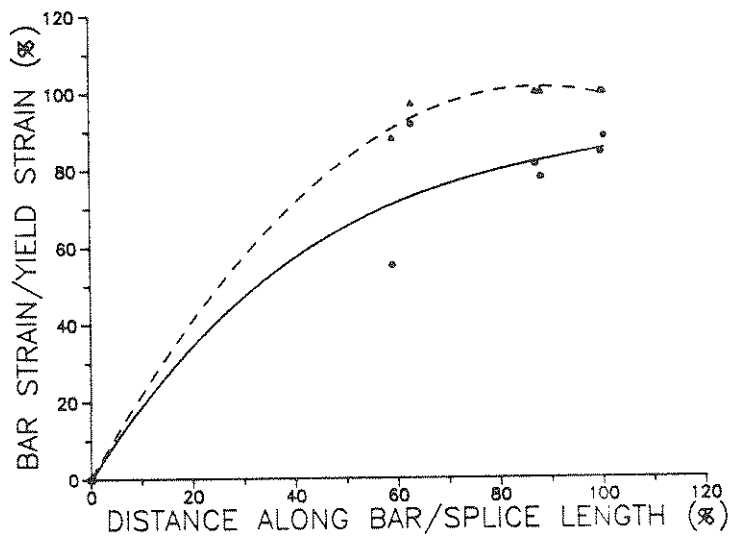
b) SPECIMEN TH6-2-5Sv

● — LOAD CYCLE 1
 ▲ - - - FAILURE LOAD CYCLE

Figure 4.9 Splice bar strain redistribution.



c) SPECIMEN TH6-6-8Sv



d) SPECIMEN TH6-8-10Sv

● — LOAD CYCLE 1
 ▲ - - - FAILURE LOAD CYCLE

Figure 4.9 (Continued) Splice bar strain redistribution.

The splice bar strain data also confirmed that greater yield penetration occurred with increasingly wider splice bar spacings. The yield penetration to at least to a distance equal to the spacing of the splice bars and beyond was confirmed in all the specimens with gages at all spacings. The direct effect on the splice bar strain distributions can be shown in Figure 4.10. In the figure any strains recorded at or above yield were plotted at the yield strain value. The redistribution is greatest for the largest spacing of the splice bars. From the limited amount of information it was not apparent that the splice bar size, the splice length, the amount and distribution of the transverse reinforcement, and the concrete strength had any effect on the splice bar strain distribution.

4.3.3.2 Transverse Reinforcement Strains

A limited study was performed on the strains of the transverse steel that investigated the effect of spacing of the splice bars and the associated effects of splice length and different distributions of transverse reinforcement. Out of 12 specimens with instrumented transverse reinforcement, only 6 had sufficient gages for a proper comparison.

As shown in Figures 4.11 through 4.15, the strains in the transverse reinforcement were dependent on spacing of the splice bars, splice length, and the reinforcement distribution. In two instrumented series, specimens with increased splice bar spacings had greater or equal transverse reinforcement strains

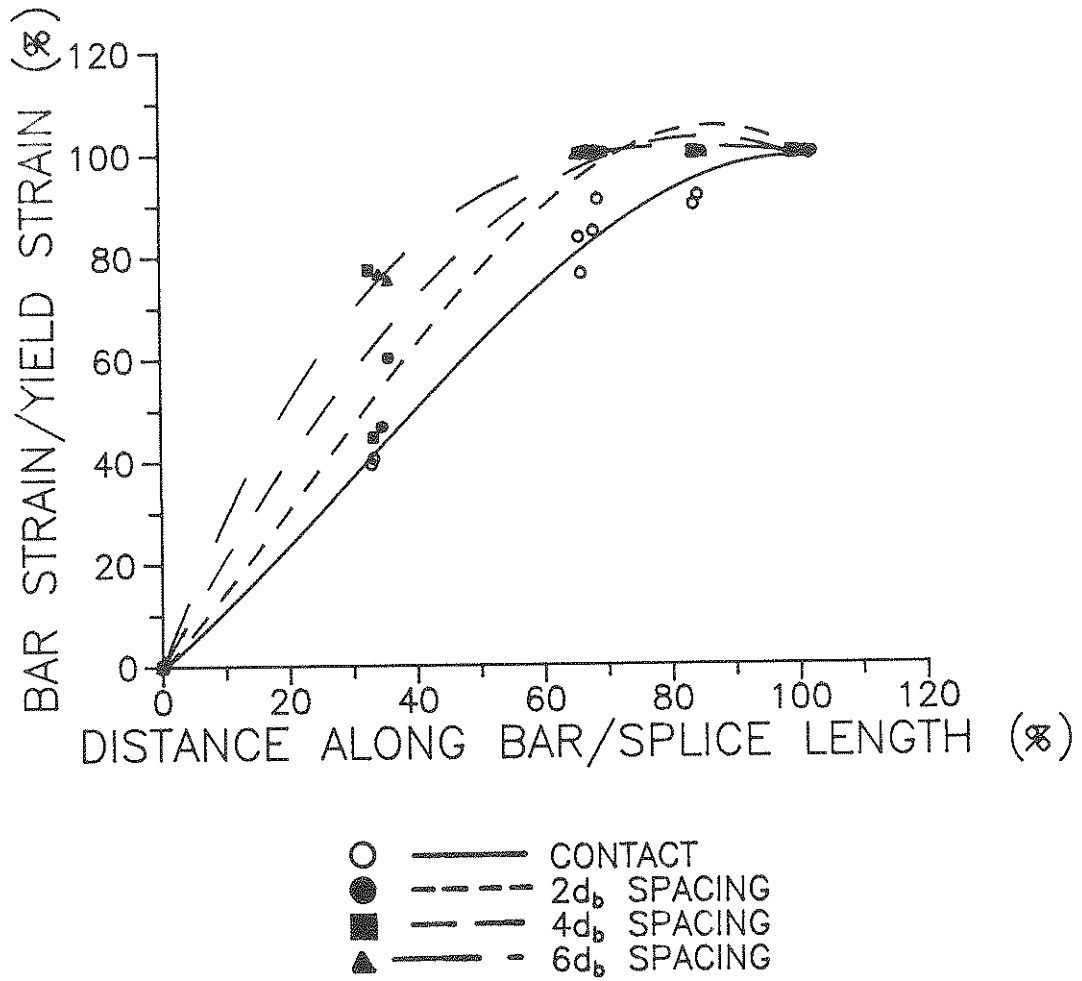
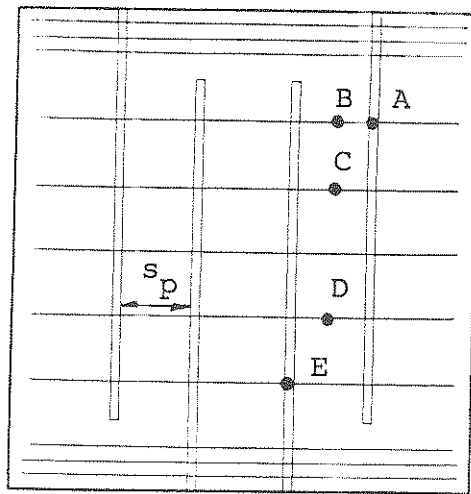


Figure 4.10 Splice bar strain distribution and the effect of splice bar spacing.



Specimen: T⁺H6-4-5Ws
 Splice bar spacing, s_p : $4d_b$

Gage	Strains (microin./in.)		
	Cycle 1	Cycle 20	Cycle 35
A*			
B*			
C	1311	1888	1496
D	320	657	806
E	893	1263	1272

Specimen: T⁺H6-8-10Ws
 Splice bar spacing, s_p : $8d_b$

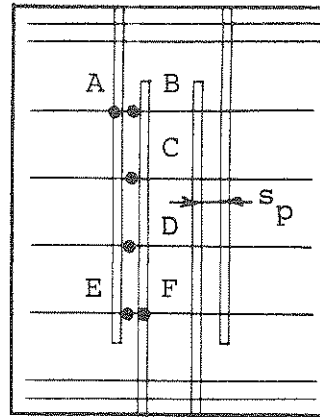
Gage	Strains (microin./in.)		
	Cycle 1	Cycle 20	Cycle 35
A	681	-	-
B	915	1227	-
C	422	2572	2699
D	87	1042	1121
E	677	2070	2189

* No gage.
 - Broken gage.

Figure 4.11 Transverse reinforcement strains and splice bar spacing, $40d_b$ splices.

Specimen: TH6-2-5Ws
 Splice bar spacing, s_p : $2d_b$

Gage	Strains (microin./in.)	
	Cycle 1	Cycle 20
A	318	938
B*		
C	394	1441
D	523	1675
E*		
F	1285	3088



Specimen: TH6-4-5Ws
 Splice bar spacing, s_p : $4d_b$

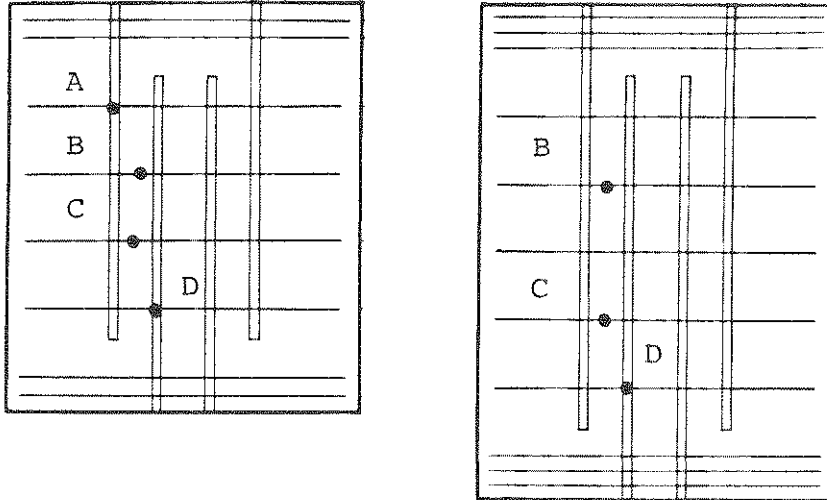
Gage	Strains (microin./in.)		
	Cycle 1	Cycle 20	Cycle 35
A	530	1216	1194
B*			
C	317	1711	1850
D	101	1542	1848
E*			
F	689	2170	3223

Specimen: T⁺H6-8-10Ws
 Splice bar spacing, s_p : $8d_b$

Gage	Strains (microin./in.)		
	Cycle 1	Cycle 5	Cycle 10
A	630	1031	Y
B	626	811	944
C	1141	1379	2147
D	1790	2402	2525
E	3150	3157	3085
F	2875	3586	4455

* No gage.
 y Yield.

Figure 4.12 Transverse reinforcement strains and splice bar spacing, $30d_b$ splices.



Specimen: TH6-4-5Ws
 Splice length, l_s : $30d_b$

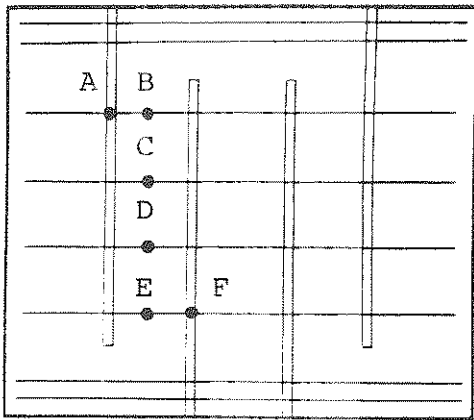
Gage	Strains (microin./in.)		
	Cycle 1	Cycle 20	Cycle 35
A	530	1216	1194
B	317	1711	1850
C	101	1542	1848
D	689	2170	3223

Specimen: T⁺H6-4-5Ws
 Splice length, l_s : $40d_b$

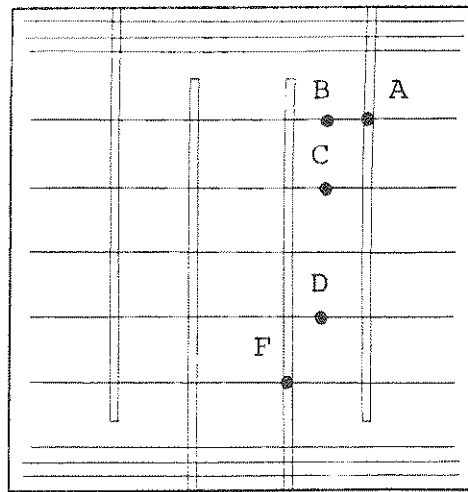
Gage	Strains (microin./in.)		
	Cycle 1	Cycle 20	Cycle 35
A*			
B	1131	1888	1496
C	320	657	806
D	893	1263	1272

* No gage.

Figure 4.13 Transverse reinforcement strains and splice length, $4d_b$ splice bar spacing.



Specimen: TH6-8-10Ws
Splice length, l_s : $30d_b$



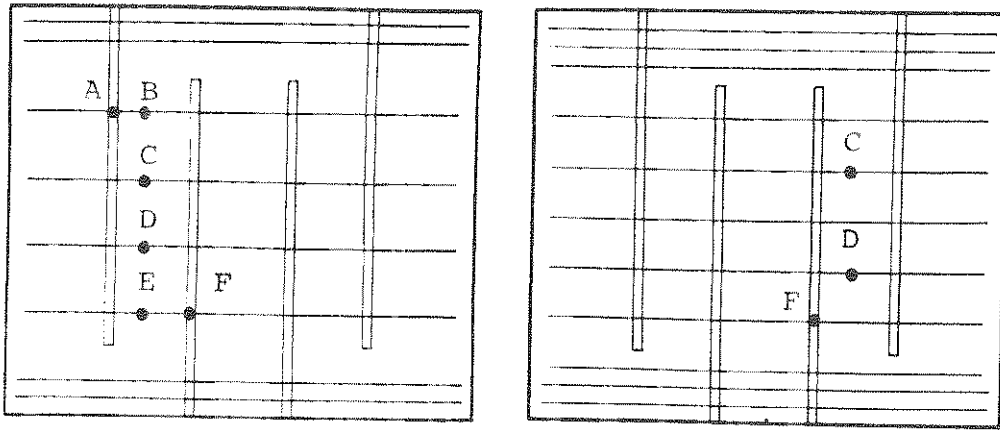
Gage	Strains (microin./in.)		
	Cycle 1	Cycle 5	Cycle 10
A	630	1031	y
B	626	811	944
C	1141	1379	2147
D	1790	2402	2525
E	3150	3157	3085
F	2875	3586	4455

Specimen: T⁺H6-8-10Ws
Splice length, l_s : $40d_b$

Gage	Cycle 1	Strains (microin./in.)		
		Cycle 5	Cycle 10	Cycle 35
A	681	862	-	-
B	915	1222	1095	-
C	422	1631	2304	2699
D	87	388	909	1121
E*				
F	677	1100	1885	2189

* No gage.
- Broken gage.
y Yield.

Figure 4.14 Transverse reinforcement strains and splice length, $8d_b$ splice bar spacing.



Specimen: TH6-8-10Ws
 Transverse reinforcement: #3 @ 5.75 inches.

Gage	Strains (microin./in.)		
	Cycle 1	Cycle 5	Cycle 10
A	630	1031	Y
B	626	811	944
C	1141	1379	2147
D	1790	2402	2525
E	3150	3157	3085
F	2875	3586	4455

Specimen: TH6-8-10Sv
 Transverse reinforcement: #3 @ 4.25 inches.

Gage	Cycle 1	Strains (microin./in.)		
		Cycle 5	Cycle 10	Cycle 35
A*				
B*				
C	460	932	1789	1963
D	91	319	1192	1424
E*				
F	537	740	1495	1781

* No gage.
 y Yield.

Figure 4.15 Transverse reinforcement strains and transverse reinforcement spacing.

than those with the splice bars at a closer spacing. When the splice length was increased in two specimens from 30 to 40 bar diameters, and the transverse reinforcing size and spacing was kept the same, the transverse steel strains were generally higher in the shorter splices, especially as the number of cycles increased. Only one set of specimens was available for the comparison of different spacings of transverse steel. The smaller sized and closer spaced transverse steel had lower strains regardless the number of cycles. Yielding did occur in the transverse reinforcement, but it occurred at locations where the concrete was significantly disturbed and cracked, such as at the end of the splice.

The significant strains recorded in the transverse reinforcement indicates the importance of the steel as a necessary link in the transfer of load in splices in thin elements. The presence of these strains can be explained by an equilibrium model. The tensile forces in the spaced splice bars of the non-contact lap splice are transferred to one another through the concrete by angled compressive struts. To counter the transverse component of the compressive stress field, a transverse tensile force must be developed. Thus the need for transverse reinforcement in noncontact lap splices.

4.3.4 Ultimate Load

The ultimate strength of lap splices subjected to repeated loading demonstrated a similar independence to splice bar

spacing. As shown in Figure 4.16, the ultimate capacity of the tensile lap splice was independent of the spacing and the number of load cycles. The figure includes all the specimens that survived more than one loading cycle except for the preliminary tension test specimens. The number of load cycles sustained by these specimens varied from 4 to 42. Also note that the yield strength is based on the specified yield strength of the splice bars which happened to be 7 to 9 ksi higher than the value of 60 ksi used in design for Grade 60 steel.

For both repeatedly and monotonically loaded specimens, the ultimate strength of the lap splice was independent of the splice bar spacing up to a clear spacing of 8 bar diameters, which is 9 inches center-to-center for a #8 bar and 7 inches, center-to-center for a #6 bar. The current maximum is 6 inches (ACI Committee 318, 1983). There was no indication that at spacings greater than these a radical difference in behavior will occur, provided certain requirements are met.

Specifically, for the ultimate strength of lap splices to be independent of splice bar spacing, the lap splice must have a similar design as used in the testing. The spacing between the splices was always greater than the spacing between the splice bars. Also, there was a minimum anchorage length of 20 bar diameters for the splice bars after the splice bar spacing was subtracted from the overall lap length. Finally, the splice was "tied" together by a sufficient amount of transverse reinforcement and concrete that provided an equilibrating force in the transverse direction.

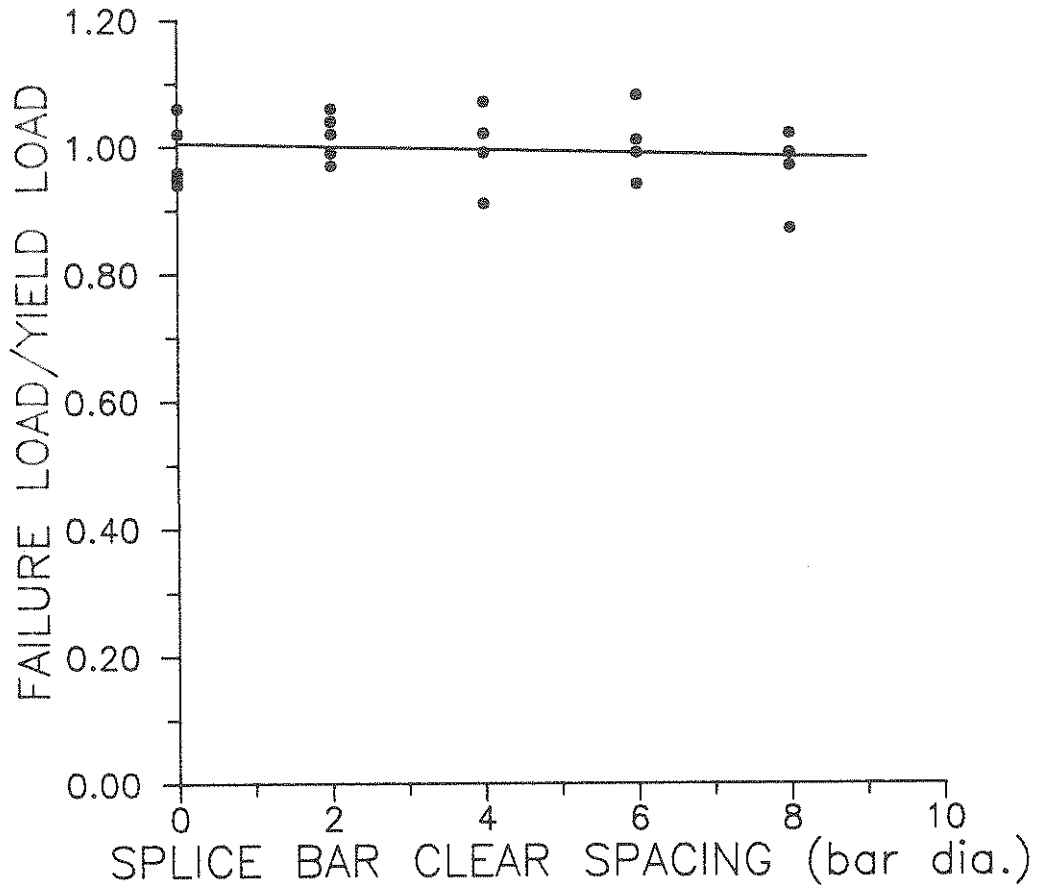


Figure 4.16 Ultimate load performance of the repeatedly loaded specimens.

4.3.5 Post-ultimate Investigation of Internal Cracking

Failure was precipitated by a concrete crack that formed in the plane of the splice bars (Figure 4.17) and was undetectable from the surface of the specimen. The failure mode formed suddenly with a significant loss of load carrying capacity to less than 20 percent of the maximum load carried earlier by the specimen. During the repeated loading, minor cracking in the concrete surrounding the deformed bars was detected by pulse-velocity measurements, but it was limited to within a bar diameter from the centerline of the bar.

As discussed earlier, the failure modes for the contact lap splice specimens matched those previously observed in wide flexural specimens. However, the noncontact lap splice introduced a new category of failure modes. The noncontact lap splice failed as a unit, regardless the spacing between the splice bars. The failure of the splice involved both bars with the splitting crack connecting the two bars as in the cross-sections shown in Figure 4.18.

Cross-section cuts and pulse-velocity readings revealed that the ultimate in-plane cracking changed with splice bar spacing. From the pulse-velocity readings it could not be determined whether or not the width of cracks changed as the spacing of the splice bars or transverse steel increased. The pulse-velocity method was able to detect that the area of the in-plane crack became less with greater spacings of the splice bars for a given

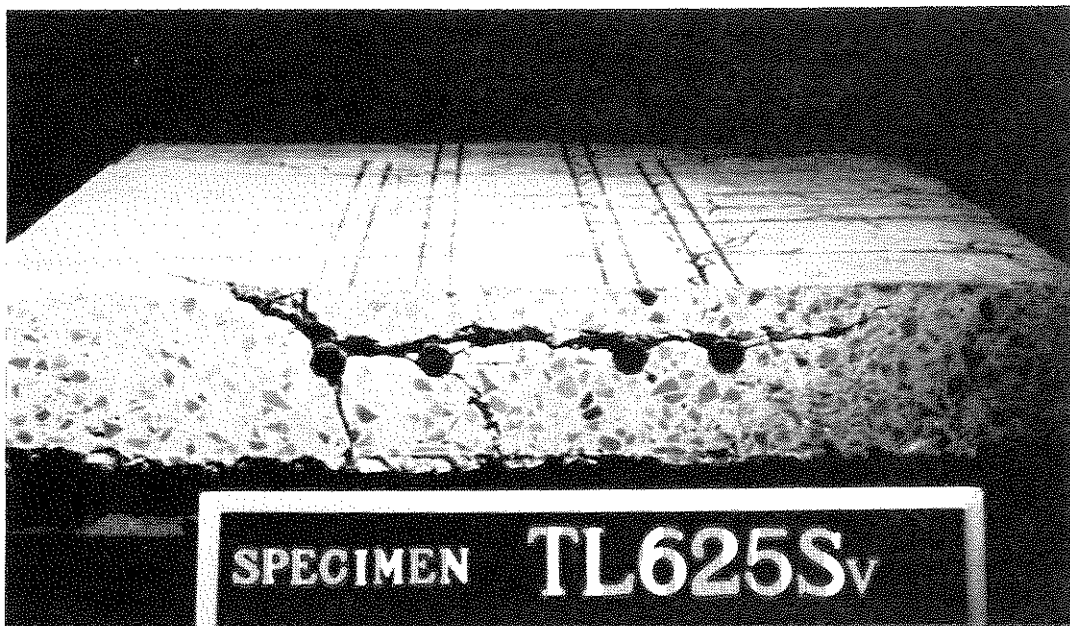


Figure 4.17 In-plane cracking of specimen TL6-2-5Sv.

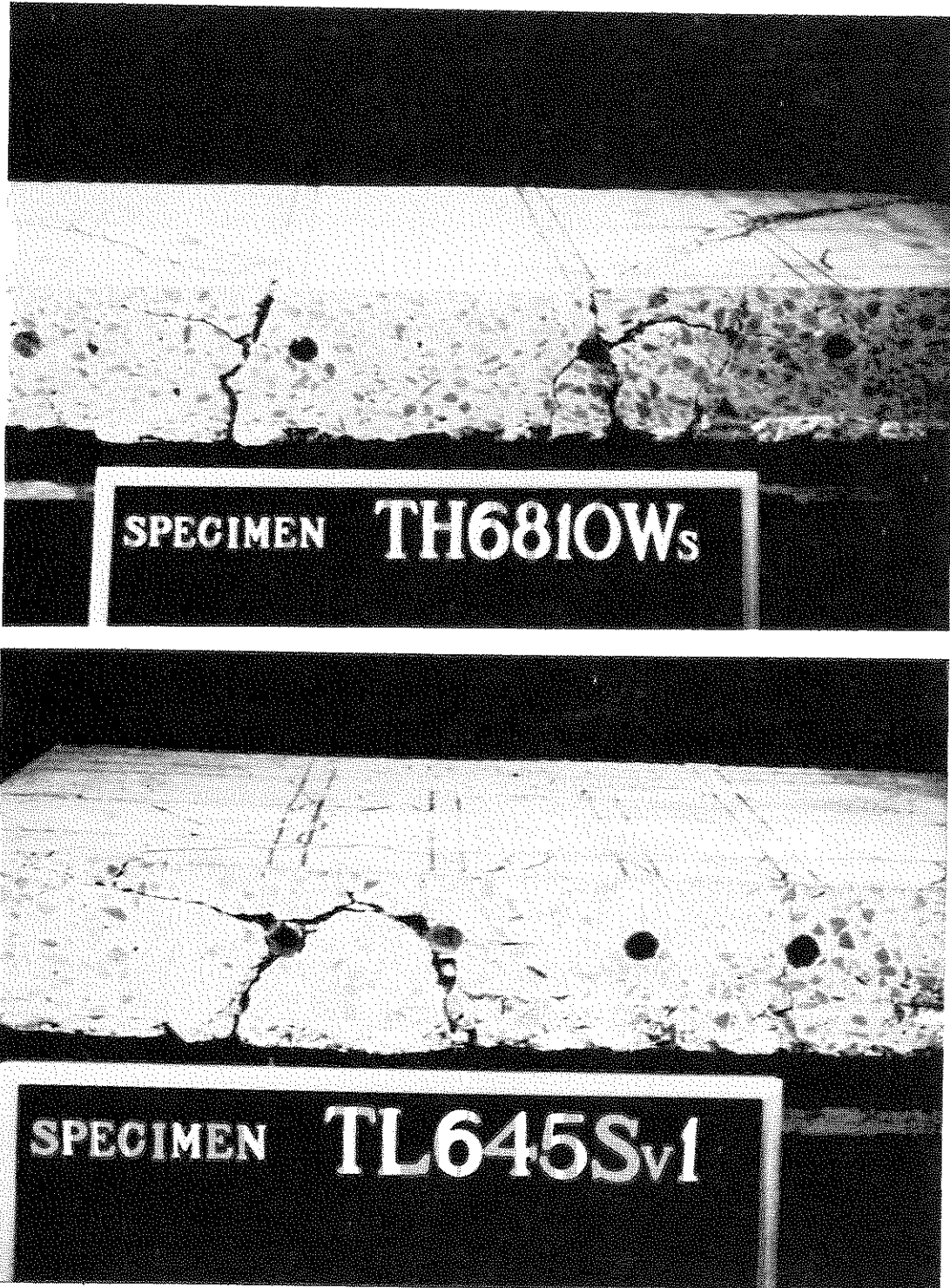


Figure 4.18 Isolated in-plane cracking failure mode.

splice. The in-plane crack was limited by the splice end crack that was diagonal between the spaced splice bars, as shown for specimen in Figure 4.19.

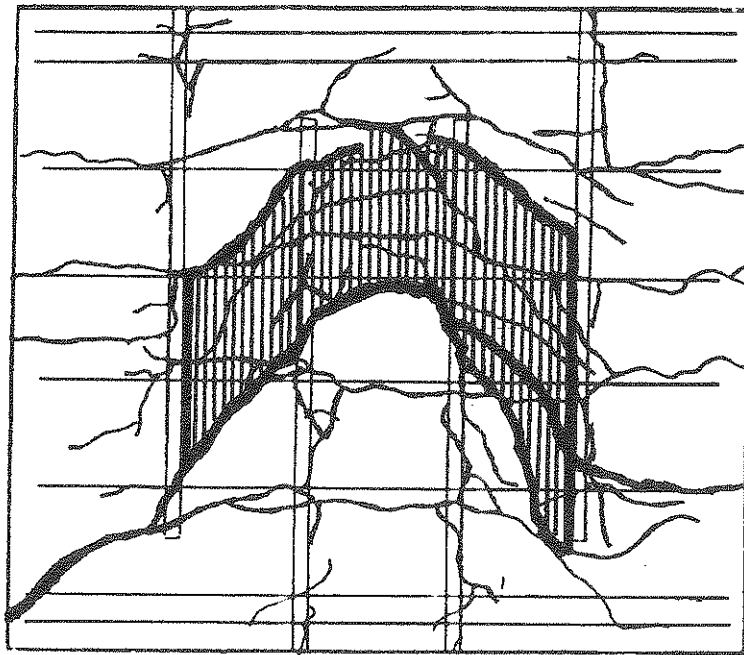
One cause for the in-plane cracking is the splice bar bond-induced bursting. The repeated cracking of the diagonal area between the bars indicates another cause. The diagonal cracks in the concrete between the splice bars resemble the compressive struts of a truss transferring the load from one splice bar to the other. A compression field would cause Poisson strains perpendicular to the plane of the splice and could contribute to the formation of the in-plane failure crack.

4.4 Summary

Through the experimental program it was determined that the splice bar spacing affected the number of inelastic load cycles attained before failure, but it did not affect the ultimate strength of a splice. Other factors affecting the behavior included the lap length, transverse reinforcement, and the concrete strength. The splice bar size did not appear to be a factor influencing noncontact splice behavior. The experimental results, including the observed changes in the reinforcement strains and their distribution along the splice, and the surface and in-plane cracking will be taken into account in the design recommendations.

28	28	27	43	65	39	26	32	26
27	33	93	58	134	42	62	27	27
26	32	94	47	26	50	43	29	26
27	32	68	30	27	30	81	40	27
26	27	27	28	26	26	26	60	26

a) Pulse-velocity measurements at failure.




b) In-plane splitting area. 

Figure 4.19 Pulse-velocity readings and in-plane cracking for specimen TH6-8-10Ws at failure.

SECTION 5

DESIGN RECOMMENDATIONS

5.1 Introduction

Previous research has shown that splices can be designed for seismic loading and the restrictions regarding their location in a structure are too conservative. Proposed seismic splice provisions neglect noncontact lap splices (Panahshahi, et al. 1987), however, and the current design guidelines for noncontact lap splices are limited and based on static behavior (ACI Committee 318, 1983). The goal of this chapter is to develop a behavioral model and design guidelines for noncontact tensile lap splices.

The basis of the design provisions will be on the behavioral model developed from test data and observations of the current and past investigations, the ACI 408 (1979) recommendations, and the latest version of the Cornell seismic lap splice design equations (Panahshahi, et al. 1987). The behavior model is a plane truss where the tensile forces from the splice bars are transferred through diagonal concrete compressive struts and equilibrium is maintained by tensile forces in the transverse reinforcement. Evidence for the truss model is presented and the noncontact tensile lap splice equations are derived and evaluated.

5.2 The Truss Model

A rational design approach in reinforced concrete for shear, torsion, and disturbed areas such as corbels and brackets have been sought for years. Recently, this topic has been the subject of many publications. For example, the 1984 Canadian reinforced concrete code contains new shear design provisions based on the compression field theory, incorporating plasticity and truss models (Collins and Mitchell 1986). Strut and tie models have been reported by Marti (1985), and Cook and Mitchell (1988). The success of these design models, along with a wealth of experimental evidence, motivated the use of a truss model to describe the behavior of noncontact lap splices. This is not the first application of a truss analogy to the lap splice; Robinson, et al. (1974) suggested a truss model for the behavior of noncontact tensile lap splices.

5.2.1 Evidence

Extensive evidence exists for the truss model of behavior for noncontact lap splices because it is based on research from the work of Chamberlin (1952) to the current investigation. The behavioral similarities between contact and spaced splices have been well documented. Researchers have reported lower average bond stresses with noncontact lap splices when compared to contact lap splices (Cairns and Jones 1982, Orangun, et al., 1975), but Reynolds and Beeby (1982) reported no difference. If noncontact lap splices are so similar in behavior when compared

to contact lap splices, why would there be differences in bond stresses? The determination of bond stress needs to be understood before this inconsistency can be resolved.

The average bond stress is equal to the tensile force developed in the deformed bar divided by the surface area of the same bar, through which the tensile load is transferred to the concrete. The average bond strength is dependent on the lap length, the assumed length of the surface area through which the tensile force is transferred.

An indication of the end of force transfer, or development, in a splice is the large crack at the end of the splice. For a contact lap splice, the crack forms at the ends of the splice, thus the actual lap length equals the transfer length. In a noncontact lap splice the end splice crack is diagonal, so the transfer length does not equal, but is shorter than the actual, or overall, lap length. This shorter transfer length, as shown in Figure 5.1, is referred to as the effective lap length. Reynolds and Beeby (1982) determined the bond stress based on a lap length from the end of the bar to the major flexural crack at the end of the splice (the effective lap length). The other researchers were using the overall lap length in their bond stress calculations.

Some of the noncontact splice experimental data from the studies performed by Cairns and Jones (1982) and Orangun, et al. (1975) were reevaluated by the author using an estimated effective lap length to see if that would remove the reported

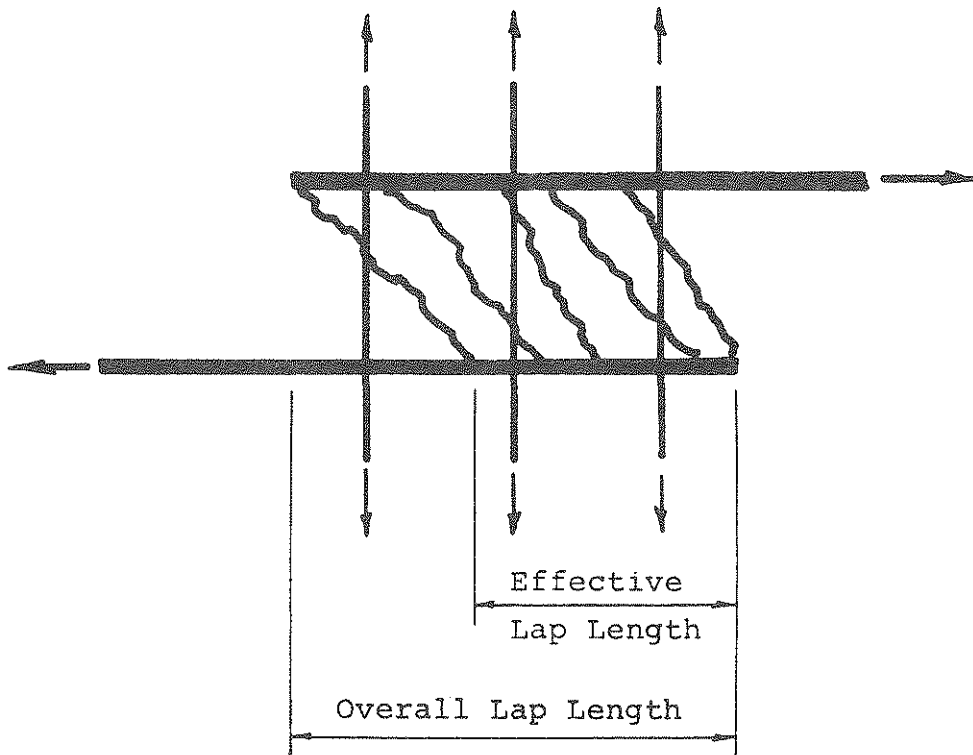


Figure 5.1 Effective lap length.

difference between average bond stresses for noncontact and contact lap splices. The results of the reevaluation along with the data from Reynolds and Beeby (1982) are listed in Table 5.1. The estimated effective lap length used was the overall lap length less the clear distance between the splice bars. In general, the bond stresses for the noncontact lap splices increased to the point where no real distinction could be made between spaced and contact lap splices when the effective lap length is used in the determination of bond stresses. The shorter effective lap length for noncontact lap splices is predicted by a truss model.

If the effective lap length is shorter with spaced spliced bars, the steel bar stress distribution would have to change with spacing. As discussed in the previous chapter, there was a change in the strain and stress distributions with splice bar spacing. It was confirmed that the yield penetration was greater for the lap splices with wider spaced bars and that it extended beyond the end of the estimated effective lap length, which was calculated the same way as in the bond stress reevaluation.

The cracking of the concrete between the bars of the splice during loading and upon failure leaves only a truss mechanism for transferring the tensile load in a noncontact lap splice. Much of the cracking, as shown in Figures 4.6 and 4.7, is diagonal and located at the splice ends and all along the splice length. The cracking angles vary between 20 and 70 degrees, but are predominantly 45 degrees. With the thin cover of only 1.5 bar

Table 5.1 Bond stress reevaluation.

Cairns and Jones (1982)

	Ultimate Bond Stress N/mm ²	
	Alignment X	Alignment Y
Contact lap	4.15	4.51
Spaced bars	3.65	3.90
Spaced, Reevaluated	4.17	4.46

Note: Reevaluation based on $l_{eff} = l_s - s_p$
 Alignment was a test variable dealing with orientation of the crescent shaped ribs of the deformed bars in a splice.

Orangun, et al. (1975)

Reevaluation of 21 plane spaced splices, Series B, from Robinson, et al. (1974)

	u_e/u_p	u_e/u_p
	Average	Standard Deviation
No adjustment	0.93	0.14
$l_{eff} = l_s - s_p$	1.05	0.17
$l_{eff} = l_s - 0.75s_p$	1.02	0.16

where u_e = experimental bond stress values.
 u_p = predicted bond stress values.

Table 5.1 (Continued) Bond stress reevaluation.

Reynolds and Beeby (1982)

All dimensions in mm.
 Normalized bond stress corrected for variation in
 concrete compressive strength.
 c/c = center to center.

Beam	l_s	l_{eff}	Splice Bar Spacing, (c/c)	Normalized Bond Stress
C1	200	-	0	0.75
C2	200	-	0	0.66
C3	200	-	0	0.66
C4	200	-	0	0.70
C5	200	-	0	0.67
C6	200	-	0	0.63
D1	300	240	60	0.71
D2	300	290	40	0.67
D3	300	-	0	0.67
D4	200	-	0	0.61
D5	200	-	0	0.51
D6	200	-	0	0.68
E1	140	-	0	0.69
E2	240	-	0	0.59
E3	150	120	40	0.69
E4	250	250	40	0.70
E5	290	-	0	0.70
E6	400	-	40	0.55

diameters, it should be a reflection of the cracking between the bars where the actual load transfer is occurring. The cracking between the bars of a splice was well documented by Goto and Otsuka (1979). Diagonal surface cracking was also observed by Ferguson and Krishnaswamy (1971) for large diameter bar contact lap splices, and by Chamberlin (1958), and Reynolds and Beeby (1982) for noncontact splices.

The ultimate failure mode cracking, the in-plane splitting, also supports the truss model of behavior. One cause for the cracking is the well-documented bursting effect of the deformed bars or splices. But the in-plane cracking between the bars of the splice is limited to the area delineated by the diagonal cracks at the ends of the splice defined in Figure 5.2. With an isolated splice failure the cracking was also limited to the concrete area between the splice bars. The limited cracking indicates that the bursting was not the only cause for the ultimate failure mode. A likely source contributing to the in-plane cracking is the compression stress field causing a Poisson out-of-plane expansion, a compression field that is predicted by the truss model. The observed splice failure mode resembles the failure mode for concrete under uniaxial compression described by Tasuji, et al. (1978) as caused "... by the formation of cracks parallel to the applied load and perpendicular to the larger unloaded surface of the specimen...".

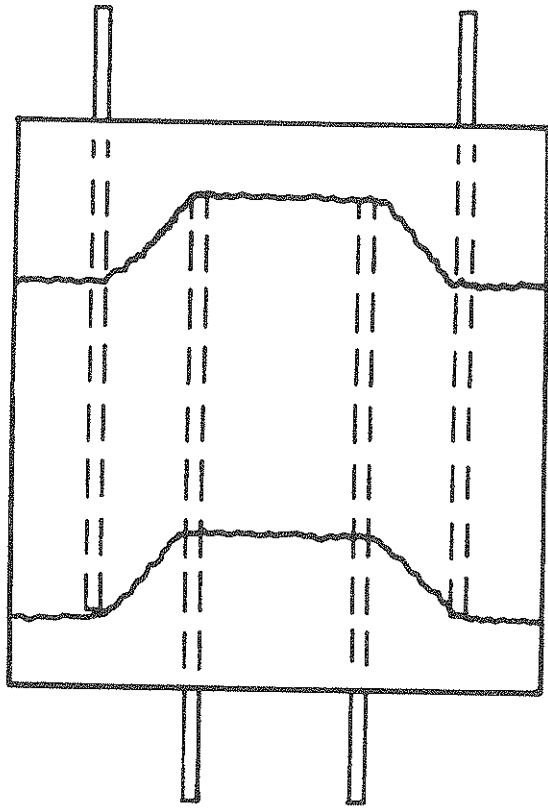


Figure 5.2 End splice crack.

5.2.2 Derivation of the Lap Splice Design Equations

Several questions remained before the actual derivation could begin. The exact stress state in the concrete and the transverse reinforcement between the splice bars is unknown, which means that which angle of the concrete struts is not known. The compressive stress will also affect the tensile strength perpendicular to the plane of the splices, which is the plane where the in-plane crack forms.

One might assume that the concrete between the splice bars is under a state of pure shear because of the end transverse crack at the ends of the splice. Then one could simply say the compressive struts form at 45 degrees. Unfortunately, the stress condition is complicated by the fact that for a noncontact splice to be in equilibrium, a transverse tensile force must exist.

The surface cracking in the concrete surrounding the splice cannot be used to define a precise angle for the compressive struts. Even in duplicate specimens there was a variation in the cracking angle. The surface cracking is caused primarily by the stress state, but is also affected by existing transverse and longitudinal cracks, the location and distribution of the transverse reinforcement and coarse aggregate of the concrete, and the cover thickness. The cracking in the concrete between the bars may not be the same as on the surface. Goto and Otsuka (1979) also reported that the angle of the concrete struts varied with lap length.

The tool used to answer the behavior questions was the compression field theory reported by Vecchio and Collins (1986), combined with a strut and tie method similar to the one summarized by Cook and Mitchell (1988). The flow of forces in the noncontact lap splice behavior was idealized as a truss and forces were determined in the truss members from statics. The capacities of the compressive struts were checked using compression field theories. The reason for using the compression field theory was that it was a rational way to explain the behavior of the noncontact lap splice and it took into account the reduction, or "softening", of the ultimate compressive strength due to the presence of transverse reinforcement, the angle of the struts, and the cracking of the concrete.

A parameter study was undertaken to quantify, if possible, the stress field in the concrete between the bars, by varying the angle of the struts, the splice bar spacing, steel reinforcement yield strength, concrete compressive strength, and transfer area. The study found that at a strut angle of 55 degrees, the minimum lap length occurred. Reasonable lap lengths resulted with angle selections of 30 to 70 degrees, and only a small lap length change occurred between 45 and 65 degrees. The load transfer area appeared to be the most reasonable at a thickness of two bar diameters, although it probably varies some with splice bar spacing.

The compression field theory could not account for the out of plane effects and resulting in-plane splitting, however. The

concrete between the loaded splice bars is in compression in one direction, but it is also in tension when resisting the bursting and splitting. The strength of concrete in one direction is dependent on the stress applied in the other direction (Nilson and Winter 1986): "When tension in direction 2 is combined with compression in the direction 1, the compressive strength is reduced almost linearly, and vice versa." Using that relationship the out of plane effect could be quantified and incorporated in a design equation, if the compressive stress in the concrete could be determined.

The compressive stress in the struts, which controls the concrete tensile strength resisting the in-plane cracking, can be predicted by the compression field theory. The maximum compressive strength is reduced due to the presence and orientation of the transverse steel. The softening magnitude varies on the angle of the struts to steel, but Marti (1985) suggested $0.6f'_c$. A compressive strut angle of 50 degrees also results in the same value. Using the biaxial strength curve from Nilson and Winter (1986), reproduced in Figure 5.3, the tensile strength is reduced to 40 percent of its uniaxial capacity when the compressive stress equals $0.6f'_c$.

Based on the compression field theory, the parameter study, biaxial concrete strength theory, and experimental evidence, a strut angle of 50 degrees was selected to characterize the compressive stress field. The 50 degree angle will be used to

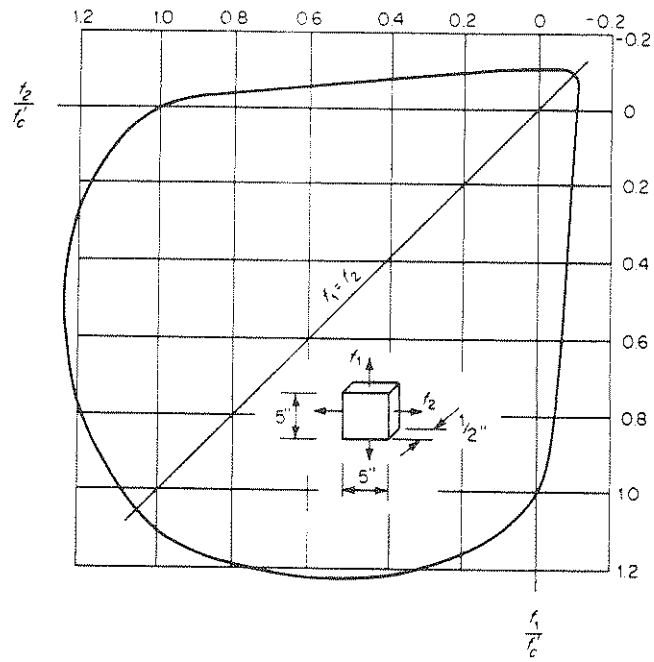


Figure 5.3 Strength in concrete in biaxial stress (Nilson and Winter 1986).

determine the effective lap length, concrete strength reductions, and equilibrium forces, all used in the noncontact lap splice derivation.

5.2.2.1 Splice Length Derivation

The derivation for the modified seismic tensile lap splice equations is based on a equilibrium model of bursting and confining forces used by Sivakumar, et al. (1982) to develop the original design equation. Sivakumar had two derivations, one for widely spaced splices and one for corner splices, both of which resulted in the same equation. The noncontact splice length derivation will follow the development of the equation for widely spaced splices.

The widely spaced splice derivation, for splices spaced greater than 4 bar diameters, only considered confinement due to the concrete. The strength of the concrete was based on a thick-walled cylinder analogy proposed by Tepfers (1979). The concrete around the deformed bars was assumed to act plastically, that is, the cylinder will crack only when the tangential stress at every part of the cylinder has reached the ultimate tensile concrete stress. The assumption is reasonable for cover to bar diameter ratios less than two.

The bursting forces come from the radial component of the bond forces. The bond force angle was assumed by Sivakumar, et al. (1982) to be 45 degrees, making the longitudinal and radial bond force components equal in magnitude. The confining

forces is provided by the surrounding concrete. For a contact lap splice, the equilibrium in a direction normal to the plane of splices, as shown in Figure 5.4, is

$$f_y d_b^2 / (4l_{eff}) + f_y d_b^2 / (4l_{eff}) = 2f_t c \quad (5.1)$$

Assuming the yield penetration to be 20 percent of the effective of the lap length, l_{eff} , the equation becomes

$$f_y d_b^2 / (1.6l_{eff}) = 2f_t c \quad (5.2)$$

When the splices are spaced, the concrete between the bars adds to the confinement. Because of the compression field in the concrete between the bars, the tensile capacity is reduced to 40 percent of its uniaxial strength. The added confinement dimension, quantified by the splice bar spacing, s_p , is limited to twice the cover dimension, c . At that spacing of the splice bars the concrete resisting the splitting becomes two separate cylinders, the size of which is dependent on the cover dimension as shown in Figure 5.5. Considering the added confinement due to the splice bar spacing, the equation becomes

$$f_y d_b^2 / (1.6l_{eff}) = 2f_t c + 0.4f_t s_p \quad (5.3)$$

Substituting in the steel yield strength of 72,000 psi based on the recommendation of Panahshahi, et al. (1987), the concrete tensile strength of $7.25(f'_c)^{0.5}$, the cover to bar diameter ratio of 1.5, both from Sivakumar, et al. (1982), and the effective lap length equation becomes

$$l_{eff} = 3100d_b / ((f'_c)^{0.5} (1.5 + 0.2s_p/d_b)) \quad (5.4)$$

where the value of s_p/d_b entered in Equation 5.4 cannot be greater than 3.0 even though the actual value may be greater.

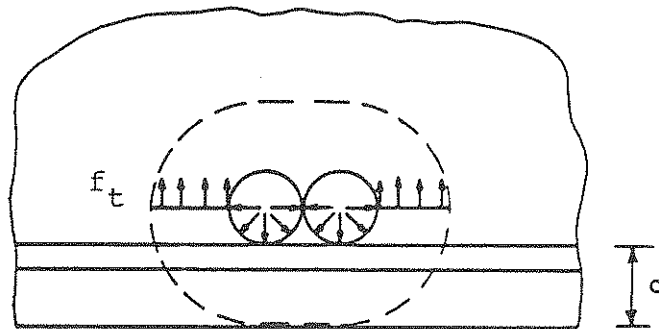
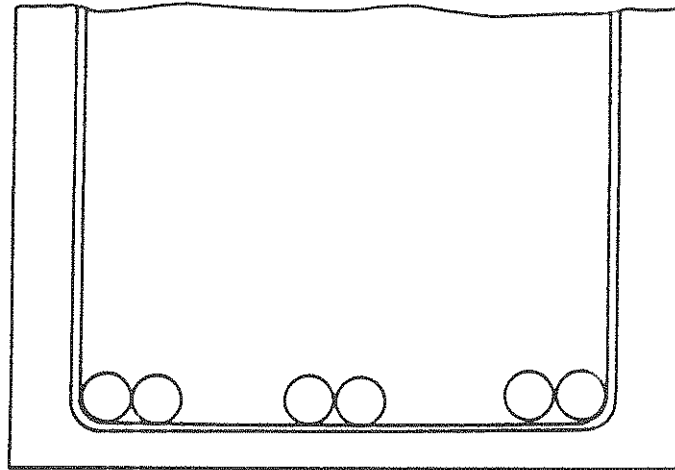


Figure 5.4 Stress diagram for interior splices not confined by supplementary stirrup-ties (Sivakumar, et al. 1982).

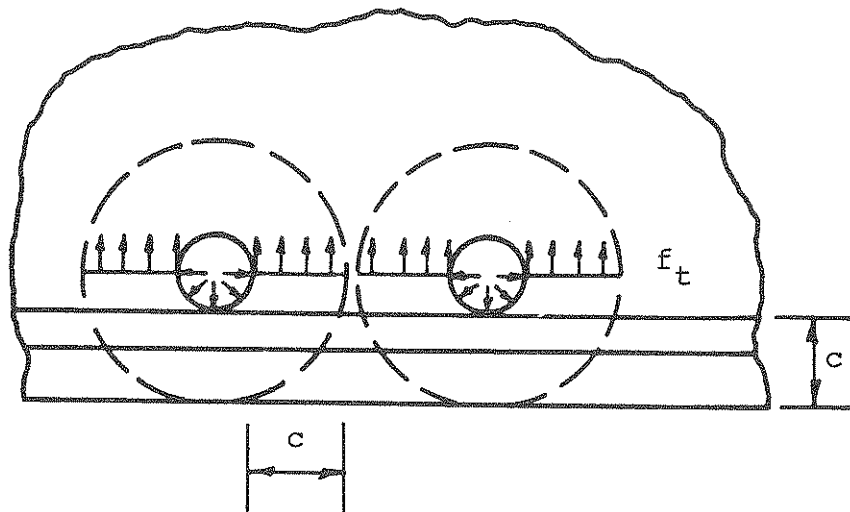


Figure 5.5 Added confinement due to splice bar spacing.

The effective lap length must not be less than $20d_b$, which is the minimum lap length allowed by Sivakumar, et al. (1983). Based on the poor performance of specimens with low concrete compressive strengths, f'_c must not be less than 3500 psi.

The overall splice lap length, l_s , is determined by adding to the effective lap length, l_{eff} , the actual splice bar clear spacing, s_p , multiplied by 0.75, which is approximately the sine of 50 degrees, the assumed angle of the compressive struts.

$$l_s = l_{eff} + 0.75s_p \quad (5.5)$$

The equation is of the same form as the one originally proposed by Sivakumar. et al. (1983). If one substitutes in a splice bar clear spacing equal to zero, which is a contact lap splice, the equation becomes the Cornell seismic splice design equation incorporating a steel yield strength of 72,000 psi.

The modifications for the monotonic tensile lap splice equations is different from the seismic design equation but uses the results of the same compression field theory parameter study. The additional confinement from the concrete between the bars of the noncontact lap splice is considered by following the procedure set forth by Orangun, et al. (1975). The spacing between the bars and the splices is determined by taking the net concrete width resisting the splitting in the plane of the bars and dividing by the number of splices. The lap length resulting from applying the ACI 408 proposal is the effective lap length. The effective lap length must not be less than 12 inches

according to ACI 318 (1983) and ACI 408 (1979). The overall lap is then the effective length plus the clear bar spacing multiplied by 0.75.

5.2.2.2 Transverse Reinforcement Derivation

The general derivation for the required transverse reinforcement is based on the truss model, equilibrium, and results of the compression field parameter study. Equilibrium in the noncontact splice truss requires that

$$P_y = P_{yt} \tan A \quad (5.6)$$

where P_y is the tensile force developed by the anchored splice bar, P_{yt} is the transverse tensile force, and A is the angle at which the compressive struts form. Substituting a value of 50 degrees for A , and the yield force in terms of yield strength and bar diameter, and solving for P_{yt} , results in

$$P_{yt} = 0.659 f_y d_b^2 \quad (5.7)$$

The maximum tensile force developed by the transverse reinforcement is dependent on the total transverse steel area, which is determined by the individual bar area A_{tr} and the spacing s along the entire splice length l_s , and is equal to

$$P_{yt} = A_{tr} f_y l_s / s \quad (5.8)$$

Equating the force required by equilibrium to the maximum force that can be developed, and solving for the transverse steel spacing s gives

$$s = 1.52 A_{tr} l_s / d_b^2 \quad (5.9)$$

Equation 5.9 is based on equilibrium and the compression field theory, with no consideration given to the demands of seismic loading. The seismic design equation for lap splice transverse reinforcement spacing derived by Sivakumar, et al. (1983) is given by Equation 5.10.

$$s = k_1 A_{tr} l_s / d_b^2 \leq 6" \quad (5.10)$$

where $k_1 = 0.375/(\text{transverse steel diameter})$.

Both transverse reinforcement equations are of the same form, but use of Equation 5.10 will result in more closely spaced transverse reinforcement than given by Equation 5.9. Noncontact lap splice specimens with transverse reinforcement designed using Equation 5.10 sustained as many load cycles as the contact lap splice specimens, even though higher transverse reinforcement strains were recorded with larger splice bar spacings. Considering the derivations and the noncontact splice performance, Equation 5.10 is satisfactory for the seismic design of noncontact tensile lap splices. The design, however, must use grade 60 reinforcement and a lap splice clear cover at least a $1.5d_b$.

Monotonic splice design in the United States does not require minimum transverse reinforcement along a splice. Based on the above derivation resulting in Equation 5.9, transverse reinforcement is required in noncontact lap splices. The derivation, however, neglects the contribution of the concrete surrounding the splice that assists in the transfer of the tensile forces transversely across the spaced splice.

Quantifying the concrete contribution is difficult, if not impossible, but if one assumes that the concrete transfers 10 percent of the load capacity of the transverse reinforcement, the spacing of the reinforcement may increase by a factor of 1.11. Multiplying Equation 5.9 by this factor results in a minimum transverse steel spacing of

$$s = 1.7 A_{tr} l_s / d_b^2 \quad (5.11)$$

Use of Equation 5.11 would require a minimum amount of reinforcement along a lap splice at nearly twice the spacing required by seismic loading.

5.3 Critical Evaluation

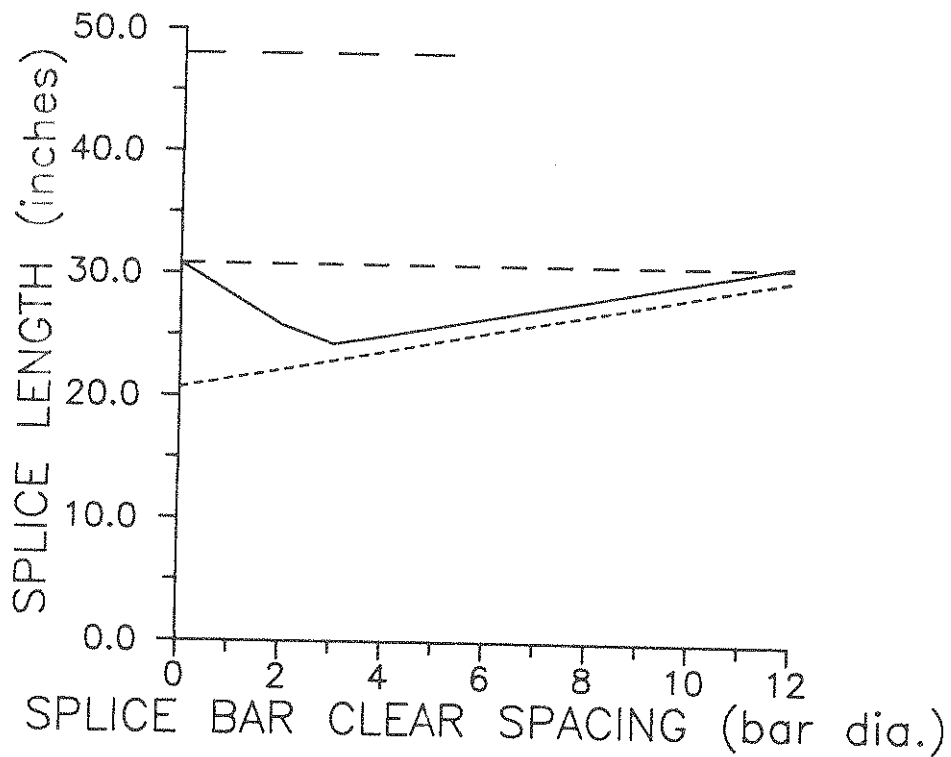
An evaluation of the noncontact lap splice design equations is required before they can be implemented in design codes. The design formulations for the seismic behavior of the noncontact lap splices explain the cyclic performance for the test series with the concrete compressive strength equal to approximately 4500 psi. As shown in Figure 4.16, the number of load cycles sustained by the specimens with a concrete compressive strength of 4500 psi increases and then decreases with the peak number of cycles occurring at a splice bar clear spacing between two and four bar diameters. The use of the noncontact lap splice design Equations 5.4 and 5.5 will result in lap lengths that decrease up to a spacing of three bar diameters, and then lap lengths will increase. The calculated lap lengths using the noncontact lap

splice equations derived above, and the Cornell seismic splice design equations from Panahshahi, et al. (1987) are presented in Figure 5.6 for #8 splice bars and a concrete compressive strength of 4500 psi.

The noncontact and the Cornell lap lengths in Figure 5.6 are also compared to lap lengths determined using both the ACI 318 (1983) requirements and the truss model/compression field theory. The lap lengths determined by the truss model/compression field theory, based on the compressive strut angle of 50 degrees, are shorter than the proposed noncontact lap splice equation. The ACI 318 lap length is significantly longer, but transverse reinforcement is not required along the splice as it is in the other design procedures.

There is no difference in the seismic transverse steel requirements for both contact and noncontact lap splices. This noncontact experimental program, as well as investigations performed by Sivakumar, et al. (1982) and Panahshahi, et al. (1987), supports the adequacy of the splice transverse reinforcement design approaches.

The tension test specimens from this investigation are evaluated in terms of repeated load performance and design according to the noncontact lap splice equations in Tables 5.2 through 5.4. The noncontact specimens generally performed better than the contact lap splice specimens. The tension contact lap splice specimens did not sustain as many load cycles as those in



SPLICE PROPERTIES:
 $f'_c = 4500$ psi
 $f_y = 72$ ksi
 $d_b = 1$ inch
 cover = 1.5 inches

- SEISMIC, NONCONTACT
- - - SEISMIC, CORNELL 1987
- · · TRUSS/COMPRESSION FIELD, A = 50°
- · - ACI 318-83, 1.7l_d

Figure 5.6 Lap length design equation comparison.

beam and column-like specimens, therefore even better performance is expected from noncontact lap splices in flexural structural members.

The monotonic lap splice design method generally produces lap lengths greater than those determined by the seismic design provisions, so the slight shortening of lap lengths by the noncontact splice provisions will have little impact on lap lengths. Table 5.1 does show, however, the beneficial influence on the correlation of the predicted and the calculated bond stresses in noncontact lap splices. The prediction equation used by Orangun, et al. (1975) is the basis for the ACI 408 (1979) splice design recommendation.

The transverse reinforcement provisions for monotonic tensile lap splice design have not changed. Only a minimum transverse reinforcement equation has been proposed, but it requires testing and further evaluation in flexural specimens. Nonetheless, for noncontact lap splices, the transverse reinforcement along the splice should satisfy equation 5.11. In any case, the beneficial influence of transverse reinforcement for both contact and noncontact lap splices is well documented and now a workable formulation exists to check the minimum reinforcement.

Although equilibrium demands truss behavior in noncontact lap splices, and design equations and methods now exist to specifically address them in design, the need for the equations

in typical design situations is splice equations should be used in special design situations. In extremely unusual situations where the noncontact lap splice equations cannot be applied, evaluating the splicing conditions in terms of a strut and tie method incorporating the compression field theory should be applied.

Table 5.2 Tension specimen evaluation based on noncontact lap splice design and performance - satisfactory.

The splices met the noncontact design requirements and had a satisfactory repeated load performance. The preliminary tension specimens were not evaluated.

Specimen I.D.	Failure Load Cycle	Comments
TN6-0-5Sv	8	
TN6-2-5Sv	16	
TN6-4-5Sv	12	
TN6-6-8Sv	12	
TN8-0-5Sv	5	
TN8-2-5Sv	8	
TN8-4-5Sv	12	
TN8-6-8Sv	9	
TN8-8-10Sv	6	
TN8-8-10Sv-1	4	
TN8-8-10Sv-2	4	
TH6-6-8Sv	29	A shorter lap length could have been used.
TH6-8-10Sv	35+	A shorter lap length could have been used.
T ⁺ H6-4-5Ws	35+	A shorter lap length could have been used.
T ⁺ H6-8-10Ws	35+	A shorter lap length could have been used.
TH8-2-5Sv	14	
TH8-4-5Sv	25	
TH8-6-8Sv	42	A shorter lap length could have been used.

Table 5.3 Tension specimen evaluation based on noncontact lap splice design and performance - marginal.

The specimen did not perform as designed, better or worse. The preliminary tension specimens were not evaluated.

Specimen I.D.	Failure Load Cycle	Comments
TH6-0-5Sv	5	Should have sustained more cycles because of a greater f'_c .
TH6-2-5Sv	11	Should have sustained more cycles because of a greater f'_c .
TH6-4-5Sv	4	Should have sustained more cycles because of a greater f'_c .
TH6-2-5Ws	23	Better performance than expected because of insufficient transverse reinforcement.
TH6-4-5Ws	35+	Better performance than expected because of insufficient transverse reinforcement.
TH6-8-10Ws	10	Better performance than expected because of insufficient transverse reinforcement.
TH8-0-5Sv	6	Should have sustained more cycles because of a greater f'_c .

Table 5.4 Tension specimen evaluation based on noncontact lap splice design and performance - unsatisfactory.

Similar contact lap splices did not perform any better than the noncontact lap splices. It indicates a generic splice design problem. The preliminary tension specimens were not evaluated.

Specimen I.D.	Failure Load Cycle	Comments
TL6-0-5Sv	2	f' _c less than 3500 psi.
TL6-2-5Sv	1	f' _c less than 3500 psi.
TL6-4-5Sv	1	f' _c less than 3500 psi.
TL6-4-5Sv-1	2	f' _c less than 3500 psi.
TL8-0-5Sv	1	f' _c less than 3500 psi.
TL8-2-5Sv	1	f' _c less than 3500 psi.
TL8-4-5Sv	1	f' _c less than 3500 psi.
TL8-6-8Sv	1	f' _c less than 3500 psi.
TL8-4-5Or	1	f' _c less than 3500 psi. Insufficient transverse reinforcement.
TL8-0-5S1	1	f' _c less than 3500 psi. Insufficient transverse reinforcement.
TL8-4-5S1	1	f' _c less than 3500 psi. Insufficient transverse reinforcement.
TL8-6-8S1	1	f' _c less than 3500 psi. Insufficient transverse reinforcement.
TN8-8-10Ws	1	Insufficient transverse reinforcement.
TN8-8-10Ws-1	1	Insufficient transverse reinforcement.
TN8-8-10Ws-2	1	Insufficient transverse reinforcement.

SECTION 6

SUMMARY AND CONCLUSIONS

6.1 Summary

This study was the final phase of an extensive investigation of the behavior of lap splices subjected to inelastic cyclic loading. The goal of the study was to understand the behavior of noncontact tensile lap splices under repeated inelastic loading and to formulate rational design guidelines and equations that parallel or conform to existing unified design equations. The investigation was motivated by the limited research on the subject and the lack of design guidelines.

Forty-seven full-scale, flat plate tension specimens were tested to determine the effects of noncontact spacing of the splice bars, bar size, concrete strength, splice length, and transverse steel area and spacing. The specimens had splice bar spacings ranging from direct contact to 8 bar diameters clear, both #6 and #8 splice bars, concrete compressive strengths ranging from 3100 to 6100 psi, splice lengths of 30 and 40 bar diameters, and splice transverse reinforcement ranging from no transverse reinforcement to amounts satisfying proposed seismic design provisions (Sivakumar, et al. 1983). The tension specimen contained two lap splices and modeled a half wall thickness. Seven specimens were used to develop the specimen configuration that modeled flexural splice behavior in the tension specimen.

A significant data base on noncontact lap splice behavior was developed. The flat plate specimens were repeatedly loaded in tension to the yield strength of the splice bars until failure occurred. Ultimate load capacities, steel reinforcement strains, and the cracking-induced failure modes were determined.

Equations for the design of noncontact lap splices for both monotonic and seismic loading were developed based on the data obtained from the experimentation and are modifications of existing state-of-the-art lap splice design equations. The derivation made use of a strut and tie analysis, incorporating the compression field theory, and investigations performed by Orangun, et al. (1975), Sivakumar, et al. (1982) and Panahshahi, et al. (1987).

6.2 Conclusions

The principal conclusions of this investigation regarding the behavior and design of noncontact tensile lap splices are presented. In general, the flat plate specimens loaded under direct tension proved to be a successful technique in testing tensile lap splices and understanding the behavior on noncontact lap splices.

6.2.1 Noncontact Lap Splice Behavior

1) Noncontact lap splice behavior has been observed and modeled as a plane truss. Load is transferred between the two

splice bars through the concrete by compressive struts. The tension ties are provided by the transverse reinforcement and surrounding concrete.

2) The ultimate load carried by a splice is independent of the splice bar spacing up to 6 inches clear for monotonic loading. Under repeated loading up to the yield strength of the splice bars (which was a testing limitation), the ultimate load (equal to the yield load) was also independent of splice bar spacing up to 8 bar diameters for both #6 and #8 bars.

3) As the splice bar spacing increases, the number of repeated inelastic tensile load cycles resisted by the splice first increases, and then decreases, peaking at a splice bar spacing between two and four bar diameters. At a clear spacing of 8 bar diameters the load cyclic performance was at least equal to that of a contact lap splice.

4) The failure mode for the spaced bar splices is an in-plane splitting crack forming between the bars of the splice. The crack is caused by the bond-induced bursting and the Poisson strains generated by the compression stress field of the force transfer.

5) The splice bars experience increased longitudinal strains along the length of the lap splice, which includes an increased yield penetration, with repeated loading and increased splice bar spacing.

6) The transverse reinforcement is a noncontact lap splice; closely spaced, uniformly distributed transverse reinforcement is required to insure proper inelastic cyclic performance.

6.2.2 Noncontact Lap Splice Design

1) The noncontact lap splice design equations take into account the added confinement of the additional concrete between the spaced bars, the reduction of the tensile strength of the concrete because of the compression force transfer stresses in the concrete between the bars, and the reduction of the effective lap length of the splice.

2) The spacing between two adjacent splice groups must be greater than the spacing between the bars of a noncontact splice.

3) For noncontact lap splices with a splice bar clear spacing not greater than 12 bar diameters, or 12 inches, and subjected to monotonic loading, the ACI 408 (1979) proposal is followed to determine the effective lap length, l_{eff} , which must be greater than 12 inches. The added confinement in the plane of the spaced splice bars is considered by taking the net concrete width resisting the splitting in the plane of the bars and dividing by the number of splices, which calculates the effective splice spacing. The overall splice lap length, l_s , is determined by adding to the effective lap length, l_{eff} , the splice bar clear spacing, s_p , multiplied by 0.75, which is approximately the sine of 50 degrees, the angle of the compressive struts.

$$l_s = l_{eff} + 0.75s_p \quad (5.5)$$

Minimum transverse reinforcement is required along the splice length and its spacing s , is dependent on the transverse reinforcement area A_{tr} , the lap length l_s , and the splice bar diameter d_b , and is determined by the following equation.

$$s = 1.7 A_{tr} l_s / d_b^2 \quad (5.11)$$

The contribution of the transverse steel can be used to reduce the lap length, provided there are at least three transverse bars crossing the splice.

4) For noncontact lap splices with a splice bar clear spacing not greater than 8 bar diameters, or 8 inches, and subjected to repeated loading, the equations proposed by Sivakumar, et al. (1983) are slightly modified to account for the splice bar spacing effects. For grade 60 reinforcement, a cover of at least 1.5 bar diameters, and a concrete compressive strength f'_c , of at least 3500 psi, the effective lap length l_{eff} , is determined by

$$l_{eff} = 3100d_b / ((f'_c)^{0.5} (1.5 + 0.2s_p/d_b)) \quad (5.4)$$

where the value of s_p/d_b entered in Equation 5.4 cannot be greater than 3.0, even though the splice bar clear spacing s_p , may be greater. The effective lap length must not be less than 20 bar diameters, as recommended by Sivakumar, et al. (1982). Equation 5.5 is again used to determine the overall lap length.

$$l_s = l_{eff} + 0.75s_p \quad (5.5)$$

where s_p is the actual splice bar clear spacing. For grade 60 transverse reinforcement, the reinforcement must be uniformly

distributed, spaced according to the Equation 5.10,

$$s = k_1 A_{tr} l_s / d_b^2 \leq 6" \quad (5.10)$$

where $k_1 = 0.375/(\text{transverse steel diameter})$, and continued a distance d past the ends of the splice. The transverse reinforcement requirements have not changed from the proposal of Sivakumar, et al. (1983).

5) In the design of the noncontact lap splice, it is conservative to ignore the effects of the splice bar spacing and design the splice as a contact lap splice provided that under monotonic loading the splice bar clear spacing is less than 12 bar diameters, or 12 inches, and under repeated loading the splice bar clear spacing is less than 8 bar diameters, or 8 inches.

6) A strut and tie model incorporating the compression field theory is strongly recommended for the design of noncontact lap splices that under monotonic loading have a splice bar clear spacing greater than 12 bar diameters, or 12 inches, and under repeated loading have a splice bar clear spacing greater than 8 bar diameters, or 8 inches.

6.3 Suggestions for Further Research

This noncontact lap splice investigation was quite thorough and there is little need to perform another extensive testing program on the subject. However, there are a few isolated topics that can be investigated. Verification of the behavior of the inelastic loading can be performed. It is the author's

opinion that the tension specimens were under a more severe loading condition than flexural members and the beams would perform better than the flat plate specimens under repeated loading. Under the more damaging fully reversed cyclic loading, flexural members should perform as well as the tension members under repeated loading provided there is sufficient confinement. Also the behavioral response of flexural members with more than two noncontact splices in a section can be examined. Finally, the transverse reinforcement contribution in noncontact splices can be studied with the goal of experimentally determining the minimum requirements for transverse reinforcement along tensile lap splices.

Advances in computer modeling of reinforced concrete behavior, which incorporate cracking of concrete and yielding of reinforcement, make it possible to investigate noncontact lap splice inelastic behavior. The computer model could be checked with results from this investigation. This analytical route could reduce the suggested experimental work.

REFERENCES

1. ACI Committee E-1, "Reinforced Concrete Building Regulations," Handbook of Reinforced Concrete Building Design, Authorized Reprint from Copyrighted Proceedings Vol. 24, American Concrete Institute, Detroit, 1928.
2. ACI Committee 116, "Cement and Concrete Terminology (ACI 116R-85)," Publication SP-19(85), American Concrete Institute, Detroit, 1985.
3. ACI Committee 211, "Standard Practice for Selecting Proportions for Normal, Heavyweight, and Mass Concrete (ACI 211.1-81), Revised 1985, American Concrete Institute, Detroit, 1986.
3. ACI Committee 318, "Building Code Requirements for Reinforced Concrete (ACI 318-63)," American Concrete Institute, Detroit, 1963.
4. ACI Committee 318, "Building Code Requirements for Reinforced Concrete (ACI 318-71)," American Concrete Institute, Detroit, 1971.
5. ACI Committee 318, "Building Code Requirements for Reinforced Concrete (ACI 318-83)," American Concrete Institute, Detroit, 1983.
6. ACI Committee 318, "Commentary on Building Code Requirements for Reinforced Concrete," Publication SP-10, American Concrete Institute, Detroit, 1965.
7. ACI Committee 318, "Commentary on Building Code Requirements for Reinforced Concrete (ACI 318R-83)," American Concrete Institute, Detroit, 1983.
8. ACI Committee 408, "Suggested Development, Splice, and Standard Hook Provisions for Deformed Bars in Tension," Report No. ACI 408.IR-79, Concrete International, Vol. 1, No. 7, July 1979, pp. 44-46.
9. Annual Book of ASTM Standards, American Society for Testing and Materials, Philadelphia, 1986.
10. Aristizobal-Ochoa, J. D., "Earthquake Resistant Tensile Lap Splices," Journal of Structural Engineering, ASCE, Vol. 109, April 1983, pp. 843-858.

11. Betzle, M., "Bond Slip and Strength of Lapped Bar Splices," Douglas McHenry International Symposium on Concrete and Concrete Structures, Publication SP-55, American Concrete Institute, Detroit, 1978, pp. 493-514.
12. Cairns, J., and K. Jones, "Bond Performance of Ribbed Reinforcing Bars in Lapped Joints," Bond in Concrete, Applied Science Publishers, London, 1982, pp. 342-352.
13. Carino, N. J., and H. S. Lew, "Reexamination of the Relation Between Splitting Tensile and Compressive Strength of Normal Weight Concrete," ACI Journal, Proceedings Vol. 79, No. 3, May-June, 1982, pp. 214-219.
14. CEB-FIP Model Code for Concrete Structures, International System of Unified Standard Code of Practice for Structures, Vol. 2, Draft 1986.
15. Cernica, J. N., Fundamentals of Reinforced Concrete, Addison-Wesley Publishing Company Inc., Reading, Massachusetts, 1964.
15. Chamberlin, S. J., "Spacing of Spliced Bars in Beams," ACI Journal, Proceedings Vol. 54, No. 8, February 1958, pp. 689-697.
16. Chamberlin, S. J., "Spacing of Spliced Bars in Tension Pull-Out Specimens," ACI Journal, Proceedings Vol. 49, No. 4, December 1952, pp. 261-274.
17. Chinn, J., P. M. Ferguson, and J. N. Thompson, "Lapped Splices in Reinforced Concrete Beams," ACI Journal, Proceedings Vol. 52, No. 2, October 1955, pp. 201-213.
18. Code of Practice for the Design of Concrete Structures NZS3101 Part 1: 1982, New Zealand Standard, Standards Association of New Zealand, July 1982.
19. Collins, M. P., and D. Mitchell, "A Rational Approach to Shear Design - The 1984 Canadian Code Provisions," ACI Journal, Proceedings Vol. 83, No. 6, November-December 1986, pp. 925-933.
20. Cook, W. D., and D. Mitchell, "Studies of Disturbed Regions Near Discontinuities in Reinforced Concrete Members," ACI Structural Journal, Vol. 85, No. 2, March-April 1988, pp. 206-216.
21. Cowell, A. D., E. P. Popov, and V. V. Bertero, "Effects of Concrete Types and Loading Conditions on Local Bond-Slip Relationships," Report No. UCB/EERC-82/17, Earthquake Engineering Research Center, College of Engineering, University of California, Berkeley, September 1982.

22. Fagundo, F. E., P. Gergely, and R. N. White. "The Behavior of Lapped Splices in Reinforced Concrete Beams Subjected to Repeated Loads," Department of Structural Engineering, Cornell University, Report 79-7, December 1979.
23. Ferguson, P. M., "Small Bar Spacing or Cover - A Bond Problem for the Designer," ACI Journal, Proceedings Vol. 74, No. 9, September 1977, pp. 435-439.
24. Ferguson, P. M., and J. E. Breen, "Lapped Splices for High Strength Reinforcing Bars," ACI Journal, Proceedings Vol. 62, No. 9, September 1965, pp. 1063-1077.
25. Ferguson, P. M., and C. N. Krishnaswamy, "Tensile Lap Splices Part 2: Design Recommendations for Retaining Wall Splices and Large Bar Splices," Research Report 113-3, Center for Highway Research, The University of Texas at Austin, April 1971.
26. Goto, Y., and K. Otsuka, "Experimental Studies on Cracks Formed in Concrete Around Deformed Tension Bars," The Technology Reports of the Tohoku University, Vol. 44 (1979), No. 1, June, pp. 49-83.
27. Hungspreug, S., P. Gergely, A. R. Ingraffea, and R. N. White, "Local Bond Between a Reinforcing Bar and Concrete Under High Intensity Cyclic Load," Report 81-6, Department of Structural Engineering, Cornell University, Ithaca, NY, January 1981.
28. Jirsa, J. O., L. A. Lutz, and P. Gergely, "Rational for Suggested Development, Splice, and Standard Hook Provisions for Deformed Bars in Tension," Concrete International, Vol. 1, No. 7, July 1979, pp. 47-61.
29. Kemp, E. L., and W. J. Wilhelm, "Investigation of the Parameters Influencing Bond Cracking," ACI Journal, Proceedings Vol. 76, No.1, January 1979, pp. 47-71.
30. Kluge, K., Gerfried Schmidt-Thro, Siegfried Stockl, and Kupfer, "Versuch uber das Verbundverhalten von Rippenstahlen bei Anwendung des Gleitbauverfahrens," Deutscher Ausschuss Fur Stahlbeton, Heft 378, Berlin 1986, pp. 63-109.
31. Lancelot, H. B., "Dowel Bar Substitution: A Hidden Strength," Forming Economical Concrete Buildings, Proceedings of the Second International Conference, Publication SP-90, American Concrete Institute, Detroit, 1986, pp. 49-69.

32. Lem, J. M., R. N. White, and P. Gergely, " The Behavior of Lapped Splices in Flat Reinforced Concrete Elements in Biaxial Tension," Department of Structural Engineering, Cornell University, Report 83-8, January 1983.
33. Lukose, K., P. Gergely, and R. N. White, "Behavior of Reinforced Concrete Lapped Splices for Inelastic Cyclic Loading," ACI Journal, Proceedings Vol. 79, No. 5, September-October 1982, pp. 355-365.
34. Lukose, K., P. Gergely, and R. N. White, " A Study of Lapped Splices in Reinforced Concrete Columns Under Severe Cyclic Loads," Department of Structural Engineering, Cornell University, Report 81-11, July 1981.
35. Lutz, L. A. and P. Gergely, "Mechanics of Bond and Slip of Deformed Bars in Concrete," ACI Journal, Proceedings Vol. 64, No. 11, November 1967, pp. 711-721.
36. Marti, P., "Basic Tools of Reinforced Concrete Beam Design," ACI Journal, Proceedings Vol. 82, No. 1, January-February 1985, pp. 46-56.
37. Neville, A. M., Properties of Concrete, Third Edition, Pitman Books Ltd., London, 1981.
38. Nilson, A. H., and G. Winter, Design of Concrete Structures, Tenth Edition, McGraw-Hill Book Co., New York, 1986.
39. Orangun, C. O., J. O. Jirsa, and J. E. Breen, "A Reevaluation of Test Data on Development Length and Splices," ACI Journal, Proceedings Vol. 74, No. 3, March 1977, pp. 114-122.
40. Orangun, C. O., J. O. Jirsa, and J. E. Breen, "The Strength of Anchored Bars: A Reevaluation of Test Data on Development Length and Splices," Research Report 154-3F, Center For Highway Research, The University of Texas at Austin, January 1975.
41. Panahshahi, N., R. N. White, and P. Gergely, "Compression and Tension Lap Splices In Reinforced Concrete Members Subjected to Inelastic Cyclic Loading," Department of Structural Engineering, Cornell University, Report 87-2, 1987.
42. Reynolds, G. C., and A. W. Beeby, "Bond Strength of Deformed Bars," Bond in Concrete, Applied Science Publishers, London, 1982, pp. 434-445.

43. Rezansoff, T., J. A. Zaccaruk, and R. Topping, "Tensile Lap Splices in Reinforced Concrete Beams Under Inelastic Cyclic Loading," *ACI Structural Journal*, Vol. 85, No. 1, January-February 1988, pp. 46-52.
44. Roberts, N. P., and R. Chung-tai Ho, "Behaviour and Design of Tensile Lapped Joints in Reinforced Concrete Beams," *Civil Engineering Public Work Review*, Vol. 68, No. 798, January 1973, pp. 35-45.
45. Robinson, J. R., T. C. Zsutty, G. Guirogodze, L. J. Lima, J. P. Hoang Long Hung und Villatoux, "La Couture des Jonctions par Adherence," *Bulletin d'Information des CEB*, Nr. 99, Marz 1974.
46. Sivakumar, B., R. N. White, and P. Gergely, "Behavior and Design of Reinforced Concrete Column-Type Lapped Splices Subjected to High-Intensity Cyclic Loading," Department of Structural Engineering, Cornell University, Report 82-11, October 1982.
47. Sivakumar, B., P. Gergely, and R. N. White, "Suggestions for the Design of R/C Lapped Splices for Seismic Loading," *Concrete International*, Vol. 5, No. 2, February 1983, pp. 46-50.
48. Sparling, B. and T. Rezansoff, "The Effect of Confinement on Lap Splices in Reversed Cyclic Loading," *Canadian Journal of Civil Engineering*, Vol. 13, 1986, pp. 681-692.
49. Tasuji, M. E., F. O. Slate, and A. H. Nilson, "Stress-Strain Response and Fracture of Concrete in Biaxial Loading," *ACI Journal*, Proceedings Vol. 75, No. 7, July 1978, pp. 306-312.
50. Tepfers, R., "Cracking of Concrete Cover Along Anchored Deformed Reinforcing Bars," *Magazine of Concrete Research*, Vol. 31, No. 106, March 1979, pp. 3-12.
51. Tepfers, R., "A Theory of Bond Applied to Overlapped Tensile Reinforcement Splices for Deformed Bars," Publication 73:2, Division of Concrete Structures, Chalmers Tekniska Hogskola (Chalmers University of Technology), Goteborg, Sweden, 1973.
52. Thompson, M. A., J. O. Jirsa, J. E. Breen, and D. Meinheit, "The Behavior of Multiple Lap Splices in Wide Sections," Research Report 154-1, Center for Highway Research, The University of Texas at Austin, January 1975.

53. Tocci, A. D., P. Gergely, and R. N. White, "The Behavior and Strength of Lapped Splices in Reinforced Concrete Beams Subjected to Cyclic Loading," Department of Structural Engineering, Cornell University, Report 81-1, May 1981.
54. Untrauer, R. E. and G. E. Warren, "Stress Development of Tension Steel in Beams," ACI Journal, Proceedings Vol. 74, No. 8, August 1977, pp. 368-372.
55. Vecchio, F. J., and M. P. Collins, "The Modified Compression-Field Theory for Reinforced Concrete Elements Subjected to Shear," ACI Journal, Proceedings Vol. 83, No. 2, March-April 1986, pp. 219-231.
56. Walker, W. T., "Laboratory Tests of Spaced and Tied Reinforcing Bars," ACI Journal, Proceedings Vol. 47, No. 5, January 1951, pp. 365-372.
57. Zsutty, T., "Empirical Study of Bar Development Behavior," Journal of Structural Engineering, ASCE, Vol. 111, No. 1, January 1985, pp. 205-219.

**NATIONAL CENTER FOR EARTHQUAKE ENGINEERING RESEARCH
LIST OF PUBLISHED TECHNICAL REPORTS**

The National Center for Earthquake Engineering Research (NCEER) publishes technical reports on a variety of subjects related to earthquake engineering written by authors funded through NCEER. These reports are available from both NCEER's Publications Department and the National Technical Information Service (NTIS). Requests for reports should be directed to the Publications Department, National Center for Earthquake Engineering Research, State University of New York at Buffalo, Red Jacket Quadrangle, Buffalo, New York 14261. Reports can also be requested through NTIS, 5285 Port Royal Road, Springfield, Virginia 22161. NTIS accession numbers are shown in parenthesis, if available.

- NCEER-87-0001 "First-Year Program in Research, Education and Technology Transfer," 3/5/87, (PB88-134275/AS).
- NCEER-87-0002 "Experimental Evaluation of Instantaneous Optimal Algorithms for Structural Control," by R.C. Lin, T.T. Soong and A.M. Reinhorn, 4/20/87, (PB88-134341/AS).
- NCEER-87-0003 "Experimentation Using the Earthquake Simulation Facilities at University at Buffalo," by A.M. Reinhorn and R.L. Ketter, to be published.
- NCEER-87-0004 "The System Characteristics and Performance of a Shaking Table," by J.S. Hwang, K.C. Chang and G.C. Lee, 6/1/87, (PB88-134259/AS).
- NCEER-87-0005 "A Finite Element Formulation for Nonlinear Viscoplastic Material Using a Q Model," by O. Gyebi and G. Dasgupta, 11/2/87, (PB88-213764/AS).
- NCEER-87-0006 "Symbolic Manipulation Program (SMP) - Algebraic Codes for Two and Three Dimensional Finite Element Formulations," by X. Lee and G. Dasgupta, 11/9/87, (PB88-219522/AS).
- NCEER-87-0007 "Instantaneous Optimal Control Laws for Tall Buildings Under Seismic Excitations," by J.N. Yang, A. Akbarpour and P. Ghaemmaghami, 6/10/87, (PB88-134333/AS).
- NCEER-87-0008 "IDARC: Inelastic Damage Analysis of Reinforced Concrete Frame - Shear-Wall Structures," by Y.J. Park, A.M. Reinhorn and S.K. Kunnath, 7/20/87, (PB88-134325/AS).
- NCEER-87-0009 "Liquefaction Potential for New York State: A Preliminary Report on Sites in Manhattan and Buffalo," by M. Budhu, V. Vijayakumar, R.F. Giese and L. Baumgras, 8/31/87, (PB88-163704/AS). This report is available only through NTIS (see address given above).
- NCEER-87-0010 "Vertical and Torsional Vibration of Foundations in Inhomogeneous Media," by A.S. Veletsos and K.W. Dotson, 6/1/87, (PB88-134291/AS).
- NCEER-87-0011 "Seismic Probabilistic Risk Assessment and Seismic Margins Studies for Nuclear Power Plants," by Howard H.M. Hwang, 6/15/87, (PB88-134267/AS). This report is available only through NTIS (see address given above).
- NCEER-87-0012 "Parametric Studies of Frequency Response of Secondary Systems Under Ground-Acceleration Excitations," by Y. Yong and Y.K. Lin, 6/10/87, (PB88-134309/AS).
- NCEER-87-0013 "Frequency Response of Secondary Systems Under Seismic Excitation," by J.A. HoLung, J. Cai and Y.K. Lin, 7/31/87, (PB88-134317/AS).
- NCEER-87-0014 "Modelling Earthquake Ground Motions in Seismically Active Regions Using Parametric Time Series Methods," by G.W. Ellis and A.S. Cakmak, 8/25/87, (PB88-134283/AS).
- NCEER-87-0015 "Detection and Assessment of Seismic Structural Damage," by E. DiPasquale and A.S. Cakmak, 8/25/87, (PB88-163712/AS).
- NCEER-87-0016 "Pipeline Experiment at Parkfield, California," by J. Isenberg and E. Richardson, 9/15/87, (PB88-163720/AS).

NCEER-87-0017 "Digital Simulation of Seismic Ground Motion," by M. Shinozuka, G. Deodatis and T. Harada, 8/31/87, (PB88-155197/AS). This report is available only through NTIS (see address given above).

NCEER-87-0018 "Practical Considerations for Structural Control: System Uncertainty, System Time Delay and Truncation of Small Control Forces," J.N. Yang and A. Akbarpour, 8/10/87, (PB88-163738/AS).

NCEER-87-0019 "Modal Analysis of Nonclassically Damped Structural Systems Using Canonical Transformation," by J.N. Yang, S. Sarkani and F.X. Long, 9/27/87, (PB88-187851/AS).

NCEER-87-0020 "A Nonstationary Solution in Random Vibration Theory," by J.R. Red-Horse and P.D. Spanos, 11/3/87, (PB88-163746/AS).

NCEER-87-0021 "Horizontal Impedances for Radially Inhomogeneous Viscoelastic Soil Layers," by A.S. Veletsos and K.W. Dotson, 10/15/87, (PB88-150859/AS).

NCEER-87-0022 "Seismic Damage Assessment of Reinforced Concrete Members," by Y.S. Chung, C. Meyer and M. Shinozuka, 10/9/87, (PB88-150867/AS). This report is available only through NTIS (see address given above).

NCEER-87-0023 "Active Structural Control in Civil Engineering," by T.T. Soong, 11/11/87, (PB88-187778/AS).

NCEER-87-0024 "Vertical and Torsional Impedances for Radially Inhomogeneous Viscoelastic Soil Layers," by K.W. Dotson and A.S. Veletsos, 12/87, (PB88-187786/AS).

NCEER-87-0025 "Proceedings from the Symposium on Seismic Hazards, Ground Motions, Soil-Liquefaction and Engineering Practice in Eastern North America," October 20-22, 1987, edited by K.H. Jacob, 12/87, (PB88-188115/AS).

NCEER-87-0026 "Report on the Whittier-Narrows, California, Earthquake of October 1, 1987," by J. Pantelic and A. Reinhorn, 11/87, (PB88-187752/AS). This report is available only through NTIS (see address given above).

NCEER-87-0027 "Design of a Modular Program for Transient Nonlinear Analysis of Large 3-D Building Structures," by S. Srivastav and J.F. Abel, 12/30/87, (PB88-187950/AS).

NCEER-87-0028 "Second-Year Program in Research, Education and Technology Transfer," 3/8/88, (PB88-219480/AS).

NCEER-88-0001 "Workshop on Seismic Computer Analysis and Design of Buildings With Interactive Graphics," by W. McGuire, J.F. Abel and C.H. Conley, 1/18/88, (PB88-187760/AS).

NCEER-88-0002 "Optimal Control of Nonlinear Flexible Structures," by J.N. Yang, F.X. Long and D. Wong, 1/22/88, (PB88-213772/AS).

NCEER-88-0003 "Substructuring Techniques in the Time Domain for Primary-Secondary Structural Systems," by G.D. Manolis and G. Juhn, 2/10/88, (PB88-213780/AS).

NCEER-88-0004 "Iterative Seismic Analysis of Primary-Secondary Systems," by A. Singhal, L.D. Lutes and P.D. Spanos, 2/23/88, (PB88-213798/AS).

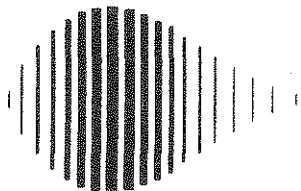
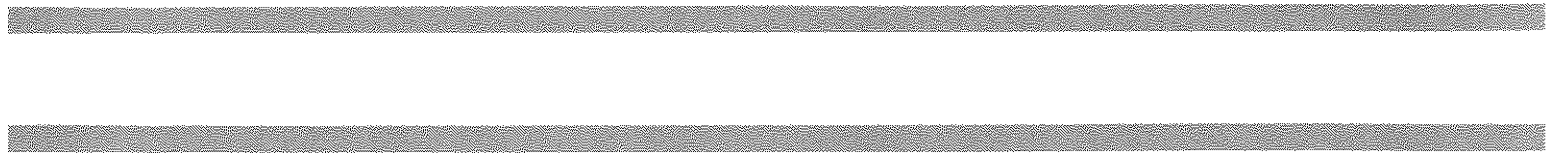
NCEER-88-0005 "Stochastic Finite Element Expansion for Random Media," by P.D. Spanos and R. Ghanem, 3/14/88, (PB88-213806/AS).

NCEER-88-0006 "Combining Structural Optimization and Structural Control," by F.Y. Cheng and C.P. Pantelides, 1/10/88, (PB88-213814/AS).

NCEER-88-0007 "Seismic Performance Assessment of Code-Designed Structures," by H.H.-M. Hwang, J.-W. Jaw and H.-J. Shau, 3/20/88, (PB88-219423/AS).

- NCEER-88-0008 "Reliability Analysis of Code-Designed Structures Under Natural Hazards," by H.H-M. Hwang, H. Ushiba and M. Shinozuka, 2/29/88, (PB88-229471/AS).
- NCEER-88-0009 "Seismic Fragility Analysis of Shear Wall Structures," by J-W Jaw and H.H-M. Hwang, 4/30/88.
- NCEER-88-0010 "Base Isolation of a Multi-Story Building Under a Harmonic Ground Motion - A Comparison of Performances of Various Systems," by F-G Fan, G. Ahmadi and I.G. Tadjbakhsh, 5/18/88.
- NCEER-88-0011 "Seismic Floor Response Spectra for a Combined System by Green's Functions," by F.M. Lavelle, L.A. Bergman and P.D. Spanos, 5/1/88.
- NCEER-88-0012 "A New Solution Technique for Randomly Excited Hysteretic Structures," by G.Q. Cai and Y.K. Lin, 5/16/88.
- NCEER-88-0013 "A Study of Radiation Damping and Soil-Structure Interaction Effects in the Centrifuge," by K. Weissman, supervised by J.H. Prevost, 5/24/88.
- NCEER-88-0014 "Parameter Identification and Implementation of a Kinematic Plasticity Model for Frictional Soils," by J.H. Prevost and D.V. Griffiths, to be published.
- NCEER-88-0015 "Two- and Three- Dimensional Dynamic Finite Element Analyses of the Long Valley Dam," by D.V. Griffiths and J.H. Prevost, 6/17/88.
- NCEER-88-0016 "Damage Assessment of Reinforced Concrete Structures in Eastern United States," by A.M. Reinhorn, M.J. Seidel, S.K. Kunnath and Y.J. Park, 6/15/88.
- NCEER-88-0017 "Dynamic Compliance of Vertically Loaded Strip Foundations in Multilayered Viscoelastic Soils," by S. Ahmad and A.S.M. Israil, 6/17/88.
- NCEER-88-0018 "An Experimental Study of Seismic Structural Response With Added Viscoelastic Dampers," by R.C. Lin, Z. Liang, T.T. Soong and R.H. Zhang, 6/30/88.
- NCEER-88-0019 "Experimental Investigation of Primary - Secondary System Interaction," by G.D. Manolis, G. Juhn and A.M. Reinhorn, 5/27/88.
- NCEER-88-0020 "A Response Spectrum Approach For Analysis of Nonclassically Damped Structures," by J.N. Yang, S. Sarkani and F.X. Long, 4/22/88.
- NCEER-88-0021 "Seismic Interaction of Structures and Soils: Stochastic Approach," by A.S. Veletsos and A.M. Prasad, 7/21/88.
- NCEER-88-0022 "Identification of the Serviceability Limit State and Detection of Seismic Structural Damage," by E. DiPasquale and A.S. Cakmak, 6/15/88.
- NCEER-88-0023 "Multi-Hazard Risk Analysis: Case of a Simple Offshore Structure," by B.K. Bhartia and E.H. Vanmarcke, 7/21/88.
- NCEER-88-0024 "Automated Seismic Design of Reinforced Concrete Buildings," by Y.S. Chung, C. Meyer and M. Shinozuka, 7/5/88.
- NCEER-88-0025 "Experimental Study of Active Control of MDOF Structures Under Seismic Excitations," by L.L. Chung, R.C. Lin, T.T. Soong and A.M. Reinhorn, 7/10/88, (PB89-122600/AS).
- NCEER-88-0026 "Earthquake Simulation Tests of a Low-Rise Metal Structure," by J.S. Hwang, K.C. Chang, G.C. Lee and R.L. Ketter, 8/1/88.
- NCEER-88-0027 "Systems Study of Urban Response and Reconstruction Due to Catastrophic Earthquakes," by F. Kozin and H.K. Zhou, 9/22/88, to be published.

- NCEER-88-0028 "Seismic Fragility Analysis of Plane Frame Structures," by H.H.M. Hwang and Y.K. Low, 7/31/88.
- NCEER-88-0029 "Response Analysis of Stochastic Structures," by A. Kardara, C. Bucher and M. Shinozuka, 9/22/88, to be published.
- NCEER-88-0030 "Nonnormal Accelerations Due to Yielding in a Primary Structure," by D.C.K. Chen and L.D. Lutes, 9/19/88.
- NCEER-88-0031 "Design Approaches for Soil-Structure Interaction," by A.S. Veletsos, A.M. Prasad and Y. Tang, to be published.
- NCEER-88-0032 "A Re-evaluation of Design Spectra for Seismic Damage Control," by C.J. Turkstra and A.G. Tallin, 11/7/88.
- NCEER-88-0033 "The Behavior and Design of Noncontact Lap Splices Subjected to Repeated Inelastic Tensile Loading," by V.E. Sagan, P. Gergely and R.N. White, 12/8/88.



National Center for Earthquake Engineering Research
State University of New York at Buffalo